

2015

Analysis of selective laser melting for additive manufacturing process

Sri Harsha Kankanala

Follow this and additional works at: <https://huskiecommons.lib.niu.edu/allgraduate-thesesdissertations>

Recommended Citation

Kankanala, Sri Harsha, "Analysis of selective laser melting for additive manufacturing process" (2015).
Graduate Research Theses & Dissertations. 1462.
<https://huskiecommons.lib.niu.edu/allgraduate-thesesdissertations/1462>

This Dissertation/Thesis is brought to you for free and open access by the Graduate Research & Artistry at Huskie Commons. It has been accepted for inclusion in Graduate Research Theses & Dissertations by an authorized administrator of Huskie Commons. For more information, please contact jschumacher@niu.edu.

ABSTRACT

ANALYSIS OF SELECTIVE LASER MELTING FOR ADDITIVE MANUFACTURING PROCESS

Sri Harsha Kankanala, M.S
Department of Mechanical Engineering
Northern Illinois University, 2015
Dr. Pradip Majumdar, Director

The additive manufacturing process or 3D printing (3DP) uses digital data obtained from a three-dimensional CAD solid model to create a physical object by building sequential layers on top of one another. The physical object is formed by sequentially printing material particles in a layer while concurrently heating, melting, and then cooling the deposited material. The process is repeated layer-by-layer to obtain a desired 3D solid physical object. The materials could be powder particles of metals, polymer, or composite. The additive manufacturing process considered in this study involve selective laser heating and fusion of metallic particles as it has a high potential to produce complex physical object with intricate internal geometries with high tolerance and precision. The objective of the research is to evaluate and characterize selective laser heating and melting of aluminum particles for fabricating layered substance using laser beam. The process of additive fabricated metallic layer will be analyzed by conducting three-dimension thermal simulation analysis of the process for fabricating a layer using spherical metallic particles and using the Selective Laser Melting (SLM). Computational algorithm will be developed to accurately melting spherical particles and forming a layer of desired thickness. The fabrication process will be iterated to ensure quality in terms of precision and resolution with varying range of operating parameters such particle size, beam diameter and power intensity, and cooling parameters to check the sensitivity on precision and resolution.

NORTHERN ILLINOIS UNIVERSITY
DEKALB, ILLINOIS

AUGUST 2015

ANALYSIS OF SELECTIVE LASER MELTING FOR ADDITIVE
MANUFACTURING PROCESS

BY

SRI HARSHA KANKANALA
© 2015 Sri harsha Kankanala

A THESIS SUBMITTED TO THE GRADUATE SCHOOL
IN PARTIAL FULFILLMENT OF THE REQUIREMENTS

FOR THE DEGREE

MASTER OF SCIENCE

DEPARTMENT OF MECHANICAL ENGINEERING

Thesis Director:

Dr. Pradip Majumdar

ACKNOWLEDGEMENTS

I would like to extend my humble thanks to Dr. Pradip Majumdar for his encouragement, advice, and guidance during all the phases of my thesis work. Also, I would like to thank Dr.Federico Sciamarella and Dr.Matt Gonser for being on my committee and also for their valuable help and guidance. I would also like to thank all the staff and faculty of the Department of Engineering for providing and maintaining the infrastructure that was needed for the successful completion of my work.

I am indebted to my parents, Prabhakar Kankanala and Sudha Parimala, my brother Madhu Balikonda, my uncle Sateesh Kankanala, and my best friends Ms.Harshada Haribabu Vuyyuri and Ms. Anusha Ravva, for being helpful during all the difficult times and also for being there for me whenever I needed them. I thank each and every one of you for being a source of strength throughout my master's program.

I am also thankful to my friends Sathwik, Narmada, Nikhilesh, Ashkan, Abhinav, and whomever help me and gave their support in times of need.

DEDICATION

To all my teachers who have moulded me into what I am and my friends and
family.

TABLE OF CONTENTS

LIST OF FIGURES	viii
1 INTRODUCTION	1
1.1 Motivation	1
1.2 Literature Review:	2
1.3 Objective	7
2 SIMULATION MODEL FOR ADDITIVE MANUFACTURING	8
2.1 Classification of Additive Manufacturing	9
2.1.1 Material Extrusion:	9
2.1.2 Material Jetting:	9
2.1.3 Binder Jetting:	9
2.1.4 Sheet Lamination:	9
2.1.5 Vat Photo polymerization:	10
2.1.6 Direct Energy Deposition:	10
2.1.7 Powder Bed Fusion:	10
2.2 Description of the Physical Model to be fabricated	13
2.2.1 Laser Beam Specifications:	13
2.3 Simulation Algorithmic Model:	14

2.3.1	Design Analysis:	17
2.4	Mathematical Formulation:	18
2.5	Energy Equation:	19
2.5.1	Heat Transfer Model:	19
2.5.2	Enthalpy Model:	21
3	COMPUTATIONAL MODEL	23
3.1	Computational Model	25
3.2	Simulation Model:	26
3.3	Geometric Model:	27
3.4	Mesh Generation:	28
4	RESULTS AND DISCUSSION	31
4.1	Physics for the model:	32
4.2	Selection of beam intensity:	33
4.2.1	Determination of the Melted Volume for multiple Beam Powers	34
4.3	Effects of parameters on part density:	47
4.3.1	Mesh Refinement study	47
4.4	Temperature Model Results	50
4.4.1	Effect of particle size – 50microns	50
4.4.2	Effect of particle size - 30microns	83
4.4.3	Effect of particle size – 10microns	96

4.5	Performing Sensitivity Analysis.....	107
4.5.1	Density calculation for particle of size 50microns	107
4.5.2	Density calculation for particle of size 30microns	108
4.5.3	Density calculation for particle of size 10microns	108
5	CONCLUSION AND FUTURE WORK	112
6	REFERENCES.....	113

LIST OF FIGURES

Figure 2-1 Selective laser melting process	12
Figure 2-2 Set of operations to be performed to manufacture a part using SLM process	14
Figure 2-3 Computational algorithm for SL beam parameters & calculating material density....	16
Figure 2-4 Geometry of powder particles	16
Figure 2-5 Geometric view of powder particles after spraying second layer and after melting it	18
Figure 3-1 Powder particles – Layer 1	28
Figure 3-2 Mesh scene	30
Figure 4-1 Table of thermo physical and laser operating properties.	31
Figure 4-2 Symmetric view	33
Figure 4-3 Temperature distribution of powder particles at beam intensity $5 \cdot 10^8$ W/m ²	34
Figure 4-4 Point probes-Temperature distribution of powder particles at intensity $5 \cdot 10^8$ W/m ²	35
Figure 4-5 Plots at section 2, 3, 4 and 5 determining temperature distribution	37
Figure 4-6 Time Vs Melted volume.....	38
Figure 4-7 Temperature distribution of powder particles at beam intensity $7.5 \cdot 10^8$ W/m ²	39
Figure 4-8 Point probes - Temperature distribution for point probe	39
Figure 4-9 Plots at section 2, 3 determining temperature distribution.....	40
Figure 4-10 Melted volume VS Time.....	41
Figure 4-11 Temperature distribution for layer 1 & beam position 1 at time 0.002s	42

Figure 4-12 Temperature distribution for layer 1 & beam position 1 at time 0.005s	42
Figure 4-13 Temperature distribution for layer 1 & beam position 1 at time 0.011s	42
Figure 4-14 Point probes - Temperature distribution for layer 1 & beam position 1	43
Figure 4-15 Point probes at the center of particles for layer 1 beam position 1	43
Figure 4-16 Plots at section 2, 3, 4 and 5 determining temperature distribution	45
Figure 4-17 Time Vs Melted volume.....	46
Figure 4-18 Time VS Temperature plot.....	47
Figure 4-19 Temperature scene representing temperature distribution for powder particles	48
Figure 4-20 Temperature scene representing temperature distribution for powder particles	49
Figure 4-21 Time VS Melted volume.....	49
Figure 4-22 Temperature distribution for layer 1 beam position 2 at 0.002 sec.....	50
Figure 4-23 Temperature distribution for layer 1 beam position 2 at 0.005 sec.....	50
Figure 4-24 Temperature distribution for layer 1 beam position 2 at 0.011 sec.....	51
Figure 4-25 Point probes - Temperature distribution for layer 1 beam position 2	51
Figure 4-26 Time Vs Melted volume.....	52
Figure 4-27 Process time Vs Highest temperature	52
Figure 4-28 Initial temperature distribution for layer 1 beam position 3 at 0.002 sec	53
Figure 4-29 Temperature distribution for layer 1 beam position 3 at time 0.05 seconds	53
Figure 4-30 Temperature distribution for layer 1 beam position 3 at 0.011 sec.....	53
Figure 4-31 Point probes - Temperature distribution for layer 1 beam position 3	54
Figure 4-32 Time VS Melted volume.....	54
Figure 4-33 Time Vs Highest temperature	55

Figure 4-34 Geometry scene for enthalpy validation	56
Figure 4-35 Mesh scene for enthalpy validation.....	57
Figure 4-36 Enthalpy scene for beam position 1	57
Figure 4-37 Enthalpy scene beam position 2.....	58
Figure 4-38 Enthalpy scene beam position 3.....	58
Figure 4-39 After melting and solidifying of layer 1.....	59
Figure 4-40 After spraying another layer of particles over the melted layer 1.....	59
Figure 4-41 Mesh scene	60
Figure 4-42 Temperature distribution at 0.02 sec.....	60
Figure 4-43 Temperature distribution at 0.05 sec.....	60
Figure 4-44 Temperature distribution for layer 2 beam position 1 at 0.011 sec.....	61
Figure 4-45 Point probes - Temperature distribution for layer 2 beam position 1	61
Figure 4-46 Time Vs Melted volume.....	62
Figure 4-47 Process Time Vs Highest temperature	62
Figure 4-48 Initial temperature distribution at 0.002 sec.....	63
Figure 4-49 Temperature distribution at time 0.05 sec.....	63
Figure 4-50 Temperature distribution for layer 2 beam position 2 at 0.011 sec.....	63
Figure 4-51 Point probes - Temperature distribution for layer 2 beam 2 position 2	64
Figure 4-52 Time Vs Melted volume.....	64
Figure 4-53 Process Time Vs Highest temperature	65
Figure 4-54 Temperature distribution at time 0.02 sec.....	65
Figure 4-55 Temperature distribution at 0.05 sec.....	66

Figure 4-56 Temperature distribution for layer 2 beam position 3 at 0.011 sec.....	66
Figure 4-57 Point probes -Temperature distribution for layer 2 beam position 3	66
Figure 4-58 Time Vs Melted volume.....	67
Figure 4-59 Time Vs Highest temperature	67
Figure 4-60 Enthalpy scene beam position 1	68
Figure 4-61 Enthalpy scene beam position 2.....	69
Figure 4-62 Enthalpy scene beam position 3.....	69
Figure 4-63 After melting and solidifying of layer 1 and 2.....	70
Figure 4-64 After spraying a new layer on the melted layer 1 and 2.....	70
Figure 4-65 Mesh scene	71
Figure 4-66 Temperature distribution at 0.002sec	71
Figure 4-67 Temperature distribution at 0.005sec	72
Figure 4-68 Temperature distribution for layer 3 beam position 1 at 0.011 sec.....	72
Figure 4-69 Point probes - Temperature distribution for layer 3 beam position 1	72
Figure 4-70 Time Vs Melted volume.....	73
Figure 4-71 Process time Vs Highest temperature	74
Figure 4-72 Temperature distribution at time 0.002 sec.....	74
Figure 4-73 Temperature distribution at time 0.005 sec.....	75
Figure 4-74 Temperature distribution for layer 3 beam position 2 at 0.011 sec.....	75
Figure 4-75 Point probes - Temperature distribution for layer 3 beam position 2	76
Figure 4-76 Time Vs Melted volume.....	76
Figure 4-77 Process time Vs Highest temperature	77

Figure 4-78 Temperature distribution at time 0.002 sec	77
Figure 4-79 Temperature distribution for layer 3 beam 3 at time 0.005 sec	78
Figure 4-80 Temperature distribution for layer 3 beam position 3 at time 0.011 sec.....	78
Figure 4-81 Point probes - Temperature distribution for layer 3 beam position 3	79
Figure 4-82 Time Vs Melted volume.....	80
Figure 4-83 Time Vs Highest temperature	80
Figure 4-84 Enthalpy scene beam position 1	81
Figure 4-85 Enthalpy scene beam position 2	82
Figure 4-86 Enthalpy scene beam position 3	82
Figure 4-87 Geometry of work piece	83
Figure 4-88 Mesh scene of the work piece	84
Figure 4-89 Temperature distribution for Layer 1 beam position 1 at time 0.008 sec	84
Figure 4-90 Temperature distribution for probe points	85
Figure 4-91 Time Vs Melted volume.....	85
Figure 4-92 Time Vs Highest temperature	86
Figure 4-93 Temperature distribution for layer 1 beam position 2 at 0.016 sec.....	86
Figure 4-94 Temperature distribution for probe points	87
Figure 4-95 Time Vs Melted volume.....	87
Figure 4-96 Time Vs Highest temperature	88
Figure 4-97 Temperature distribution for layer 1 beam position 3 at time 0.024 seconds	88
Figure 4-98 Temperature distribution for probe point	89
Figure 4-99 Time Vs Melted volume.....	89

Figure 4-100 Time Vs Highest temperature	90
Figure 4-101 Enthalpy scene beam position 1	90
Figure 4-102 Enthalpy scene beam position 2	91
Figure 4-103 Enthalpy scene beam position 3	92
Figure 4-104 Part formed after melting layer 1	92
Figure 4-105 A new powder layer is sprayed over the processed layer	93
Figure 4-106 Mesh scene	93
Figure 4-107 Temperature distribution for layer 1 beam position 1 at time 0.008 sec.....	94
Figure 4-108 Temperature distribution for probe point.....	94
Figure 4-109 Enthalpy scene for layer 3 beam position 3	95
Figure 4-110 Time Vs Melted volume.....	95
Figure 4-111 Time Vs Highest temperature	96
Figure 4-112 Geometry scene	97
Figure 4-113 Mesh scene	97
Figure 4-114 Temperature distribution for layer 1 and beam position 1 at 0.006 sec	98
Figure 4-115 Temperature distribution for point probes	98
Figure 4-116 Time Vs Melted volume.....	99
Figure 4-117 Temperature distribution for layer 1 beam position 2 at 0.012 sec.....	99
Figure 4-118 Probe points temperature distribution	100
Figure 4-119 Time Vs Melted volume.....	100
Figure 4-120 Temperature distribution of powder particles at 0.018 sec	101
Figure 4-121 Temperature distribution for probe point.....	101

Figure 4-122 Time Vs Melted volume.....	101
Figure 4-123 Enthalpy scene beam position 1	102
Figure 4-124 Enthalpy scene beam position 2.....	103
Figure 4-125 Enthalpy scene beam position 3.....	103
Figure 4-126 Geometry scene after melting the layer 1	104
Figure 4-127 After spraying another layer of particles over the melted layer 1	104
Figure 4-128 Temperature distribution of powder particles	105
Figure 4-129 Temperature distribution for probe points	105
Figure 4-130 Enthalpy Scene for Layer 3 beam position 3	106
Figure 4-131 157 Time Vs Melted volume.....	106
Figure 4-132 Particle size Vs Process time.....	110
Figure 4-133 Particle size Vs Part density.....	111

1 INTRODUCTION

1.1 Motivation

3D printing or additive manufacturing process is increasingly getting popular as an alternative to traditional machining or manufacturing process such as machining, molding and stamping. Additive manufacturing process is particularly attractive in creating intricate internal shapes such as the complex flow multiple gas flow micro channels and internal cooling channels.

It can be clearly stated that 3D printing or additive manufacturing (AM) has a vast potential to become one of the top most inventions ever made by mankind. 3D printing has now become very popular across the mass media. The people opinion of what really this 3D printing is, will put an end to all other traditional manufacturing techniques.

3D printing is one among the many branches in Additive Manufacturing process tree. This manufacturing process can handle multiple machining operations such as machining, molding and stamping. In a brief explanation it can be stated that, 3D printing is the process, in which successive layers of material (may be metal powder or metal spray) are laid one after the other. It is particularly attractive in creating intricate internal shapes which otherwise are very complex to create by other conventional machining processes. It is very difficult to manufacture a part with multiple channels and grooves by using a milling or welding operation

(conventional machining processes), but where as in 3D printing it is very easy to create such a part. This process is also very useful for mass production.

3D printing is a far advanced technology. In the beginning it was used only by large scale industries, as it was a costly as well as time consuming process. As the time and technology advanced it has reached our homes, now people are using mobile 3D printers at home. Even though it is an easy process to create a part or an assembly by 3D printing, the final part should carry all the characteristics as per customer satisfaction as well as the application where the part is used. If product doesn't meet the application tolerances, its waste of material, time, man power as well as money. There are many parameters that influence the density, strength, time taken to manufacture a unit in 3D printing. The main ones are Powder particle size, Beam diameter, Beam Power Intensity, Powder particle shape, Scan speed. Selection of all these parameters requires a lot of skill. So it's always better to run an analysis by selecting a small part of the desired part. The process to be followed is, design the part in any cad software, run a thermal analysis. The main advantage in running a complete analysis is that all the thermal properties, time taken to create the part and the density of the final product can be calculated even before manufacturing the part in 3D printing. If the analyzed part meets all the requirements, then it can be manufactured.

1.2 Literature Review:

Gusarov et al. [1] conducted experiments to study the mechanics in heat transfer of selective laser melting and how SLM stability varies with scanning speeds. From the experiments it was concluded that SLM include radiation transfer of laser in powder media which produces

volumetric heat source, related heat transfer and melt flow due to surface tension. The stability of this process can be achieved only in an interval of scanning speeds for the melting of powder. The melted tracks or layers are broken (unstable) in any scanning velocity other than this interval. Explanation was given as balling effect at high velocities by Plateau–Rayleigh capillary instability of a liquid cylinder and they found that by reducing the length-to-circumference ratio and increasing the width of the contact with the substrate would stabilize SLM by reducing the scanning velocity.

Zeng et al. [2] studied on laser sintering temperature distribution and effects of process parameters to temperature states through Fourier Equations, which are commonly used for describing the temperature distribution in various models, even though they cannot be solved completely. This study explains that FE has proven reliable as compared to other numerical methods whereas temperature distribution method has been used for measuring actual temperature distribution in SLM processes. It also recommends analytical and simulation modeling, experimental measurement and control side, laser beam distribution, energy penetration, material absorption ratio and thermal properties such as thermal conductivity, density of powder before and after laser scanning as areas of analysis for better understanding and control of SLM processes.

Kruth et al. [3] carried out a study to classify SLS and SLM processes based on binding mechanism occurring in both processes. On this basis they classified SLS/SLM processes into “solid state sintering”, “chemically induced binding”, “liquid phase sintering – partial melting”

and “full melting”. Explanation was given that exploration of full melting metal powders has increased over years supported by improving process parameters which result in better mechanical properties compared to selective laser sintering.

Yadroitsev et al. [4] carried out parametric analysis of SLM process for Inox 904L (Stainless Steel - Grade 904L) powder with particle size less than 20mm. The powder layer thickness and power input per unit speed to be 50mm and P/V ratio to be 270-420 Ws/m. Results concluded that as P/V ratio increases, the melted vector also increases and width of single vectors formed at different scanning speeds decreases. It was determined that for forming thin walls, the process has to be carried out in lengthwise direction by applying correction factor to make dimensions of the part equal to those specified in CAD.

Li et al. [5] developed a three-dimensional finite-element model to analyze effects of processing parameters on temperature. Results showed that by lower scan speed, higher laser power, and shorter scan interval parameters a distinguished high temperature in the powder bed and wider melting line width could be obtained. Also the curve of temperature versus time was studied which exhibited fluctuating variation with transverse scan mode, while moderate variation with lengthwise scan mode was observed in curve.

Brown and Arnold [6] conducted case studies to improve the efficiency of photovoltaic and optoelectronic devices. After the case study an explanation was given that the light propagation in materials, energy absorptions mechanics (absorption coefficient derived from material's

dielectric function and conductivity), heat equation based on conservation of energy and Fourier's law of heat conduction, material response, surface melting and ablation (removal of material from substrate due to absorption of laser energy) form the fundamentals of Laser Surface Processing.

Kumar and Pityana [7] through their study compared the different processes used for manufacturing of metal products such as Selective Laser Melting (SLM), Laser Engineered Net Shaping (LENS), and Laminated Object Manufacturing (LOM) etc. Results explain that SLM is not energy-efficient when it comes to manufacturing a product of small size as they lack versatility in size and they require high amount of powders. LENS on the other hand has feedback control due to which high quality and desired mechanical properties could be obtained. Electron Beam Melting has high scan speeds which can increase productivity and add to value of process. But these processes are not suitable for integration of sensors. Ultrasonic Consolidation and LOM are suitable for easy-to-machine materials such as aluminum and magnesium alloys as they start with metal sheets instead of powder.

Yadroitsev and Smurov [8] carried out a study on effects of processing parameters on surface morphology for SLM. Results stated that the properties of a product depend highly on each laser-melted track, each layer and strength of connections between them for which SLM is suitable. Results also found that changing the hatch distance modifies the geometric characteristics of tracks and hence surface morphology. In addition, to obtain a smooth surface,

the maximum shift distance should not exceed the average width of continuous track. In order to manufacture a one-pass thin wall, layer thickness and scanning speed are important in SLM.

Basu and Srinivasan et al. [9] studied the molten pool under steady state conditions for a flow pattern. In order to get the momentum equation for molten region they assumed top-hat heat flux distribution and used vorticity stream function method. Simulations resulted in stating the existence of two contra-rotating cells in flow pattern.

Basu and Date et al. [10] took an axisymmetric model and investigated the steady state and transient laser-melting problems. Gaussian distribution of heat flux was used, they analyzed the flow field and heat transfer by varying the beam powder density and beam radius of pure metals.

Ravindran and Srinivasan et al. [11] used the Galerkin Finite Element Method for laser melting analysis. An examination of the flow field and heat transfer in laser melting of an alloy using apparent capacity method was carried out. But this analysis of flow field and heat transfer was carried out for a typical range of surface tension values of steel.

Dharani and Majumdar et al. [12] analyzed the laser heating and melting of metals by developing a computational enthalpy-based model. A solution algorithm and a code estimate was developed by them to estimate temperature distribution, solid-liquid interface location and shape and size of molten metal.

Kasula and Majumdar et al. [13] studied the temperature and stress distribution and the size of molten metal formed due to Gaussian Laser Beam. A multidimensional transient heat and mass transfer equations were used to develop a mathematical model and a three-dimensional finite element model was used to obtain a numerical solution.

1.3 Objective

The objective of the research is aimed at developing an integrated design and manufacturing model to design and manufacture high performance gas flow-field or bipolar plates, typically used for fuel cell or electric battery storage using Selective Laser Melting (SLM)-based Additive Manufacturing (AM) process.

The main objective of this thesis is to design a computational model of Selective Laser Melting (SLM) process and have a clear understanding of this process by performing a complete micro structural analysis. A computational simulation model will be developed to characterize the SLM-AM process by laser melting of the selected section of the pre-deposited particles and forming different layers of desired part, so as to optimize the key parameters such as laser beam power, spot size, beam scan speed, scan spacing and particle size. Our efforts will be focused on analyzing effect of laser beam parameters and particles size on the densities of the powdered materials formed layer by layer. An iterative methodology will be utilized in controlling the parameters in order to achieve a targeted density of the fabricated parts.

2 SIMULATION MODEL FOR ADDITIVE MANUFACTURING

The additive manufacturing process or 3D printing (3DP) uses digital data obtained from a three-dimensional CAD solid model to create a physical object by building sequential layers on top of one another. The physical object is formed by sequentially printing a material particle/resin mixture in a layer while concurrently heating, melting, and cooling the deposited material. There has been a steady growth in the use of high power lasers in the additive manufacturing process. The additive manufacturing process is repeated layer-by-layer to obtain a desired 3D solid physical object. Additive Manufacturing concept involves a series of operations such as Material Development, Design, Modeling, Simulation, Material processing, Layering and Final Product. Additive Manufacturing materials that can be processed by this technique are Metallic materials namely the aluminum, titanium & stainless steel and their alloys; Polymeric materials, Ceramic materials and Organic materials. These feedstock materials can be in liquid form, powder form, filament form, as well as in strips.

ASTM F2792 – 12a Standard Terminology for Additive Manufacturing Technologies classifies it as into seven different processes.

2.1 Classification of Additive Manufacturing

2.1.1 Material Extrusion: Another name for Extrusion process is Fused Deposition Modeling. This process involves fusion of a Build material filament, which is deposited on the build platform with part supporters to create an exclusive part. Thermoplastic components can be easily manufactured by this process. In addition to build material, a spool of support material especially wax is added to the final part by extrusion nozzles.

2.1.2 Material Jetting: In Material Jetting process, the jetting head moves around the build tray jetting liquid polymer. Ultraviolet light is projected on to the model material to solidify it. This process is done layer by layer and is highly recommendable due to its high resolution. The main advantage of Material Jetting is that varieties of materials can be processed at once.

2.1.3 Binder Jetting: In this process the inkjet print head deposits liquid adhesives on to a bed of powder metal or polymer. Another layer of powder is deposited over this by the leveling rollers and the same process is repeated again. After multiple layer depositions, our final part is achieved.

2.1.4 Sheet Lamination: Also known as laminated object manufacturing (LOM). In the sheet lamination process layers of paper, plastic or metals are fused with resins using heat and pressure. This process has a set of mirrors over the platform. A computer controlled laser beam is incident on this set of mirrors, which reflects the beam on to the moving optic head and this would cut the sheet metal in desired shape and dimensions.

2.1.5 Vat Photo polymerization: Stereo lithography (SL) is a unique AM process that uses Stereo lithography Apparatus (SLA) to create a printing over the UV curable liquid. A UV light source passes through this liquid that converts the liquid plastic into solid objects.

2.1.6 Direct Energy Deposition: Direct Energy Deposition has different forms which can be attained by varying the heat sources and feedstock materials. Generally a Laser beam uses powder particles as feedstock, Electron beam uses metal wire and Arc plasma uses flat sheet strips.

2.1.7 Powder Bed Fusion: In this process a bed of powder (metal or polymer) is melted using a laser beam. Materials that can be processed through powder bed fusion are aluminum, titanium, stainless steel, nickel and nylon. These powder materials can be of different shapes and sizes. Acicular, flake, dendritic, rounded, porous, angular and spherical shapes are the commonly used ones.

Direct Metal Laser Sintering (DMLS): Direct Metal Laser Sintering is a high temperature additive manufacturing process where the layers of powdered metal are fused in a chamber of inert gas. This process builds up the part layer by layer at a time. After finishing a layer, the powder bed which is attached to the platform moves down, and automated rollers which are attached at both ends add a new layer of powdered particles, which are further sintered. DMLS is an AM process very similar to Selective Laser Sintering (SLS), but the main difference in DMLS technique is it is only used to process metal particles whereas SLS is used to process both metal and plastic process.

Selective Laser Sintering (SLS): SLS is a costly as well as time effective technology. In the selective laser sintering process the layer of powder materials are fused by the high energy lasers beams. After finishing a layer, the powder bed which is attached to the platform moves down, and automated rollers which are attached at both ends add a new layer of powdered particles. This process is also done in a layer by layer sequence. In the SLS process plastics, ceramics, glass and metal powders can be sintered.

Selective Laser Melting Process:

Selective Laser Melting is a process of 3D printing where a laser is used to melt the powder particles. These powder particles are melted to a particular dimension so that they create a fine layer with good surface finish on the top. Once this layer is finished, the powder bed moves a step down and the automated rollers which are connected on both sides move to the center spreading another layer of powder particles over the melted layer. Again this layer is melted and the process is being repeated till the final product is manufactured as per the required dimension. If an extremely dense and strong part has to be manufactured meeting the customer requirement, SLM is an ideal technique of all the Additive Manufacturing processes. The part strength and densities are very high because the powder material is melted completely creating a melt pool in which the powder particles are consolidated before cooling to form a solid structure with no void spaces between the particles, unless like the SLS process where the powder materials are just fused to create a new part. Void spaces between the powder particles remain the same reducing the density of the final part.

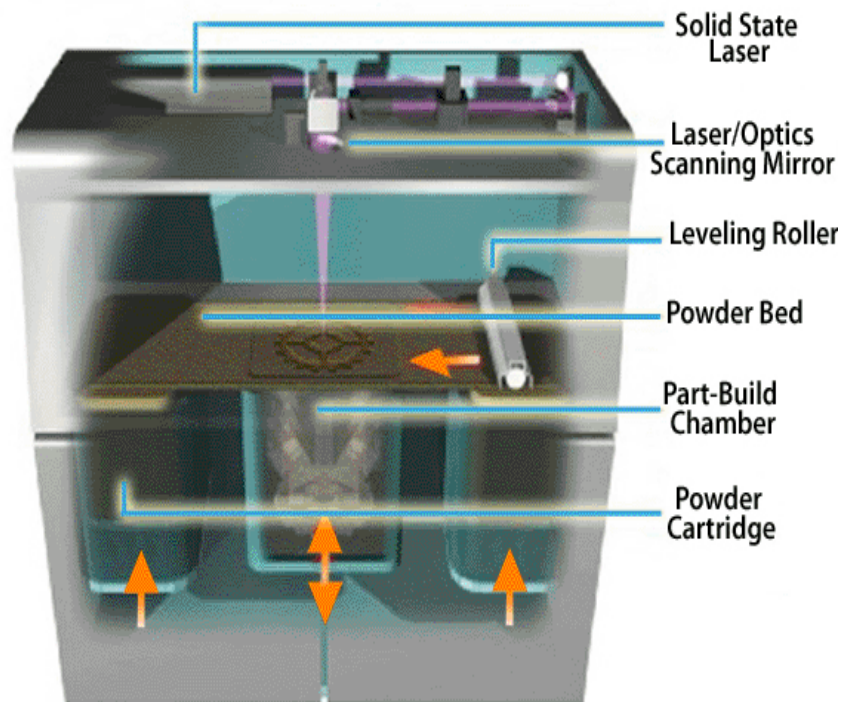


Figure 2-1 Selective laser melting process

Lasers are very precise and easily usable tool. The main principle of laser machining involves the incidence of high energy laser beam on a small area. The focal area depends on the diameter of the projected beam. The heat intensity from a laser beam can melt as well as vaporize the material on which it is projected. Lasers don't have many limitations and can be used extensively to perform various manufacturing operations like welding, drilling, cutting, hardening, surface finishing and so on. The use of high energy laser is an important aspect in SLM process. The main advantages of using a high energy laser are the precise control over

beam power, unidirectional property, high quality consistency and increased production with greater speed.

2.2 Description of the Physical Model to be fabricated

The main parameters to be considered for the SLM process are Powder Size, Shape and Material Properties: The materials that are generally used in the manufacturing process are Aluminum & its alloys, Titanium & its alloys, Stainless Steel. The work piece is assumed to be a stationary part with a layer of powder particles over it. The grain structure of the powder particles are rounded, flat, angular or spherical in shape. The top surface of the powder particles are subjected to laser beam and bottom surface is set to convective cooling. The surrounding temperature is considered as ambient.

2.2.1 Laser Beam Specifications:

A laser beam with constant or Gaussian power distribution is incident at the centre of the surface. As per the application and working power range, Nd-YAG laser, CO₂ laser and fiber laser are most commonly used.

Power Intensity: A laser beam with a constant power distribution is incident on the surface of the material. As the laser beam is incident, the heat is absorbed at the surface of the powder particles based on the absorptivity of the material. The energy formed evolves as heat and the powder particles get completely heated up as the heat is dissipated to the cooler regions inside the particle due to conduction. As more and more heat is dissipated, the temperature increases and the material start melting. As the local material temperature exceeds the melting

temperature of the material, there is phase change from solid to liquid. The region of this solid-liquid interface is established based on the melting temperature of the material. A significant amount of this heat is lost to the surrounding from the surface due to convection.

Scan speed: Scan speed is defined as the rate at which the laser spot moves on the surface of the work piece. There are mainly two types of scanning, traverse direction scanning and lengthwise direction scanning. In this project we deal with traverse direction scanning.

Scan speed = Distance travelled by the beam/ Time taken to melt the work piece

Hatch Space: Hatch Space is the distance between the centers of two adjacent metal particles.

2.3 Simulation Algorithmic Model:

Computational Algorithm for Selecting Laser Beam Parameters and Calculating Material Density

A sequence of operations to be followed to manufacture a part using Selective laser melting the SLM process.

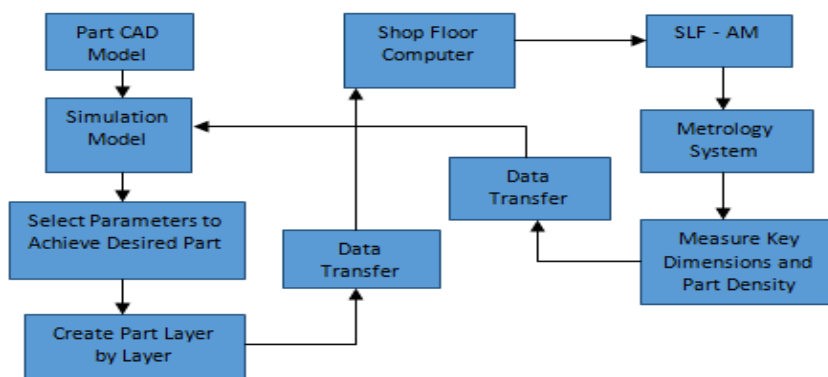


Figure 2-2 Set of operations to be performed to manufacture a part using SLM process

Computational Algorithm for Selecting Laser Beam Parameters and Calculating Material Density

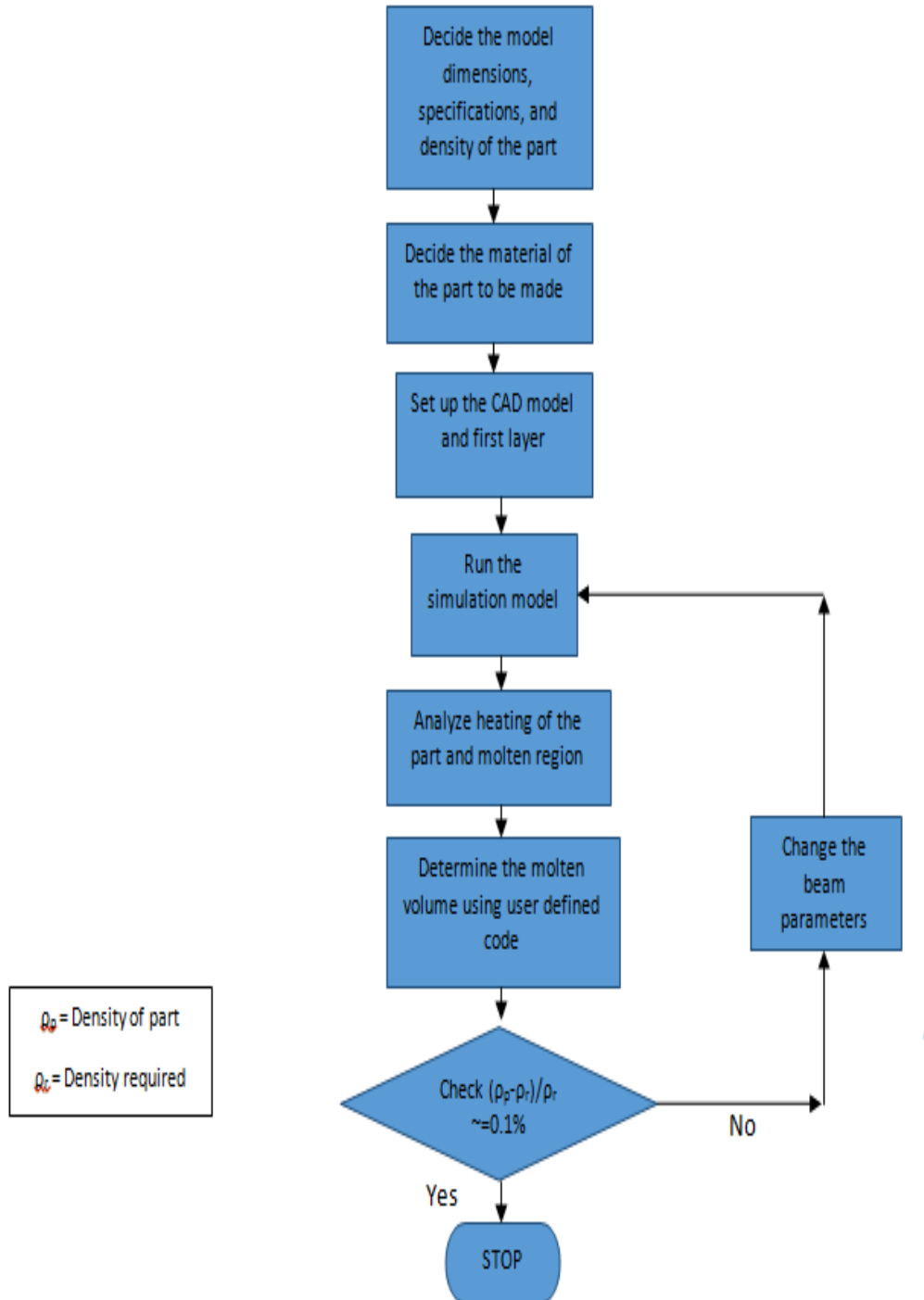
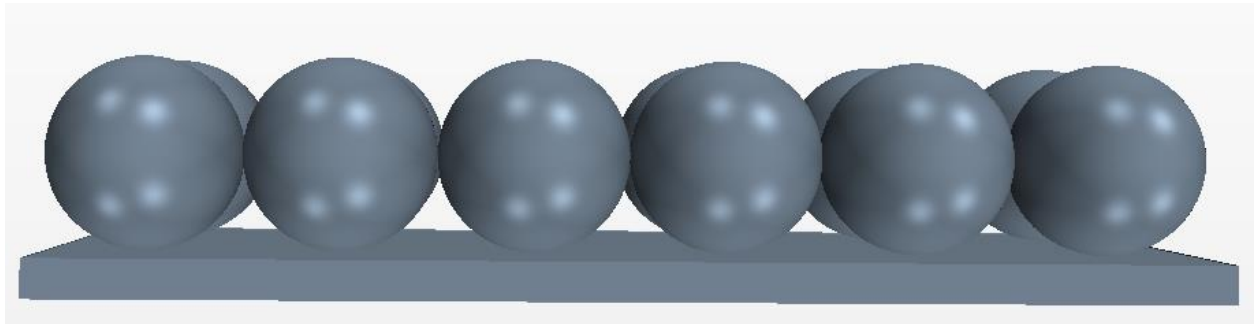
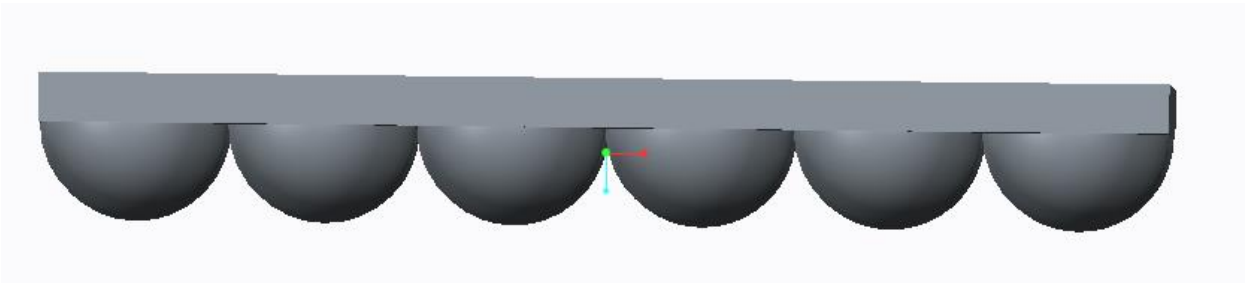


Figure 2-3 Computational algorithm for SL beam parameters & calculating material density

A series of operations to be followed in order to compute for the laser beam parameters as per the density requirement. In this project we are trying to calculate the density of a particular part by performing sensitivity analysis before that part is actually machined. Before performing the analysis, all the characteristics of the laser beam (laser beam intensity and laser beam diameter) and the material specifications (powder size) are decided beforehand. Set up the CAD model as per dimensions and material specifications. This model has a layer of powder particles over a rectangular beam of support.



(a)



(b)

Figure 2-4 Geometry of powder particles

After setting up the CAD model, a laser beam is projected on the powder particles with a certain beam intensity. Over time the powder particles start to melt. The beam characteristics are to be decided by taking in to consideration of the volume required to be melted. The laser beam has a particular scan speed and it melts the powder particles to such an extent that it fills the void spaces between the powder particles. In order to determine the volume required to fill the void spaces, a simple user defined code is scripted in VB, this will determine the volume required to be melted.

2.3.1 Design Analysis:

The work piece is a multi layered set of powder particles over a rectangular flat plate. All the powder particles are spherical in shape. The material used to manufacture the work piece is aluminum. The top surface of the powder particles are subjected to laser beam and bottom surface is set to convective cooling.

Once the model is set up, run the simulation model analyzing the volume to be melted. If this volume reaches the required volume as per the user define code, we take a note of all the parameters that are used and we calculate the density of the part.

After finishing a layer, a fresh layer of powder particles are sprayed on the processed layer and we repeat the same process for multiple layers.

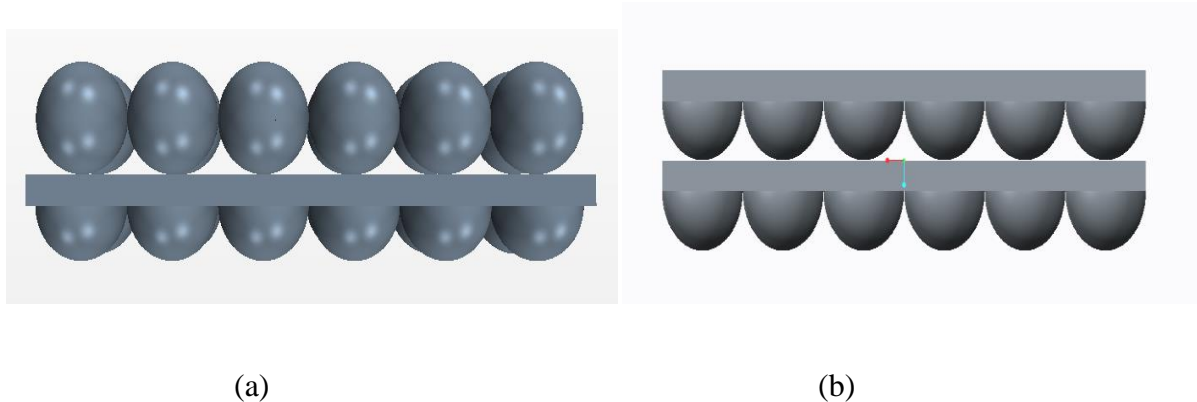


Figure 2-5 Geometric view of powder particles after spraying second layer and after melting it

After analyzing the parameters, the data is transferred to shop floor computer. This computer sends the manufacturing parameters such as beam intensity, beam diameter, scan speed and specifications of the powder particles for further set up. After receiving the data from the computer, a set up resembling the simulation set up is constructed. This set up is now processed and a final part is manufactured. This manufactured part is sent to metrological system to measure the dimensions as well as part densities. If this manufactured part exactly resembles the product of the simulated part, we end the process. If it doesn't, we transfer the data back to the simulation model, where the changes are made and this process is repeated over again till we reach the desired density. The main advantage of this process is no wastage of material and time & this process is very efficient.

2.4 Mathematical Formulation:

Laser Beam Characteristics: The laser beam intensity which strikes the surface of a work piece is expressed as I_o .

Beam Intensity, $I_o = P_o / A_o$

Where

$$A_o = \pi R_o^2$$

P_o = Laser beam power

I_o = laser beam intensity

R_o = laser beam spot radius.

Absorbed Heat Energy at the metal surface: $q_s'' = \alpha I_o$

2.5 Energy Equation:

2.5.1 Heat Transfer Model:

Following assumptions are made in deriving the heat transfer model: (1) The material is stationary but the laser is moving in traverse direction with a variable scan speed; (2) The constant heat transfer coefficient depicts the heat losses due to both convection and radiation; (3) The material is a solid part with a constant energy absorption at the surface and is invariable with temperature; (4) The net heat input to the material is the heat flux absorbed at the surface of the part with constant absorptivity; (5) The heat transfer inside the material is in all the X, Y and Z-directions; (6) Absorbed laser intensity is not high enough to cause evaporation of the aluminum part from solid state to vapor state; (7) The material is considered to be an isotropic substance; and 8) No effect of inert gas on intensity of the laser beam or surface absorptivity of the material.

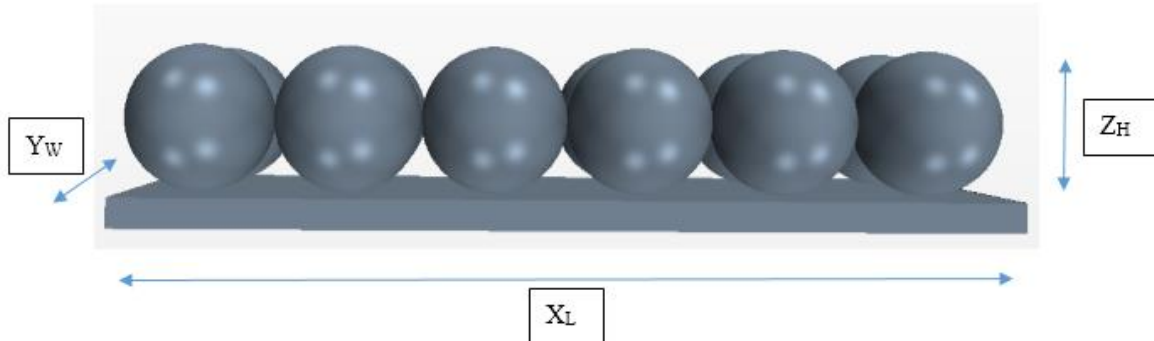


Figure 2-6 Geometric view (X axis, Y axis, Z axis)

Governing equation:

$$\frac{\partial}{\partial x}(K_x \frac{\partial T}{\partial x}) + \frac{\partial}{\partial y}(K_y \frac{\partial T}{\partial y}) + \frac{\partial}{\partial z}(K_z \frac{\partial T}{\partial z}) = \rho \cdot c_p \frac{\partial T}{\partial t}$$

Boundary conditions

At $Z=0$, $-d \leq X \leq d$ and $-d \leq Y \leq d$

$$\pm K_z \frac{\partial T}{\partial z} + \alpha I_0 = h_c (T - T_\infty)$$

$$\text{At } Z=2H, \quad -K_z \frac{\partial T}{\partial z} = h_c (T - T_\infty)$$

$$\text{At } X=-L \text{ and } X=L, \quad -K_x \frac{\partial T}{\partial x} = h_c (T - T_\infty)$$

$$\text{At } Y=-W \text{ \& } Y=W, \quad -K_y \frac{\partial T}{\partial y} = h_c (T - T_\infty)$$

At $Z=0$, $-L \leq X \leq -d$ and $d \leq y \leq L$, $-W \leq Y \leq -d$ and $d \leq y \leq W$

$$-K_z \frac{\partial T}{\partial z} = h_c (T - T_\infty)$$

2.5.2 Enthalpy Model:

The heat equation in terms of temperature is now converted to enthalpy for further validation.

The enthalpy model helps us to reduce the computational difficulties that are associated with the solid-liquid moving boundary condition of the current problem. So the enthalpy based governing equation is as follows

$$\frac{\partial}{\partial x} \left(A_x \frac{\partial h}{\partial x} \right) + \frac{\partial}{\partial y} \left(A_y \frac{\partial h}{\partial y} \right) + \frac{\partial}{\partial z} \left(A_z \frac{\partial h}{\partial z} \right) = \rho \cdot \frac{\partial h}{\partial t}$$

$$\text{Where } A_x = \frac{K_x}{c_p}, A_y = \frac{K_y}{c_p} \text{ and } A_z = \frac{K_z}{c_p}$$

Boundary conditions for the above enthalpy model are

At $Z=0$, $-d \leq X \leq d$ and $-d \leq Y \leq d$

$$\pm A_z \frac{\partial h}{\partial z} + \alpha I_0 = \frac{h_c}{c_p} (h - h_\infty)$$

$$\text{At } Z = 2H, \quad -A_z \frac{\partial h}{\partial z} = \frac{h_c}{c_p} \cdot (h - h_\infty)$$

$$\text{At } X = -L \text{ and } X = L \quad -A_x \frac{\partial h}{\partial x} = \frac{h_c}{c_p} \cdot (h - h_\infty)$$

$$\text{At } Y = -W \text{ \& } Y = W, \quad -A_y \frac{\partial h}{\partial y} = \frac{h_c}{c_p} \cdot (h - h_\infty)$$

At $Z=0$, $-L \leq X \leq -d$ and $d \leq Y \leq L$, $-W \leq Y \leq -d$ and $d \leq Y \leq W$

$$-A_z \frac{\partial h}{\partial z} = \frac{h_c}{c_p} \cdot (h - h_\infty)$$

Here,

d is the beam diameter,

h is the heat transfer coefficient,

C_p is the specific heat,

T is the temperature of the body

T_∞ is the temperature of surroundings.

$$h = \int_0^t C_p dT + \phi L$$

L is the latent heat of melting.

Considering an isothermal phase change for a pure metal, the molten volume and the density of the work piece is determined from the melting temperature T_{melt} of all the powder particles with sizes of 10, 30 and 50 microns which is estimated as

$$T_{\text{melt}} = \frac{h_{\text{melt}}}{C_p}$$

Where h_{melt} = enthalpy at T_{melt},

C_p=specific heat of the material.

3 COMPUTATIONAL MODEL

The application of computational techniques in Additive Manufacturing has become an important aspect because to its ability to simulate the dynamic model that would specify the volume to be melted to fill up the void spaces between the spherical region. The Computational Fluid Dynamic simulations also helps us to calculate all the physical quantities such as heat flux required, time taken to manufacture the final product and density of the final product. All these advanced Software available now in the market are a lot helpful to analyze any scalar function even in a miniature structure with a very colorful and distinct imaging. This would indeed help a lot of manufacturing companies to run a complete analysis of the final product and have a proper study on its physical quantities before manufacturing it. With the help of this CFD studies, one can go a step further ahead by visualizing the temperature distribution and change in enthalpy which are very difficult to estimate for a minute work piece using experimental techniques. In spite a lot of limitations and assumption made, the main objective of the study is to compute and characterize the formation of material layers using Selective Laser Melting (SLM) of Powder Bed Particles. Without CFD analysis or by any other convectional manufacturing process it is almost impossible to predict the intensity of the laser beam and melted volume required to fill up the void spaces between the spherical particles, but with CFD analysis it's very easily predictable. The CFD techniques are also very helpful

to analyze the temperature distribution at each section inside a minute spherical shaped aluminum powder particle [15].

Initial development of the simulation model was primarily restricted to a single sphere. Such a model can provide a close realistic analysis on heating and melting of spherical particles to establish the optimum operating parameters in terms of the particles size and laser beam parameters. In this project CFD simulations were carried out by considering the dimensions of the spherical particles as 50 μm , 30 μm , 10 μm in diameter. The heat flux required to melt the spherical particles depending on the application as well as density requirement is calculated by trial and error method. The heat transfer coefficients which depends on the particle size and fluid properties are also calculated. After setting up the model and running the simulations the total process time which is a very important aspect of SLM process could be calculated for each layer.

A 3-dimensional computational model as per the required dimensions of the work piece is modeled in PTC Creo. The required work piece is designed part by part and is then assembled. This final assembled model is imported to commercial CFD software called STAR CCM+, which uses control volume-based discretization method for solving Governing equations of heat flow patterns. The work piece is built layer by layer [15].

3.1 Computational Model

The application of computational techniques in Additive Manufacturing has become an important aspect because to its ability to simulate the dynamic model that would specify the volume to be melted to fill up the void spaces between the spherical region. The Computational Fluid Dynamic simulations also helps us to calculate all the physical quantities such as heat flux required, time taken to manufacture the final product and density of the final product. All these advanced Software available now in the market are a lot helpful to analyze any scalar function even in a miniature structure with a very colorful and distinct imaging. This would indeed help a lot of manufacturing companies to run a complete analysis of the final product and have a proper study on its physical quantities before manufacturing it. With the help of this CFD studies, one can go a step further ahead by visualizing the temperature distribution and change in enthalpy which are very difficult to estimate for a minute work piece using experimental techniques. In spite a lot of limitations and assumption made, the main objective of the study is to compute and characterize the formation of material layers using Selective Laser Melting (SLM) of Powder Bed Particles. Without CFD analysis or by any other convectional manufacturing process it is almost impossible to predict the intensity of the laser beam and melted volume required to fill up the void spaces between the spherical particles, but with CFD analysis it's very easily predictable. The CFD techniques are also very helpful to analyze the temperature distribution at each section inside a minute spherical shaped aluminum powder particle.

The first important step is the selection of material and parameters according to the required density. The main parameters to be considered are the particle size, scan speed, beam intensity

and beam diameter. The specifications, objectives and the impact of all these parameters has been theoretically explained in the chapter 2. In this chapter a complete practical validation of all the parameters will be explained with valid examples for better understanding.

3.2 Simulation Model:

Initial development of the simulation model was primarily restricted to a single layer of spheres. Such a model can provide a realistic analysis on heating and melting of spherical particles to establish the optimum operating parameters in terms of the particles size and laser beam parameters. In this project CFD simulations were carried out by considering the dimensions of the spherical particles as 50 μm , 30 μm , 10 μm in diameter. The heat flux required to melt the spherical particles depending on the application as well as density requirement is calculated by trial and error method. The heat transfer coefficients which depends on the particle size and fluid properties are also calculated. After setting up the model and running the simulations the total process time can be calculated for each layer.

A 3-dimensional computational model as per the required dimensions of the work piece is modeled in PTC Creo. The required work piece is designed part by part and is then assembled. This final assembled model is imported to commercial CFD software called STAR CCM+, which uses control volume-based discretization method for solving Governing equations of heat flow patterns. The work piece is built layer by layer.

The melting point for aluminum metal is 933.3 K. Calculate the volume of the powder particles that is melted (reached over 933.3K) by using enthalpy based model. Calculate the process

time for every beam projection. For further analysis over this, plot the graphs for Process Time VS Melted Volume and also Process time VS Maximum Temperature Reached.

3.3 Geometric Model:

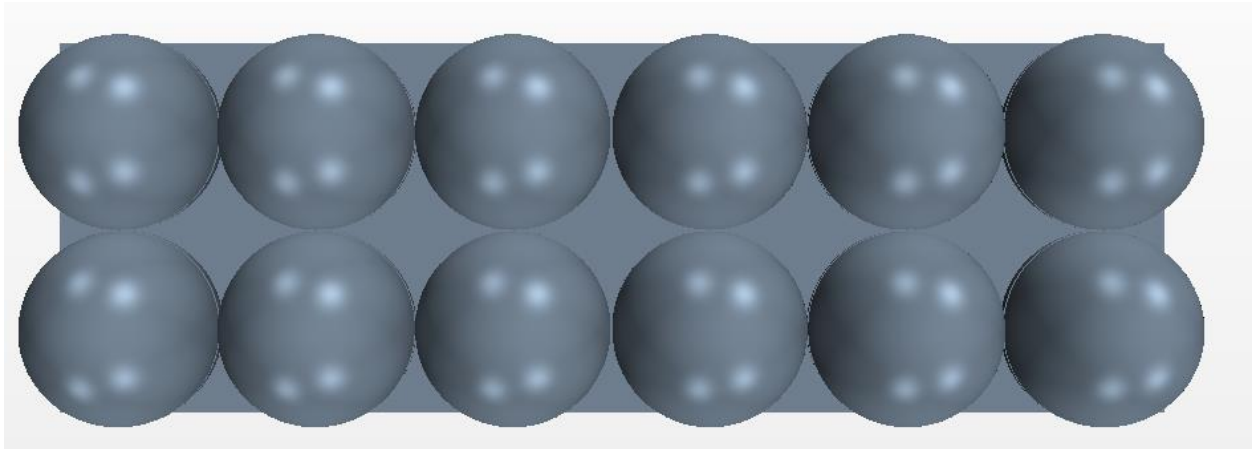
The geometric models have been designed using Creo Parametric 2.0 with dimensions of the spherical shaped powder particles 50 μm , 30 μm and 10 μm . The space between the centers of two adjacent particles is same as the diameter. So this clearly explains that the powder particles are aligned adjacent to each other. In this geometry the size of the powder particles was constructed based on the average size used in additive manufacturing. The material being selected to manufacture final work piece is aluminum metal. Each and every powder particle in the model is divided in to two halves. On one surface laser beam is incident and it is a inlet surface for the heat flux whereas the other half's surface is given a convective boundary. All these powder particles are aligned on a rectangular plate. The contact area between any two adjacent powder particles is very minimal and the contact area of these powder particles with the rectangular flat plate is also minimal. CFD analysis has been performed for three different cases 50 μm (Case 1), 30 μm (Case 2), 10 μm (Case 3) and is analyzed to observe the temperature distribution, enthalpy distribution and process time.

Let Particle size be = 50 microns

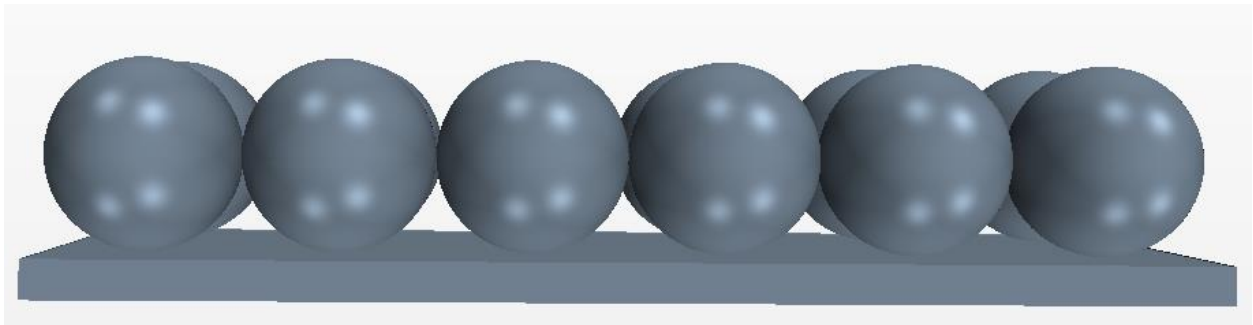
Radius of the spherical powder particles is 0.025mm

Geometry X axis -0.05 to 0.05; Y axis 0.025 to -0.275; Z axis -0.025 to 0.025

Origin is (0, 0, 0)



(a)



(b)

Figure 3-1 Powder particles – Layer 1

3.4 Mesh Generation:

In finite volume method it is very important to discretize the complete geometrical domain into number of cells using a particular grid size. The generated mesh mainly depends the size of grid size, type of grid and number of cells and faces generated. In order to resolve the complex changes in the scalar field functions such as temperature, enthalpy and so on, the grid size needs to be significantly small. This will increase the accuracy of the CFD Solution.

Star-CCM+ contains four different types of meshing models

- Polyhedral – Volumetric Polyhedral shaped cells

- Tetrahedral- The complete volume has tetrahedral shaped cells
- Prism layer- Orthogonal prismatic thin mesh

In this study the Prism layer mesher is selected as it provides a robust and Efficient method of producing a high quality mesh for both simple and complex structures. In general if your structure is a regular shaped part then prism layer is selected. Polyhedral is generally selected for irregular shapes.

For this model we select Prism layer mesher, Trimmer and Surface remesher. The curvature refinement is checked for both trimmer and surface remesher model, as the region where the heat flux given is curved for our geometry. So in general the

Prism Layer Mesher resolves the boundary layer,

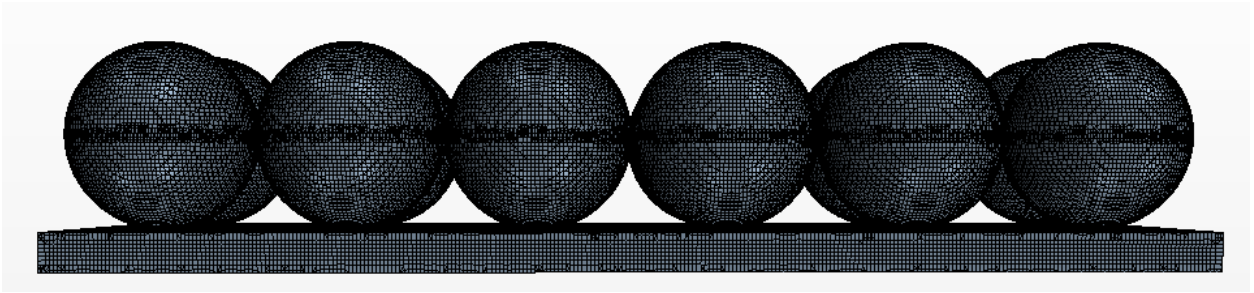
Trimmer trims the hexahedral volume meshes, and the

Surface Remesher tries to improve the triangulation of wrapped surface.

The mesh base size is 0.001mm



(a)



(b)

Figure 3-2 Mesh scene

Number of cells generated: 1094725

Number of faces generated: 3180160

Visual basic code

In order to analyze the density of the powdered material layer by layer and as well as for the final part, the key parameter to be calculated is the molten volume required to fill the void spaces. Here particle diameter is the main variable and the whole code runs on it. By using this user defined code, the physical parameters such as molten volume required to fill the void spaces, height of the cap (melted region) and width of the cap are calculated.

4 RESULTS AND DISCUSSION

A laser beam with constant power distribution is incident on the top surface of the powder particles. The laser beam used in this project is Nd-YAG laser. The working power range of this laser is about 150W-500W. The beam diameter is around 120microns. Its emission wavelength is 1064nm. When the top surface of the powder starts melting, it flows in to the void space between the spherical particles creating a rectangular plate.

Material	Aluminum
Melting temperature, T_m (K)	933.3
Latent heat of evaporation, h_{ig} (J/kg)	$3.88 \cdot 10^5$
Surface absorptivity, α_o	0.15
Density, ρ (kg/m ³)	2700
Thermal diffusivity, α (m ² /s)	$0.961 \cdot 10^{-4}$
Thermal conductivity, K (W/mk)	237
Laser power, P (W)	300
Beam radius, R (μ m)	120
Convective heat transfer coefficient, h (W/m ² k)	1185
Surrounding air temperature, T_a (K)	300

Figure 4-1 Table of thermo physical and laser operating properties.

4.1 Physics for the model:

After the mesh generation, physics should be assigned to the work piece for performing the thermal analysis. So the physical models are selected as per the physics of the work piece and boundary conditions. As the geometry of the final work piece is solid, the following physics are to be selected. They are

Three dimensional

Gradient

Solid - Aluminum

Implicit Unsteady

Constant Density

Segregated Solid Energy

After the physics is applied, we then assign the properties of aluminum to the physics and assign the physics to all the regions.

Calculation of density and scan speed of the laser beam are the main aspects.

Volume of the whole sphere is $65.4 \times 10^{-6} \text{ mm}^3$

As per the visual basic code

The volume required to be melted up is $9.4 \times 10^{-6} \text{ mm}^3$

So the shape of the volume after the melting is

In general when you consider the sphere, the melted part is the spherical cap of the sphere. In the figure it clearly explains that b is the height of the spherical cap where as a is the length of the chord of that spherical cap. With the user defined code,

For Radius of sphere is 0.025mm

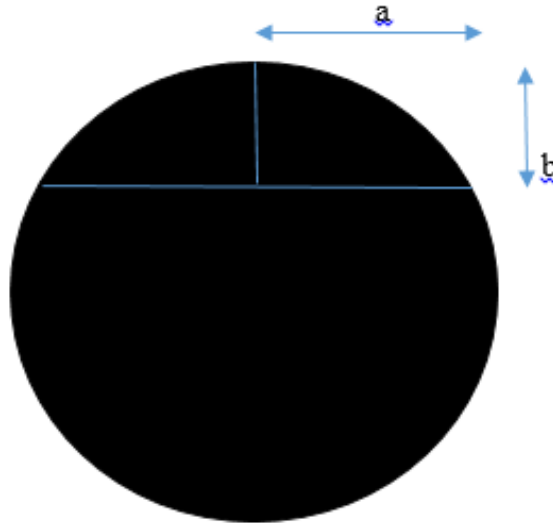


Figure 4-2 Symmetric view

a is 0.04249mm

b is 0.0119mm

Simple Analysis explains that as the required height of Spherical cap (Volume to be melted) is 0.0119mm, whereas the Z axis -0.025mm to 0.025mm

The sphere should be melted to the section -0.025 and -0.020mm completely and the sections -0.015 and -0.010 partially to meet the requirements.

4.2 Selection of beam intensity:

When the laser beam is incident on powder particles, the volume required to be melted is the volume to fill up the void spaces between the powder particles. There are three cases to be considered where we built the work piece layer by layer. For case1, where the melted volume

fills up only the void spaces on the upper layer. The final model is constrained to three layers and sensitivity analysis is performed after melting. So, the selection of power intensity of the laser beam required to melt the powder particles exactly as per the requirement is calculated by trial and error method. As the dimensions of the powder particles are minute, the heat flux required to melt them is marginally small. Selection of power intensity is a critical task, because the melted volume should exactly fill the void spaces. If a high intense laser beam is projected, this may result in over melting of the powder particles increasing the manufacturing time as well as solidifying time. It may even result in vaporizing the metal work piece. The melting point for aluminum metal is 933.3 K.

4.2.1 Determination of the Melted Volume for multiple Beam Powers

4.2.1.1 Intensities of the Laser Beam

Initially let the heat flux incident on the beam be $5 \cdot 10^8 \text{ W/m}^2$

Beam Intensity: $5 \cdot 10^8 \text{ W/m}^2$

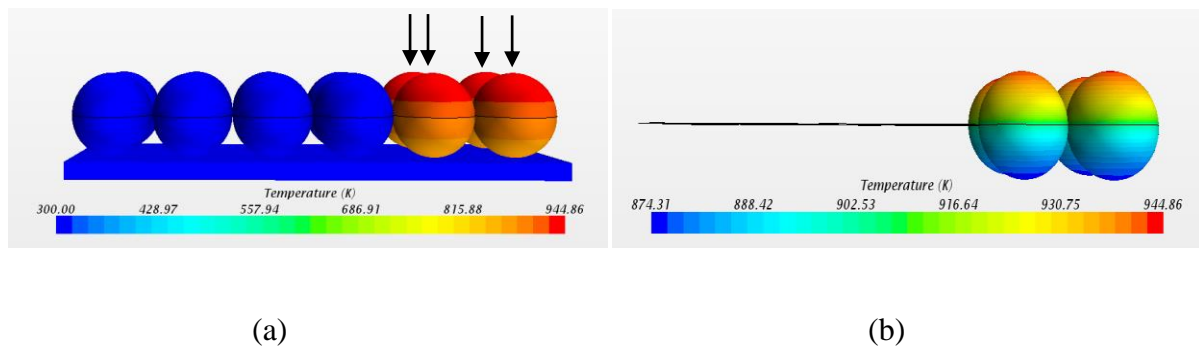


Figure 4-3 Temperature distribution of powder particles at beam intensity $5 \cdot 10^8 \text{ W/m}^2$

Now for the calculation of volume of the melted region, point probes are created all over the powder particles where the beam is incident on. Distance between each consecutive probe point is 0.00005mm and these point probes are created section wise filling the whole volume of the powder particles.

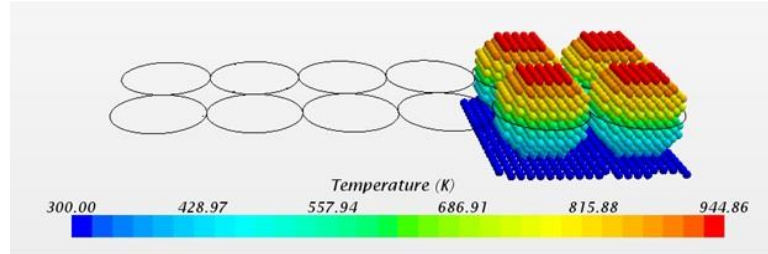
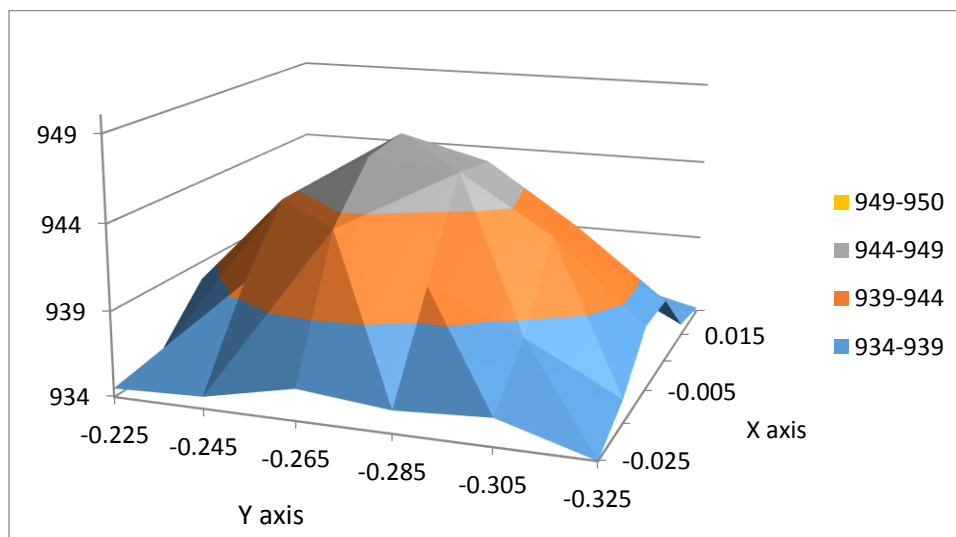


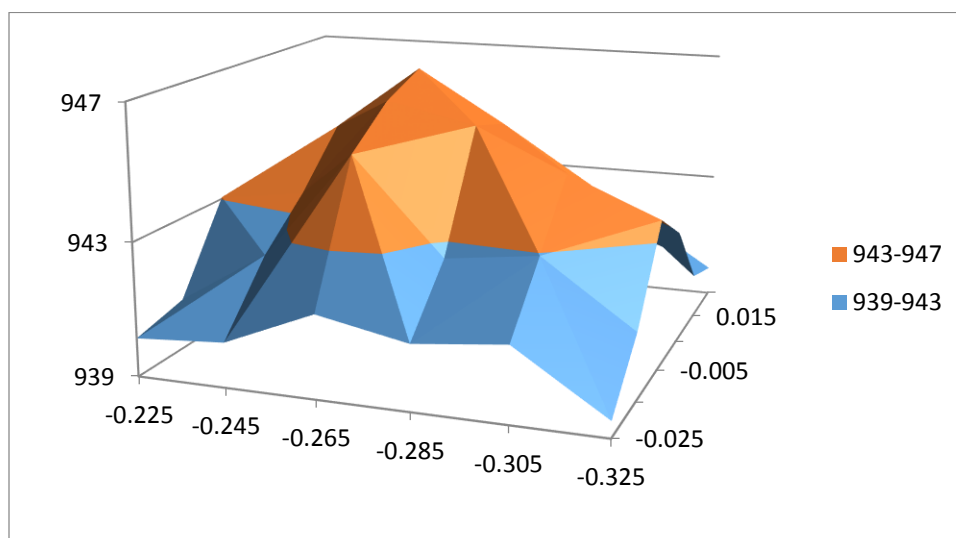
Figure 4-4 Point probes-Temperature distribution of powder particles at intensity $5 \cdot 10^8$ W/m²

In order to identify the time required to melt a selected volume of material for the given beam intensity, temperature variations in the particles are monitored and compared with the melting temperature to identify the molten volume. In figure 4.1 variation of material temperature in small temperature band (5 C) are demonstrated in a 3-D plot that displays the exact molten volume. As the height of the particle is represented by Z axis which varies from $Z = -0.025$ mm to $Z = 0.025$ mm, the plots are plotted for multiple sections: Section (1) $Z = -0.025$ mm to -0.020 mm; Section (2) $Z = -0.020$ mm to -0.015 mm, Section (3) $Z = -0.015$ mm to, -0.010 mm, Section (4) $Z = -0.010$ mm to, -0.005 mm and Section (5) $Z = -0.005$ mm to 0 mm.

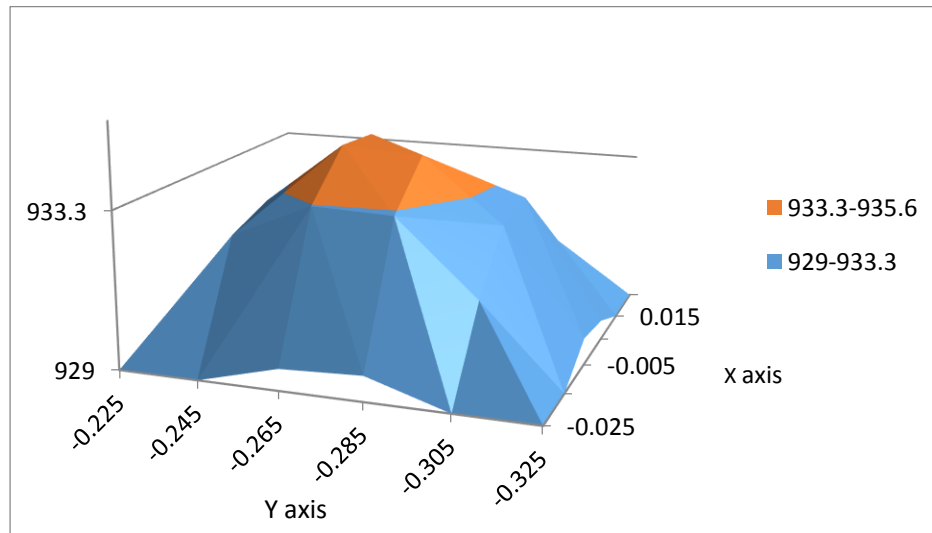
From the Figure 4-2, it is clearly visible that the Section (1) at -0.025 mm is completely melted as the temperature of all the points in that section are well over 933.3 k. So the plots are taken at other sections.



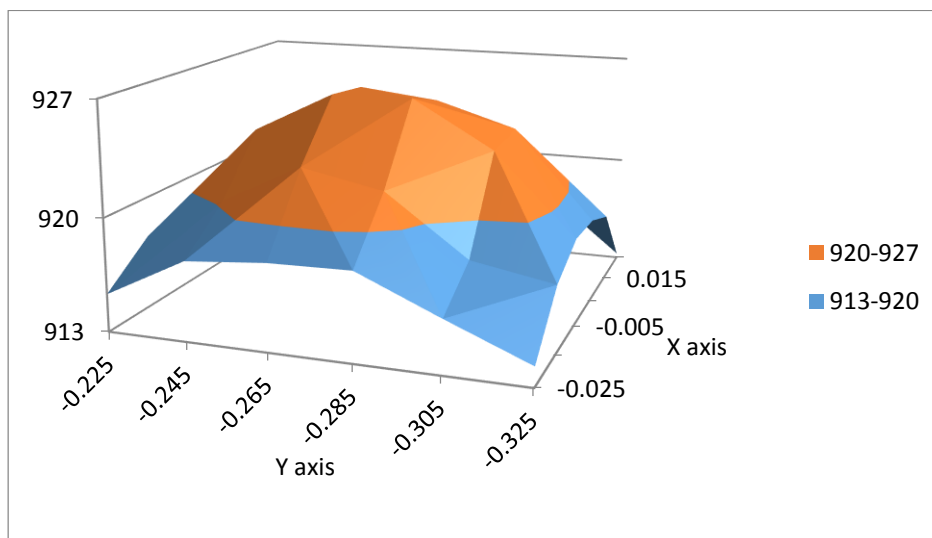
(a) Section - 2



(b) Section - 3



(c) Section - 4



(d) Section - 5

Figure 4-5 Plots at section 2, 3, 4 and 5 determining temperature distribution

So by the graphs it is clearly indicated that the sections at -0.025mm, -0.020mm are completely melted, whereas the section -0.015 is partially melted and the section at -0.01mm is completely solid.

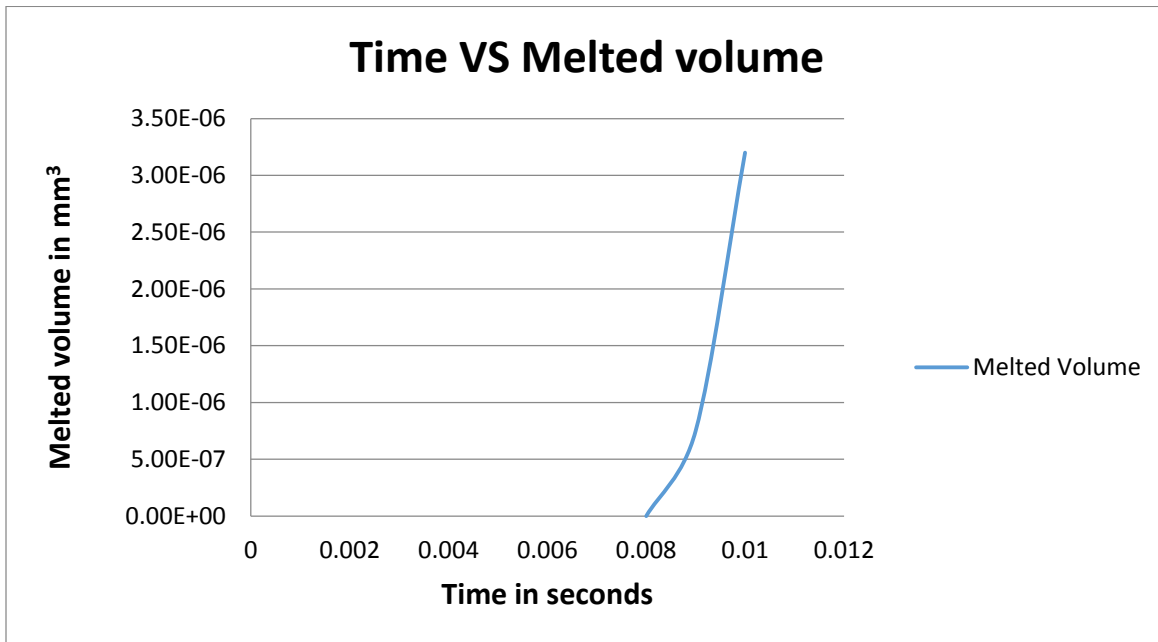


Figure 4-6 Time Vs Melted volume

Here the melted volume is $3.2 \times 10^{-6} \text{mm}^3$, which is less than the required melted volume to fill up the void spaces in the upper layer.

As the heat flux 5×10^8 was not adequate to melt the powder particles to fill up the void spaces, we increase the heat flux to $7.5 \times 10^8 \text{W/m}^2$

Beam Intensity: $7.5 \times 10^8 \text{ W/m}^2$

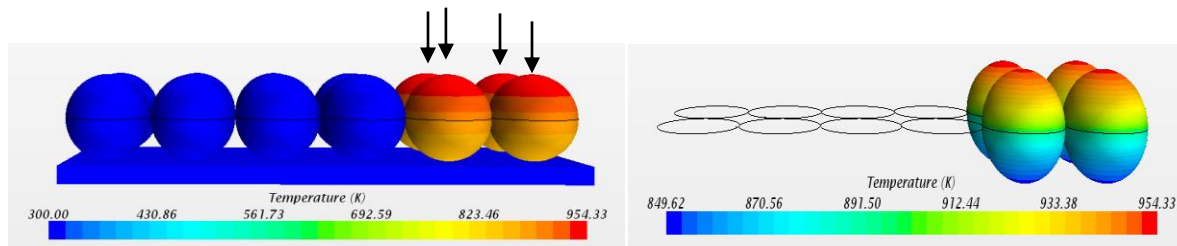


Figure 4-7 Temperature distribution of powder particles at beam intensity $7.5 \times 10^8 \text{ W/m}^2$

Now for the calculation of volume of the melted region, point probes are created all over the powder particles where the beam is incident on. Distance between each consecutive probe point is 0.00005mm and these point probes are created section wise filling the whole volume of the powder particles.

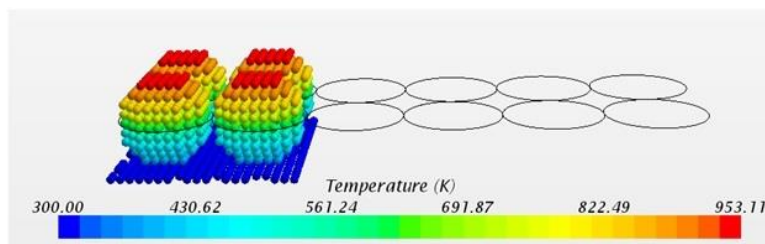
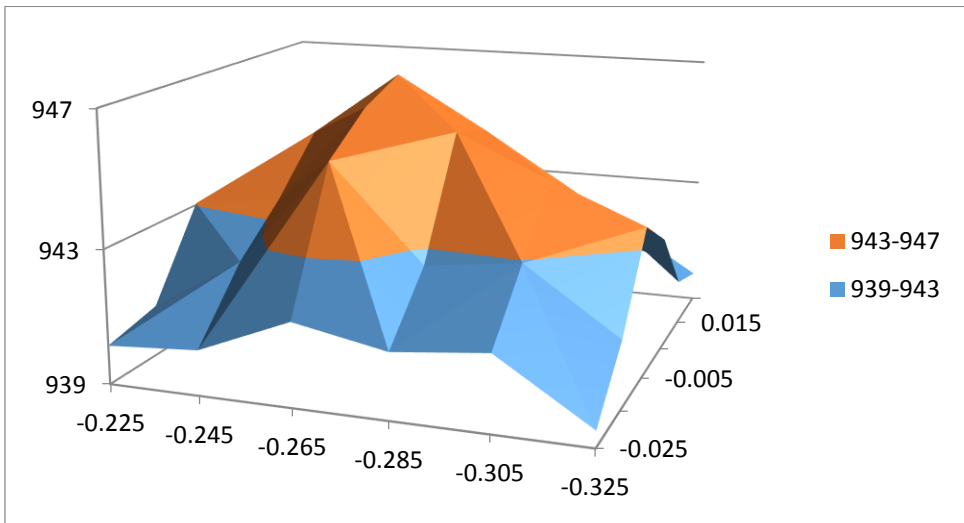


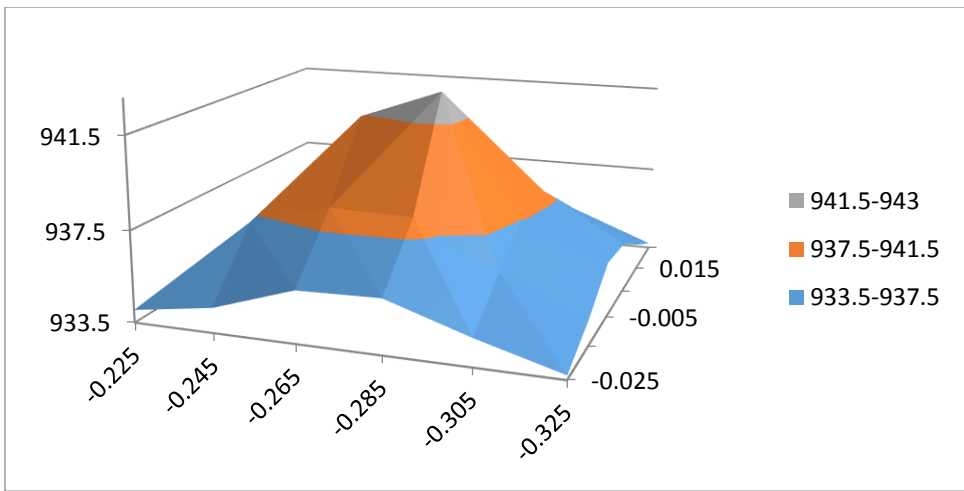
Figure 4-8 Point probes - Temperature distribution for point probe

To calculate the exact molten volume, plot a 3d graph that shows the temperature distribution at every section. As the height of the particle is represented by Z axis which varies from -0.025mm to 0.025mm, the plots are plotted for section of points at -0.025mm, -0.020mm, -0.015mm, -0.010mm, -0.005mm are per requirement.

From the Figure 2, it is clearly visible that the section at -0.025mm is completely melted as the temperature of all the points in that section are well over 933.3k. So the plots are taken at Section 2 and Section 3.



(a) Section 2



(b) Section 3

Figure 4-9 Plots at section 2, 3 determining temperature distribution

So by the graphs it is clearly indicated that the Sections 1 & 2 (at -0.025mm, -0.020mm) are completely melted, whereas the Section 3 (at -0.015) is partially melted and the Section 4 & Section 5 (at -0.01mm, -0.005mm) are completely solid.

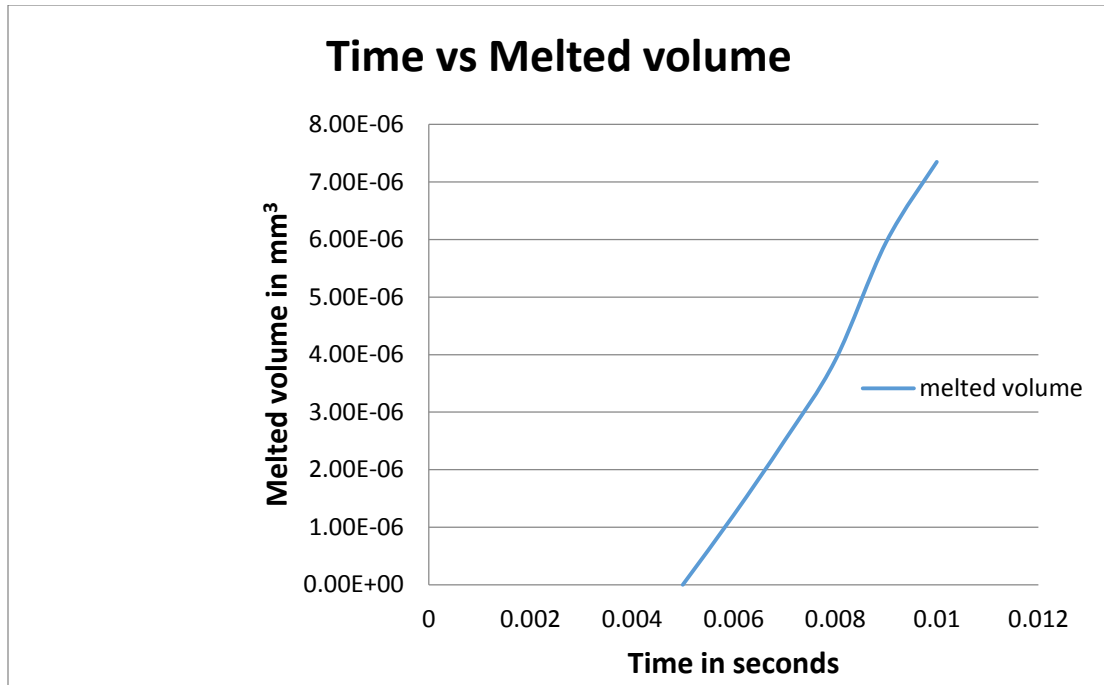


Figure 4-10 Melted volume VS Time

Here the melted volume is $7.5 \times 10^{-6} \text{mm}^3$, which is less than the required melted volume to fill the void spaces in the upper layer.

Further increase the heat flux to $1.0 \times 10^9 \text{W/m}^2$

Consider a single layer of powder particles and the laser beam is at position 1.

Layer 1 & Beam Position 1

Initially at time 0.002 seconds

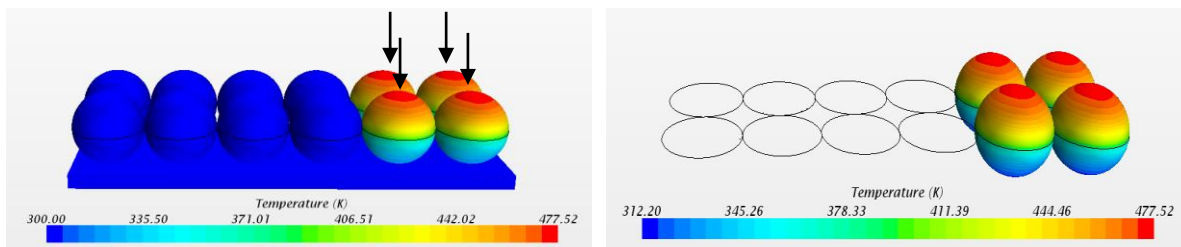


Figure 4-11 Temperature distribution for layer 1 & beam position 1 at time 0.002s

When the beam is incident on the powder particles, the temperature rises steadily with respect to time.

After 0.005 seconds of laser beam exposure

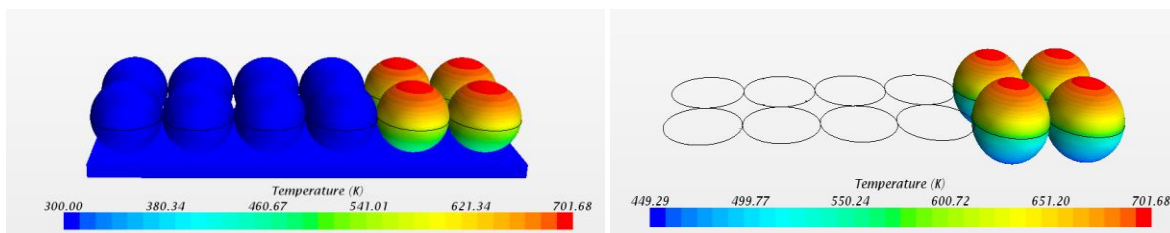


Figure 4-12 Temperature distribution for layer 1 & beam position 1 at time 0.005s

After 0.011 seconds

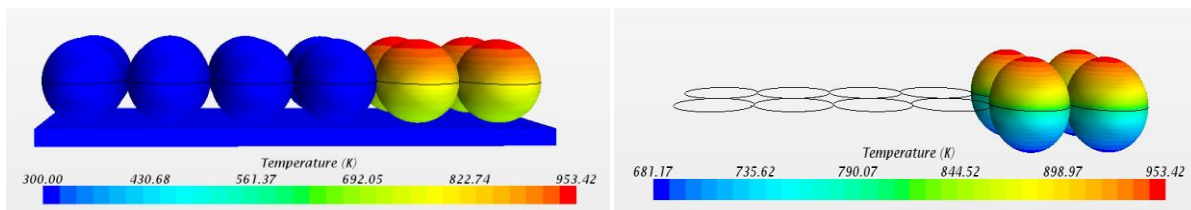


Figure 4-13 Temperature distribution for layer 1 & beam position 1 at time 0.011s

Now for the calculation of volume of the melted region, point probes are created all over the powder particles where the beam is incident on. Distance between each consecutive probe point is 0.00005mm and these point probes are created section wise filling the whole volume of the powder particles.

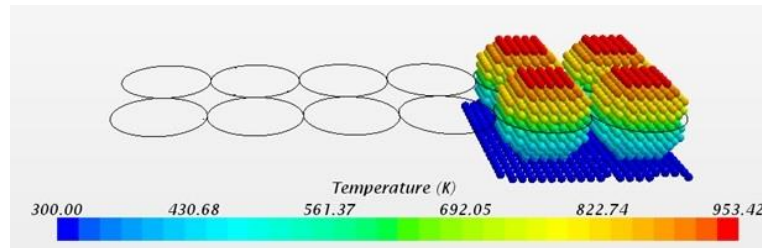


Figure 4-14 Point probes - Temperature distribution for layer 1 & beam position 1

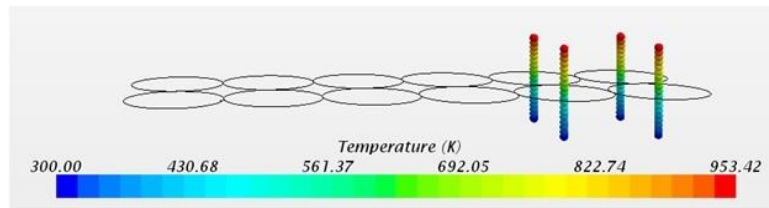
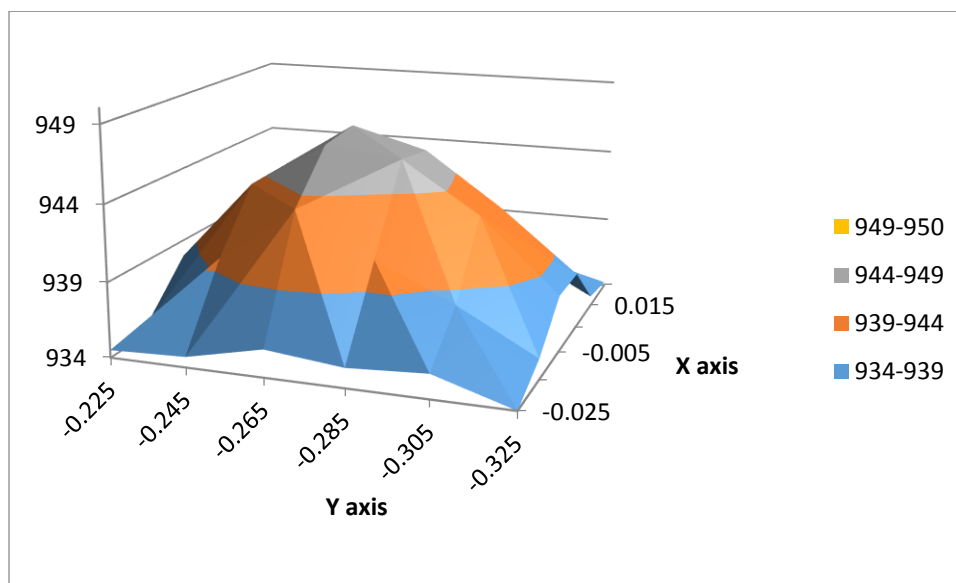


Figure 4-15 Point probes at the center of particles for layer 1 beam position 1

The process time for the completion of melting process is 0.011sec

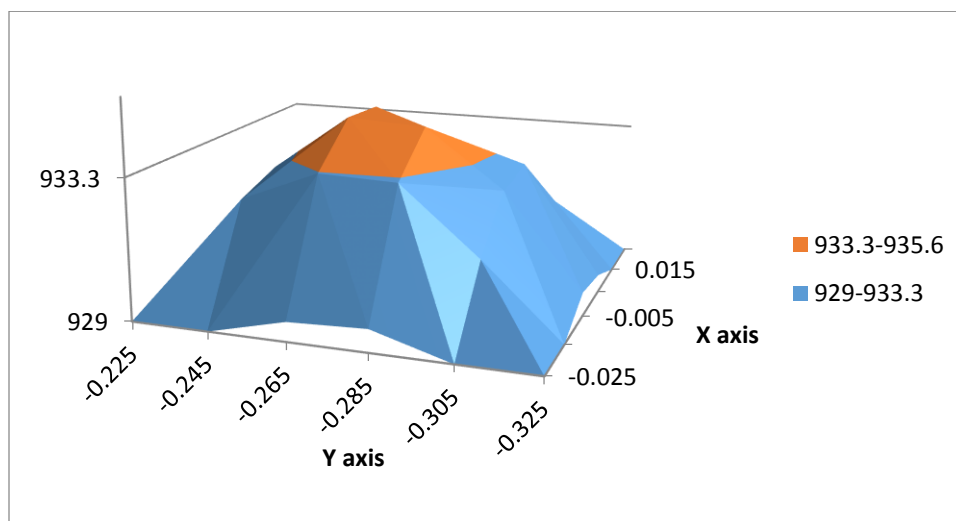
From the Figure 2, it is clearly visible that the section at -0.025mm is completely melted as the temperature of all the points in that section are well over 933.3k. So the plots are taken at Section 2, 3, 4 & 5.

Z -0.020mm



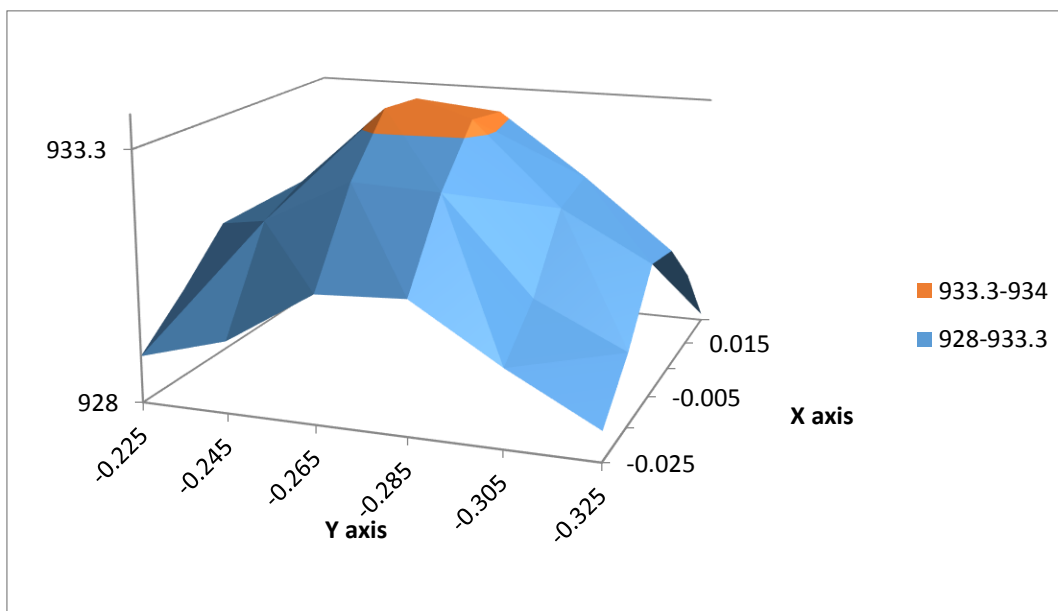
(a) Section 2

Z -0.015mm



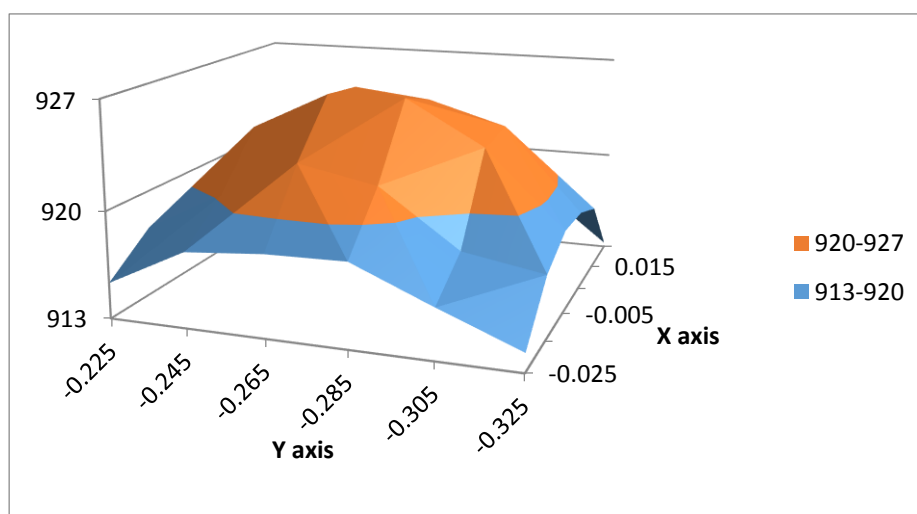
(b) Section 3

Z -0.01mm



(c) Section 4

Z -0.005mm



(d) Section 5

Figure 4-16 Plots at section 2, 3, 4 and 5 determining temperature distribution

So by the graphs it is clearly indicated that the sections at Section 1 & 2 are completely melted, whereas the Section 3 & 4 is partially melted and the Section 5 is completely solid.

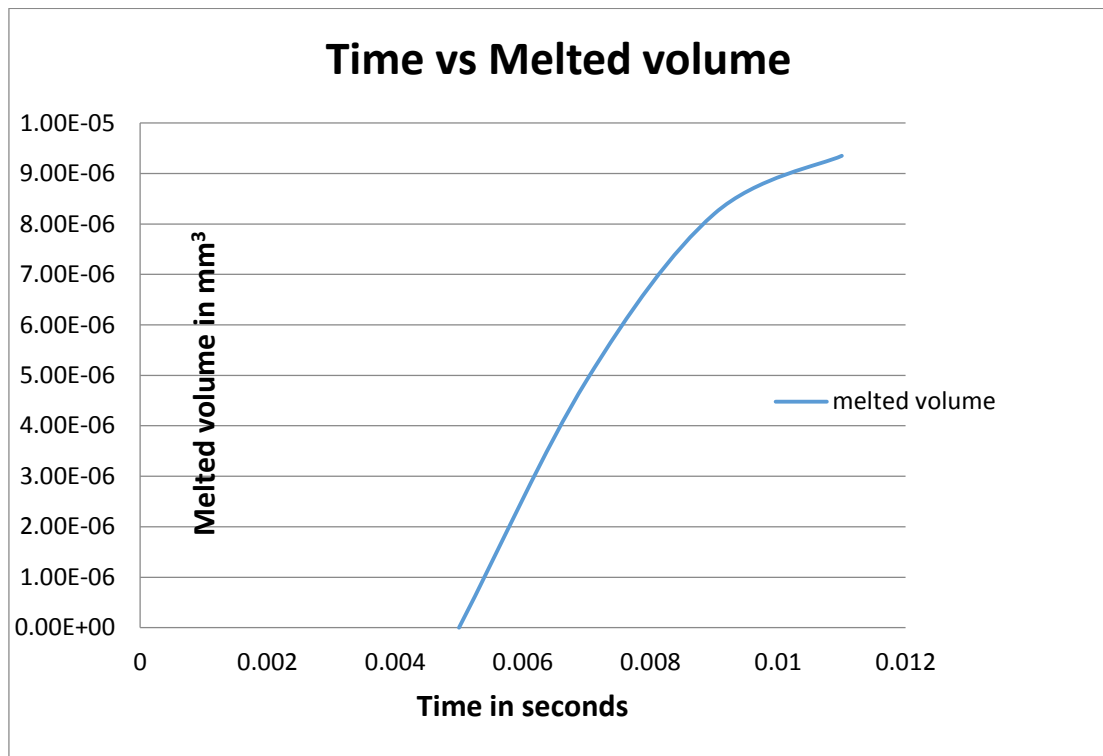


Figure 4-17 Time Vs Melted volume

Here the melted volume is $9.38 \times 10^{-6} \text{ mm}^3$, which is the required melted volume to fill up the void spaces in the upper layer. So we set up the beam power to $1 \times 10^9 \text{ W/m}^2$.

As the melted volume of the powder particles exactly fills up the void spaces, the laser beam is set to this intensity.

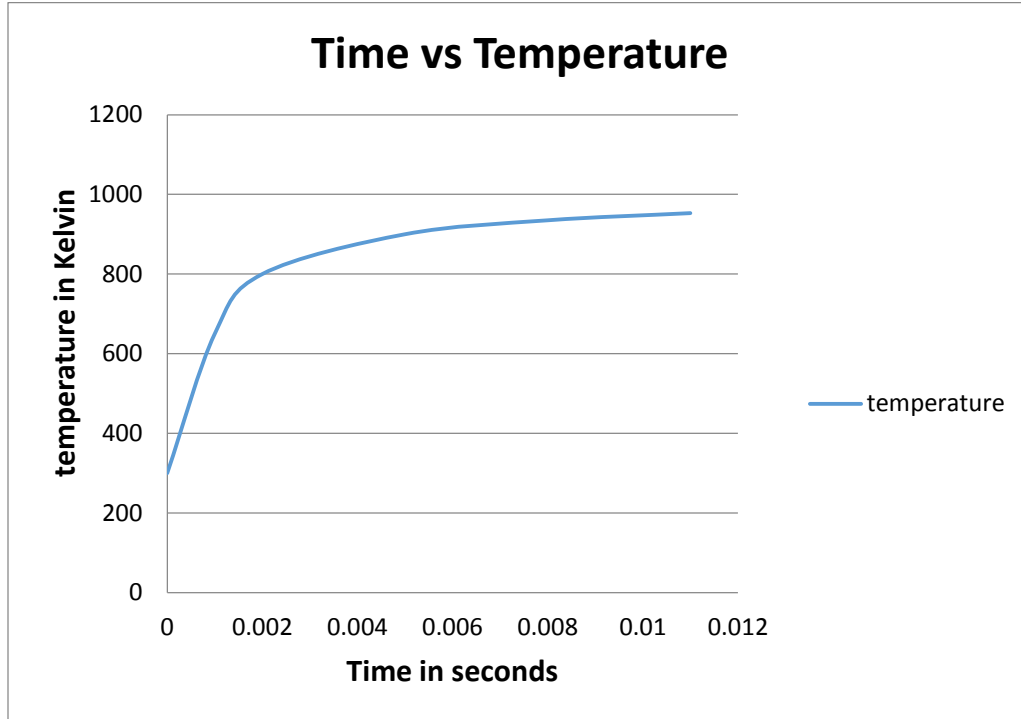


Figure 4-18 Time VS Temperature plot

4.3 Effects of parameters on part density:

4.3.1 Mesh Refinement study

Mesh refinement is a prominent condition in the simulation process for better results. In this case, the temperature distribution across the sectional planes of the powder particles can be stabilized by using better mesh models and base size. In general the mesh models and the base size is chosen, depending on the geometry of the work piece. In some cases we require a finer mesh to get better results, in some cases it's not required.

Case 1 - For base size 0.0005mm

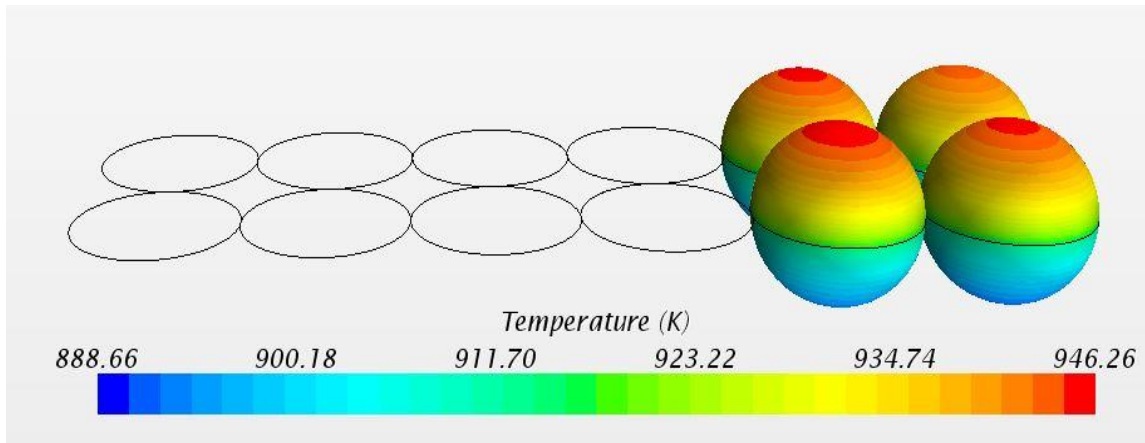


Figure 4-19 Temperature scene representing temperature distribution for powder particles

Even though the intensity of the laser beam incident on all the powder particles is constant, the temperature distribution throughout particles is not the same. There are a few factors that may be responsible for this irregular temperature distribution, namely the meshing models, mesh base size, simulation cycle and relaxation factor. Initially the base size was 0.0005mm with V simulation cycle and 0.99 relaxation factor. But all these factors resulted in an irregular temperature distribution among the powder particles. So the base size was increased to 0.001mm with Prism layer mesher, Surface Remesher and Trimmer as meshing models, the simulation cycle was changed to W and the relaxation factor to 0.97. All these changes resulted in a variation in temperature distribution.

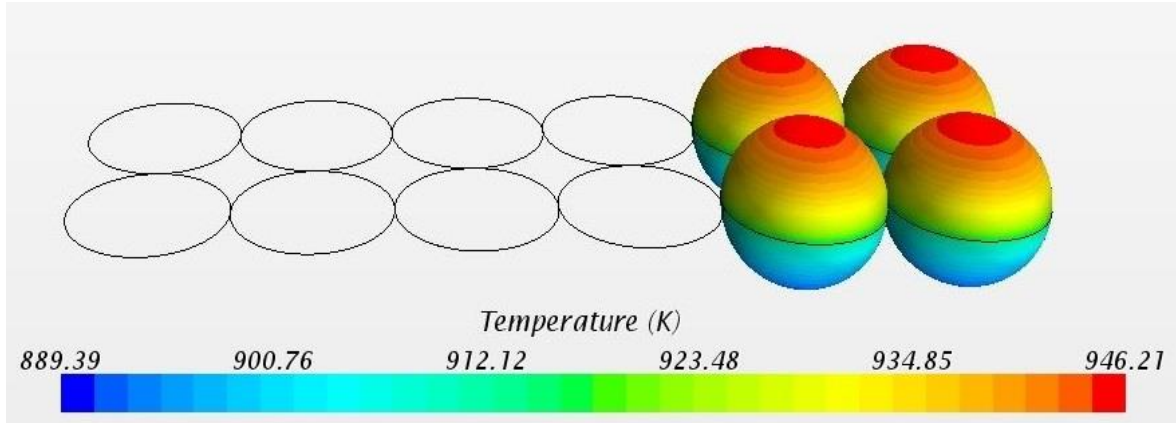


Figure 4-20 Temperature scene representing temperature distribution for powder particles

The difference in the temperature scenes clearly explain the variation in temperature distribution of powder particles. These changes in the simulation model creates a regular temperature scene providing better results for further analysis. So, this model clearly explains the importance of mesh refinement resulting in more accurate analysis.

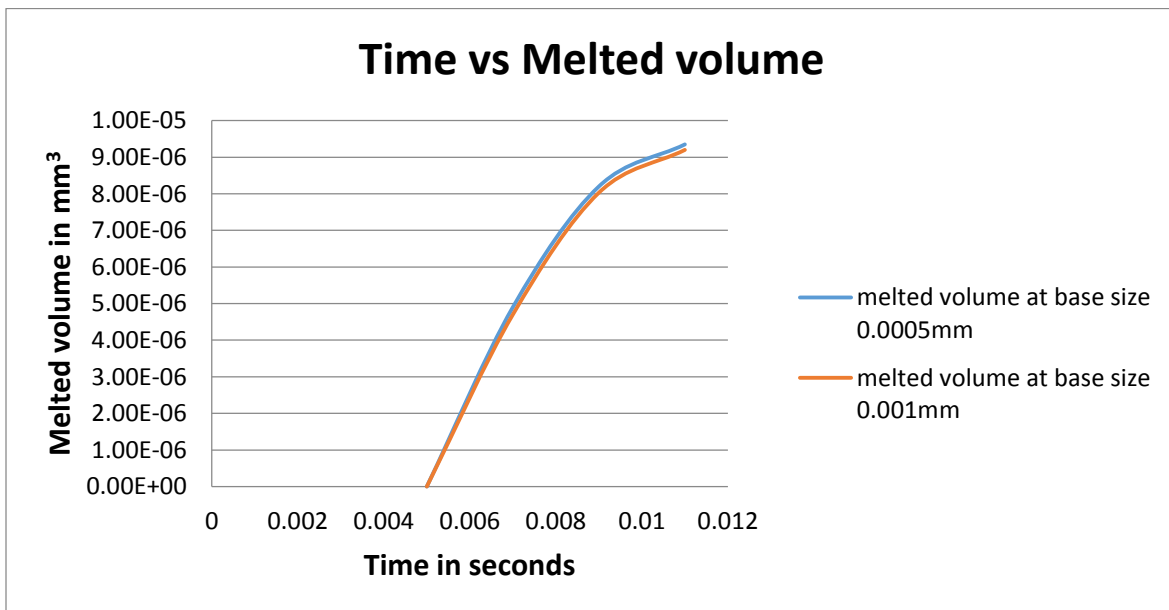


Figure 4-21 Time VS Melted volume

On inspection, it's clearly visible that the graph plotted with the base size 0.001mm has a sharp curve and the graph with a base size 0.0005mm has a very smooth curve. Here the change is within the base size which modifies the result to a very minute variance which would indeed help to analyze any issue.

4.4 Temperature Model Results

4.4.1 Effect of particle size – 50microns:

Now the beam is shifted to next set of powder particles.

Laser 1 - Beam position 2

Initially after 0.002 seconds

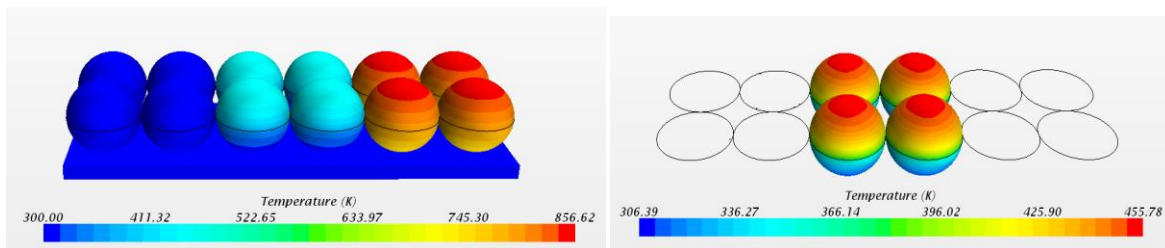


Figure 4-22 Temperature distribution for layer 1 beam position 2 at 0.002 sec

Time 0.005 seconds

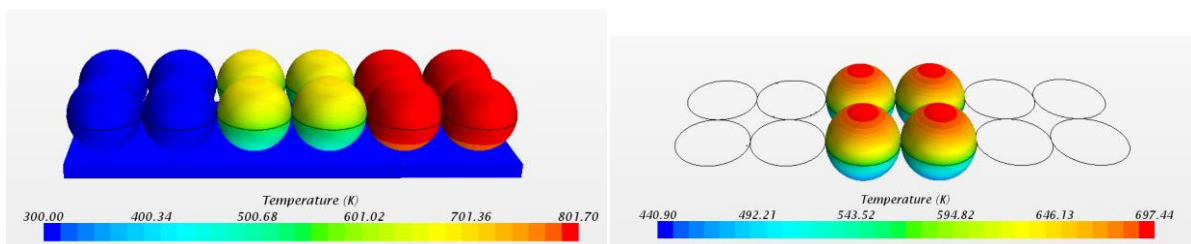


Figure 4-23 Temperature distribution for layer 1 beam position 2 at 0.005 sec

Time 0.011 seconds

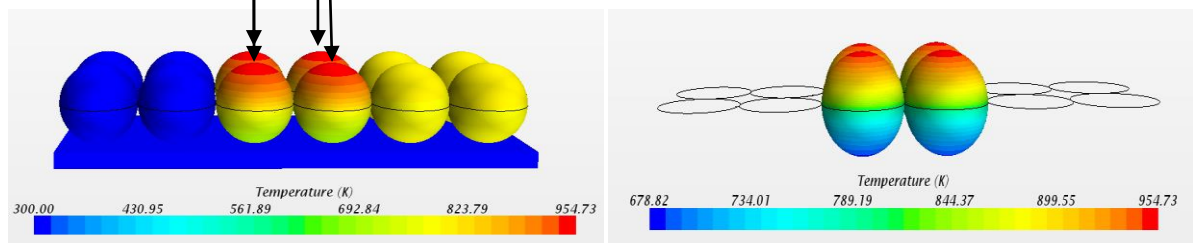


Figure 4-24 Temperature distribution for layer 1 beam position 2 at 0.011 sec

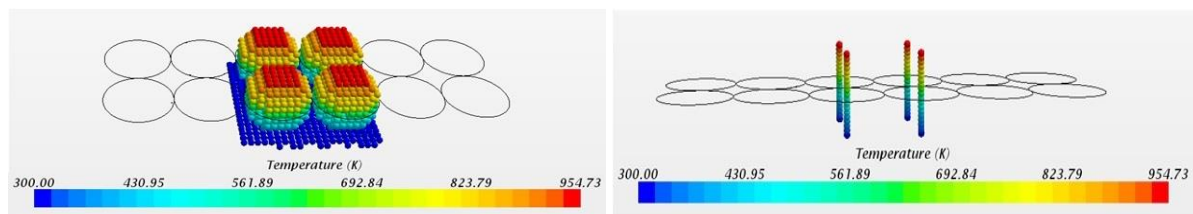


Figure 4-25 Point probes - Temperature distribution for layer 1 beam position 2

The process time for the laser beam to melt up the required volume is 0.011 seconds.

So the total process time will be $0.011+0.011=0.022\text{sec}$

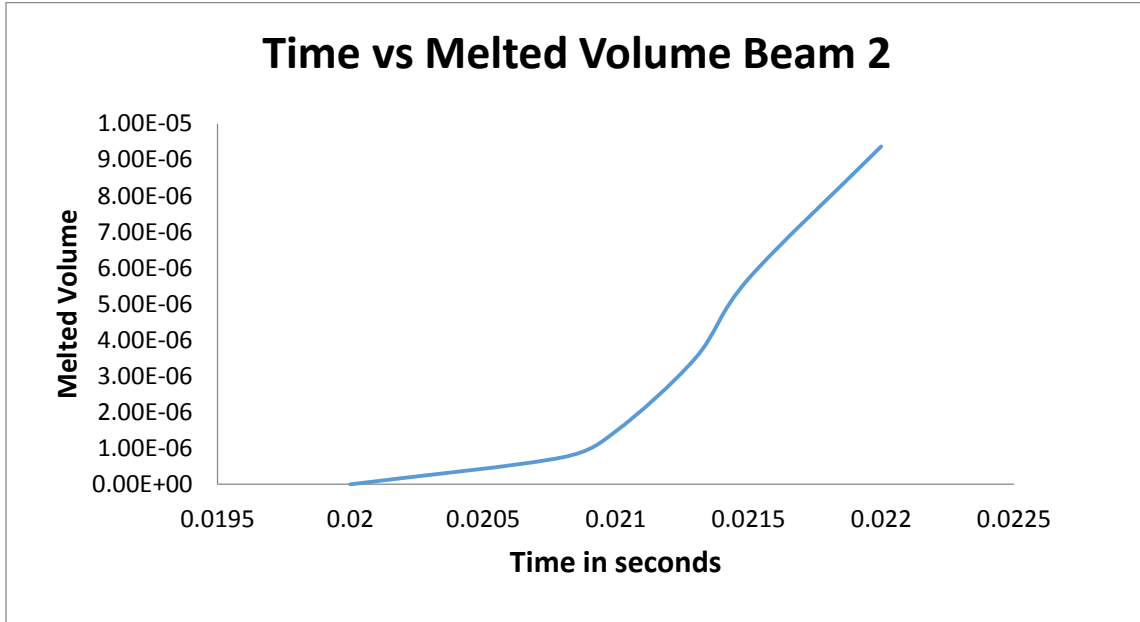


Figure 4-26 Time Vs Melted volume

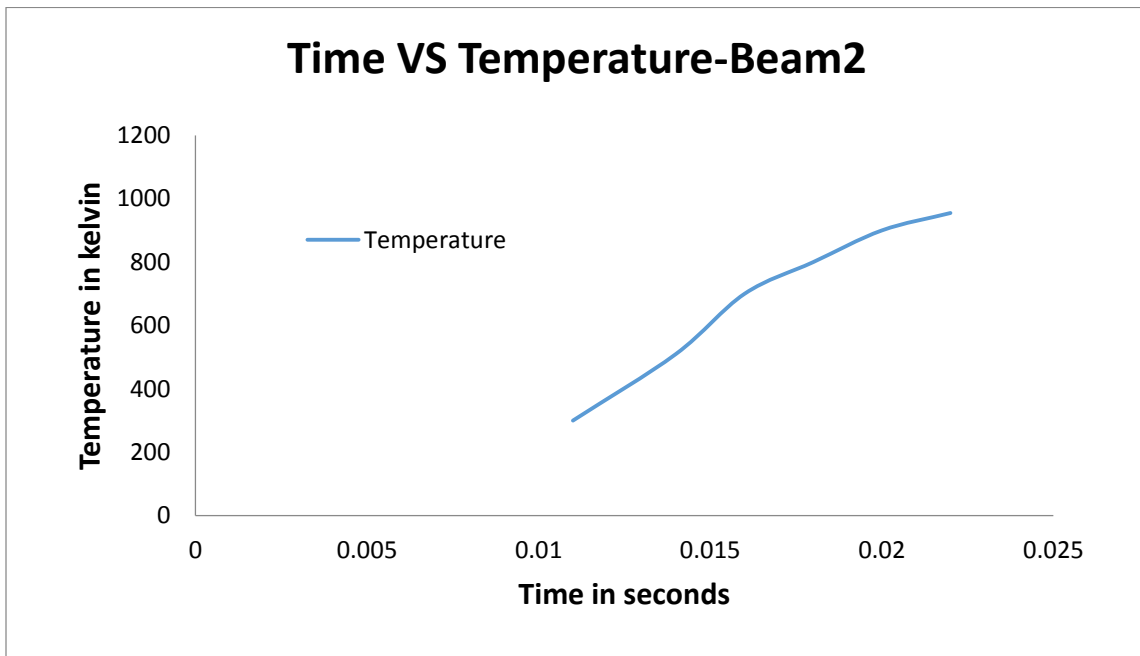


Figure 4-27 Process time Vs Highest temperature

Layer 1 – Beam position 3

Initially at Time 0.002 seconds

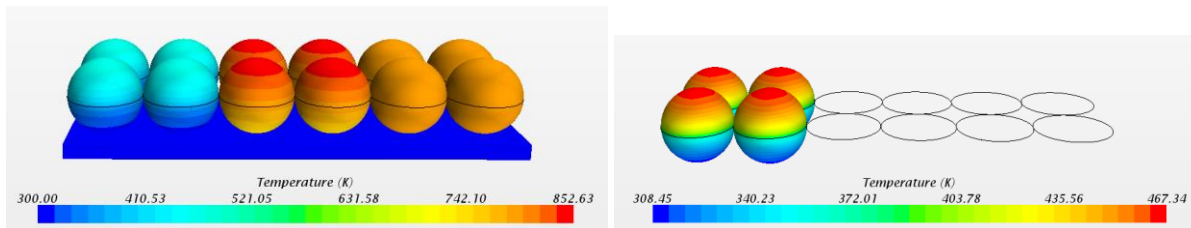


Figure 4-28 Initial temperature distribution for layer 1 beam position 3 at 0.002 sec

At time 0.005 seconds

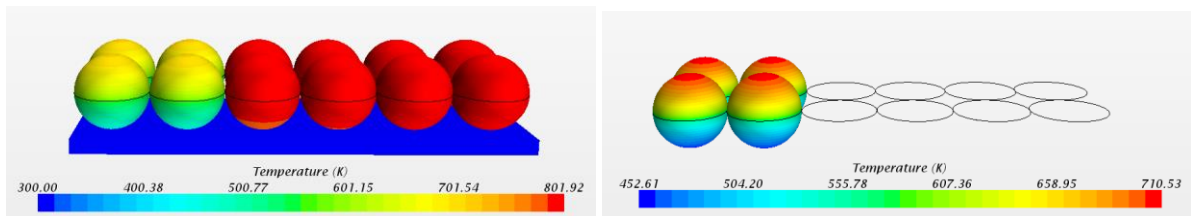


Figure 4-29 Temperature distribution for layer 1 beam position 3 at time 0.05 seconds

Time 0.011 seconds

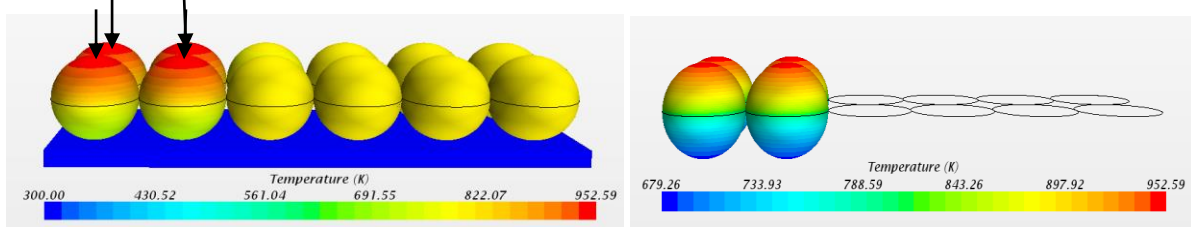


Figure 4-30 Temperature distribution for layer 1 beam position 3 at 0.011 sec

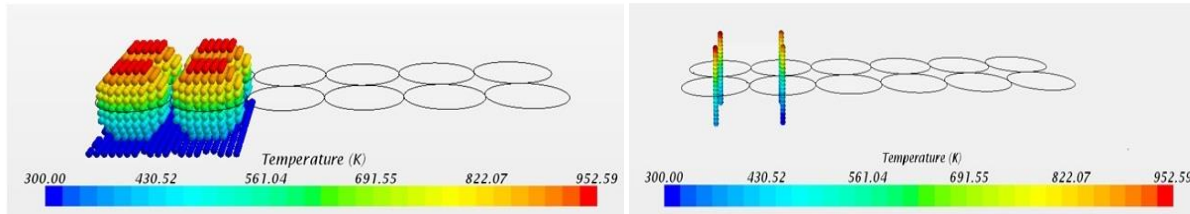


Figure 4-31 Point probes - Temperature distribution for layer 1 beam position 3

The process time for the laser beam to melt up the required volume is 0.011 seconds.

So the total process time will be $0.011 + 0.011 + 0.011 = 0.33\text{sec}$

Plots

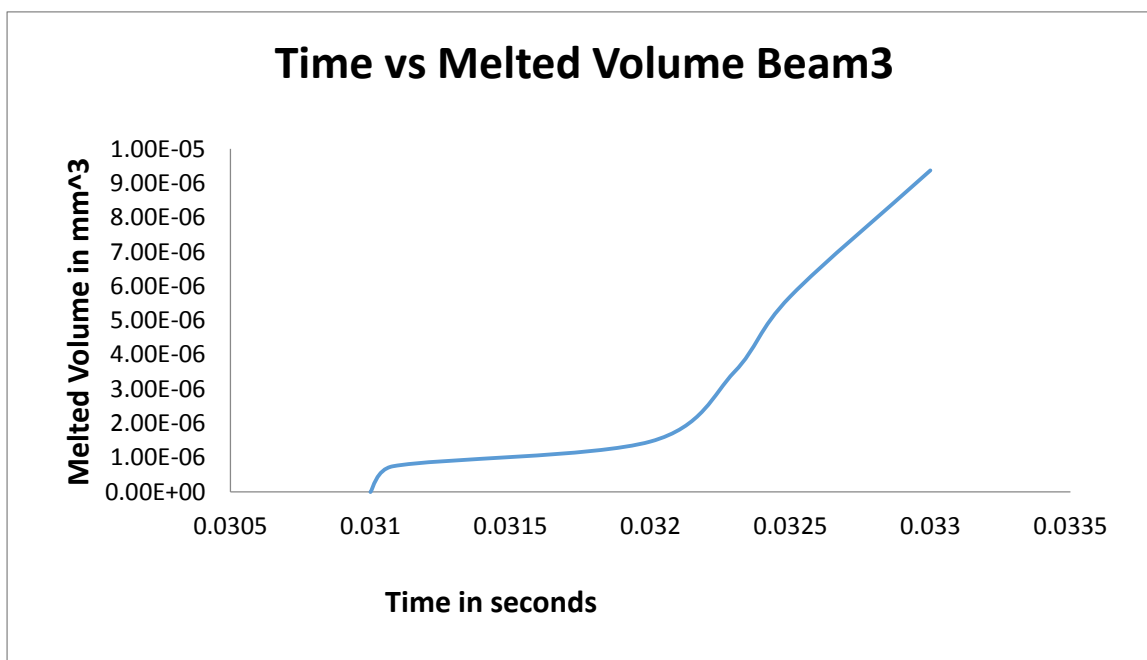


Figure 4-32 Time VS Melted volume

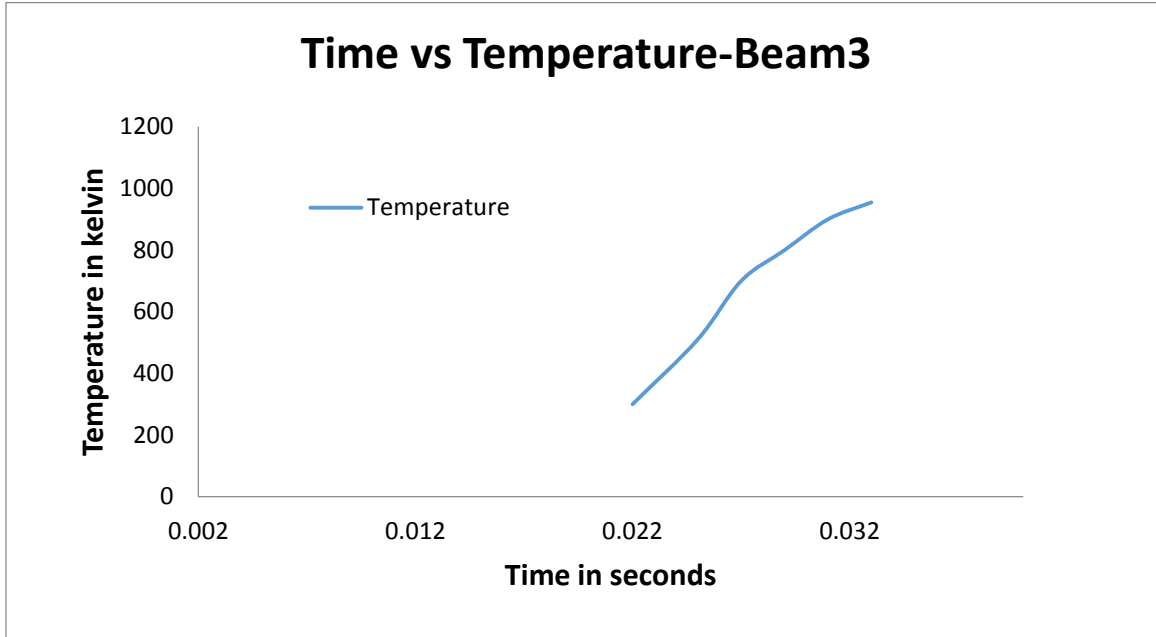
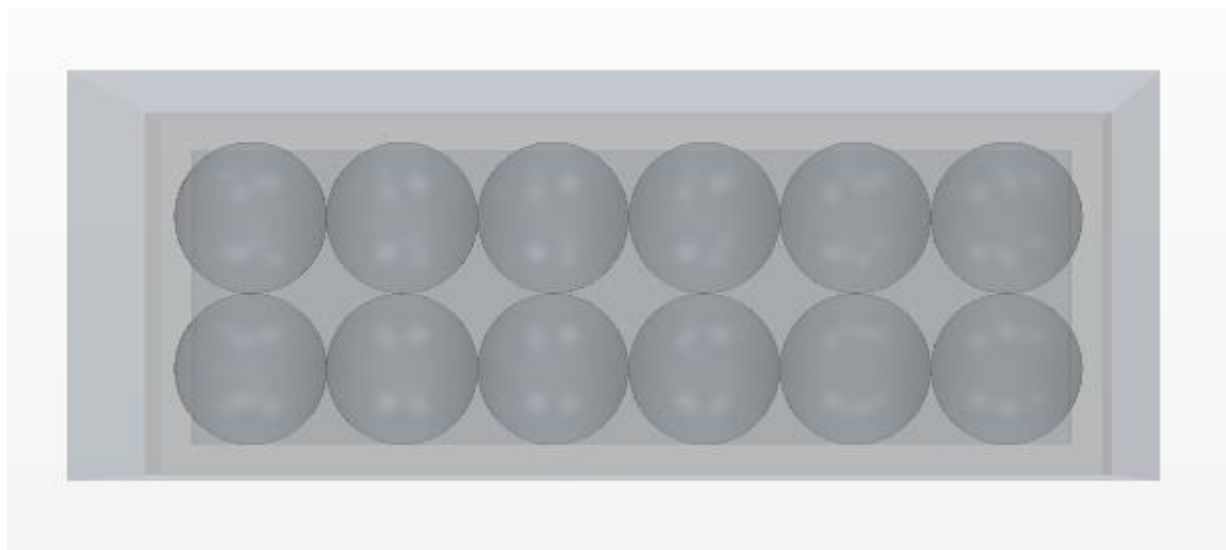


Figure 4-33 Time Vs Highest temperature

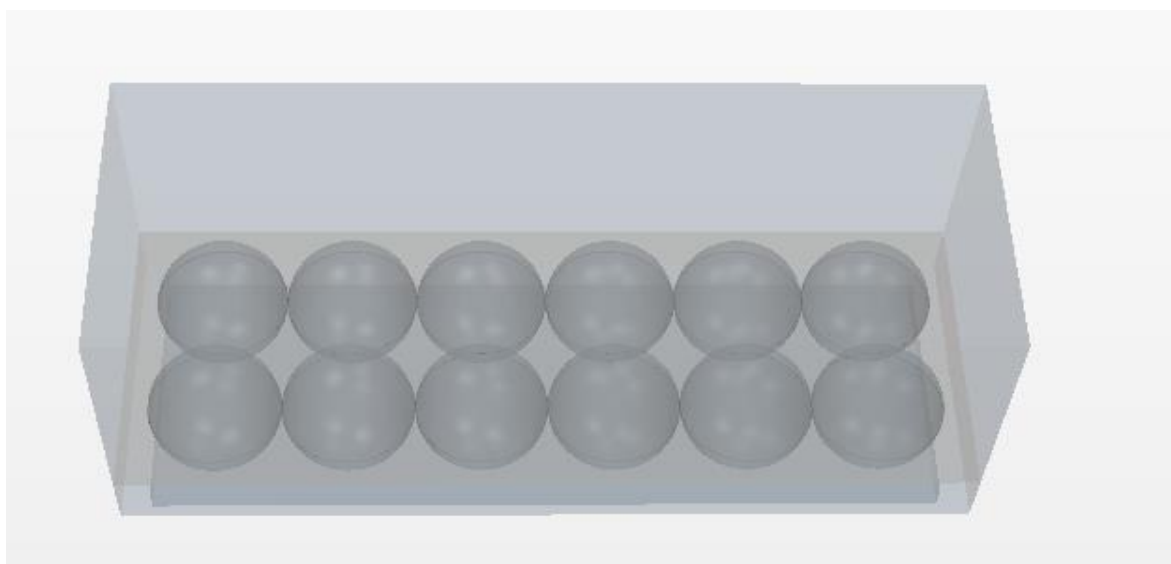
Enthalpy Validation

- Particle diameter = 50microns
- Beam diameter = 120 microns
- Beam intensity = $1 \cdot 10^9$ W/m²
- Latent heat of aluminum = 301290 J/kg

Geometry scene - With a layer of particles and air



(a)



(b)

Figure 4-34 Geometry scene for enthalpy validation

Mesh scene a

Base size 0.001mm

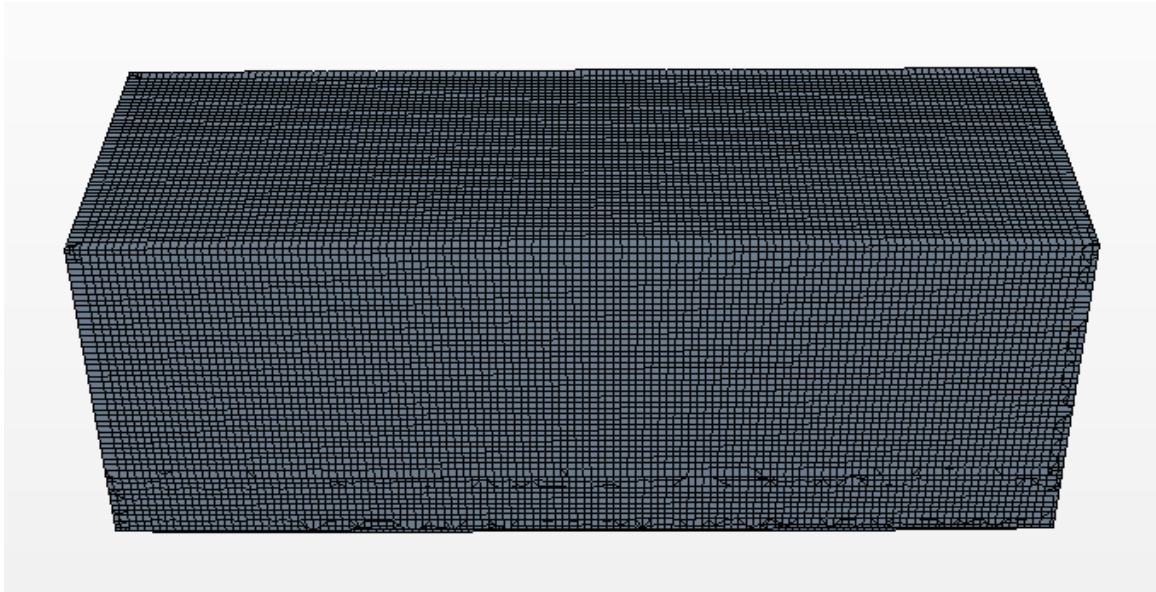


Figure 4-35 Mesh scene for enthalpy validation

Enthalpy scenes

Layer 1 & Beam position 1

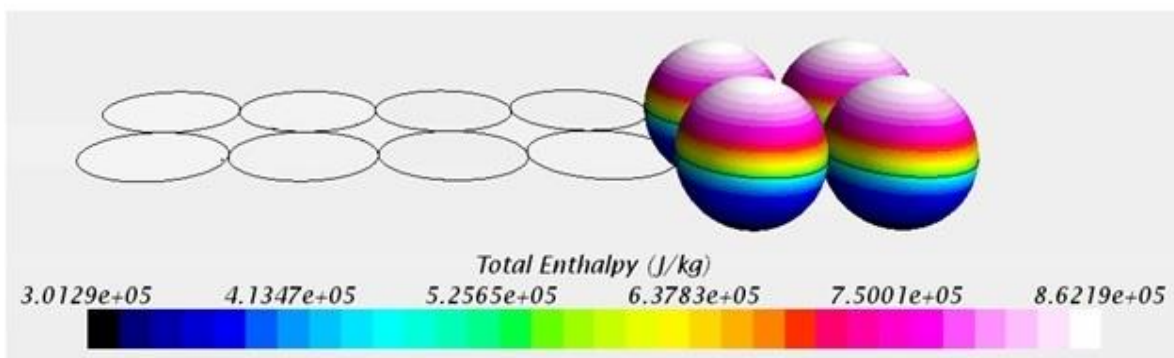


Figure 4-36 Enthalpy scene for beam position 1

Enthalpy is 862190 J/kg

$$T_{\text{melt}} = h_{\text{melt}}/C_p$$

$$= 862190/903$$

$$= 952.8\text{k}$$

So this is the temperature that we got from the temperature scene by projecting a laser beam on to the aluminum particles.

Beam position 2

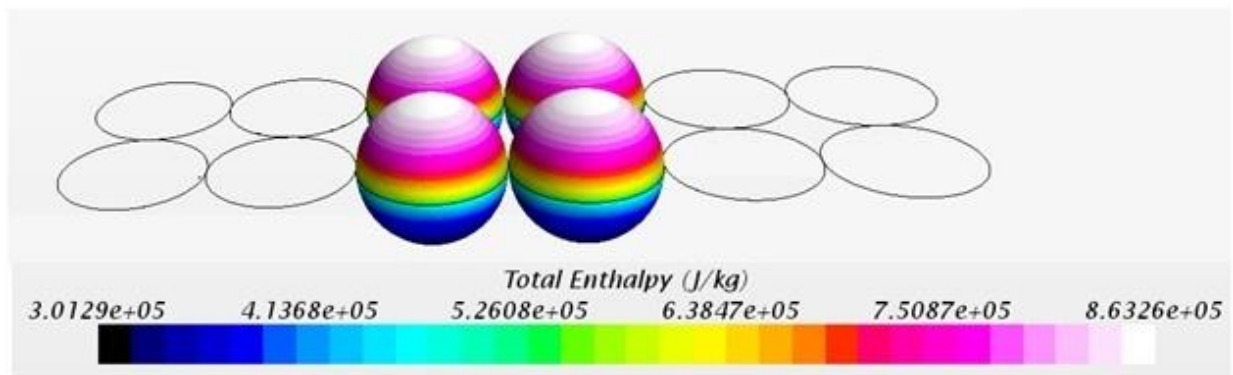


Figure 4-37 Enthalpy scene beam position 2

Beam position 3

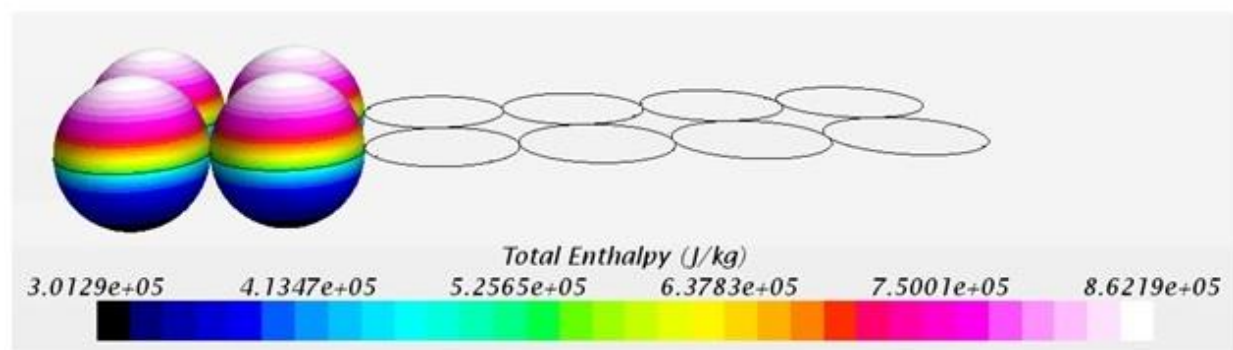


Figure 4-38 Enthalpy scene beam position 3

The slow melting of the powder particles, results in deposition of the molten volume in void spaces, creating a rectangular bar on top of it. The height of the rectangular plate formed by melting the upper region of the layer 1 of powder particles and filling up the void spaces is 0.01308mm. Multiple layers of powder particles are considered for better results and validation. So, spray another fresh layer of powder particles over that manufactured layer1.

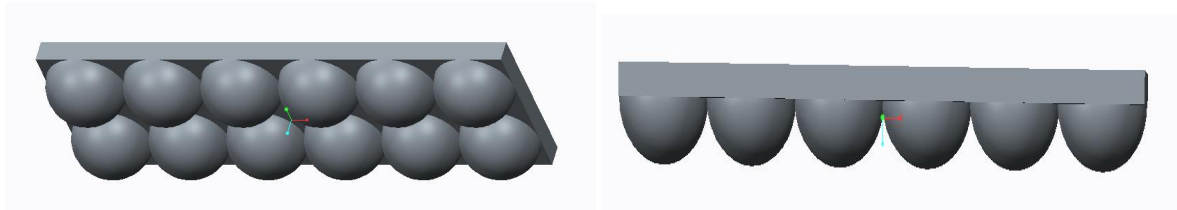


Figure 4-39 After melting and solidifying of layer 1

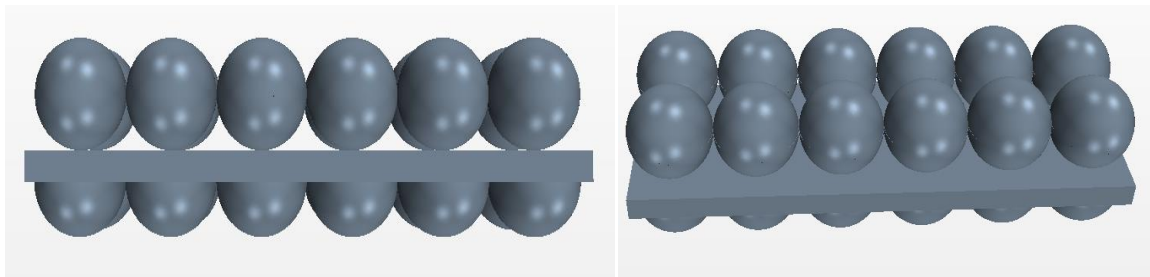


Figure 4-40 After spraying another layer of particles over the melted layer 1

Mesh Base size = 0.001mm

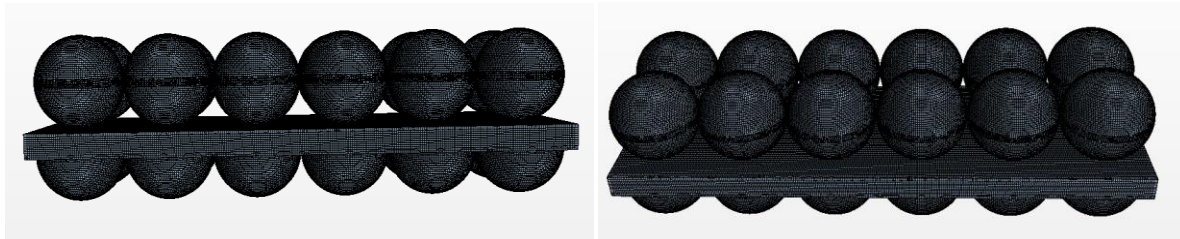


Figure 4-41 Mesh scene

The position of laser beam is at Layer 2 & Beam position 1

Initial Time = 0.002 seconds

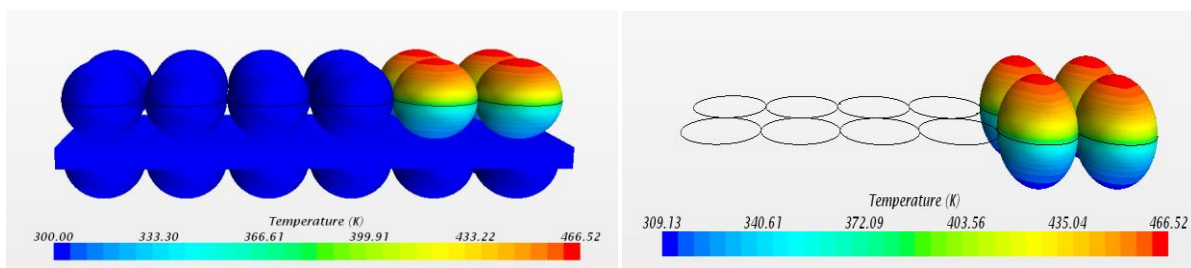


Figure 4-42 Temperature distribution at 0.02 sec

Time = 0.005 seconds

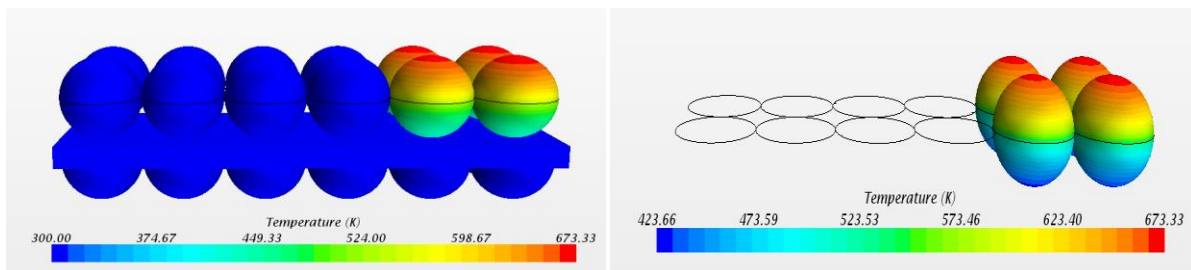


Figure 4-43 Temperature distribution at 0.05 sec

Final time = 0.011 sec

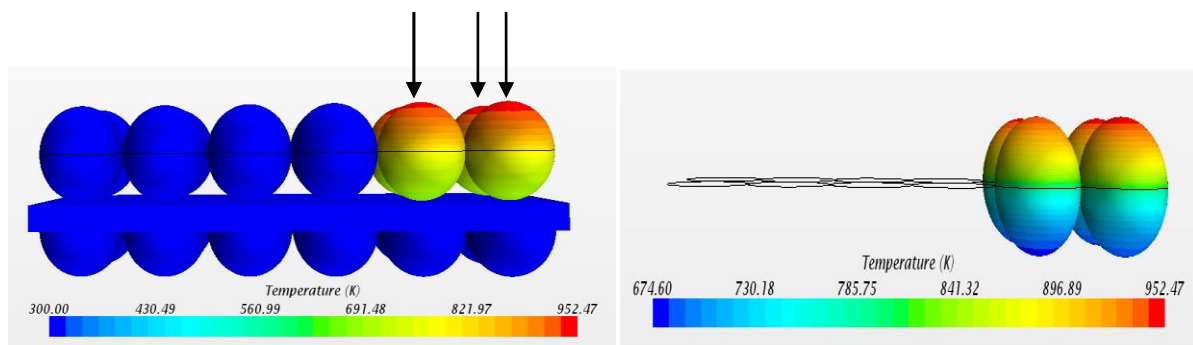


Figure 4-44 Temperature distribution for layer 2 beam position 1 at 0.011 sec

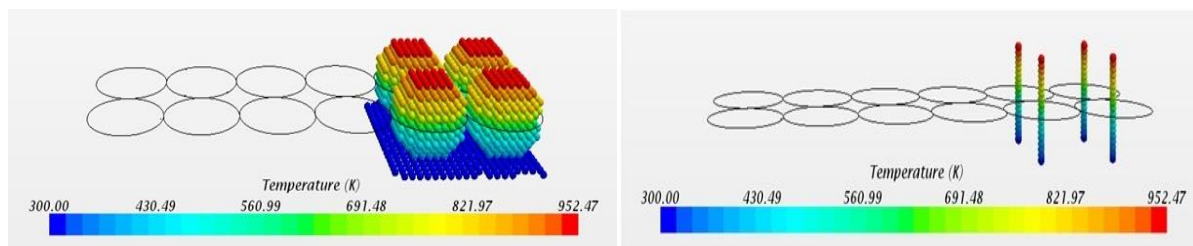


Figure 4-45 Point probes - Temperature distribution for layer 2 beam position 1

The process time for melting powder particles at Position 1 is 0.011 sec

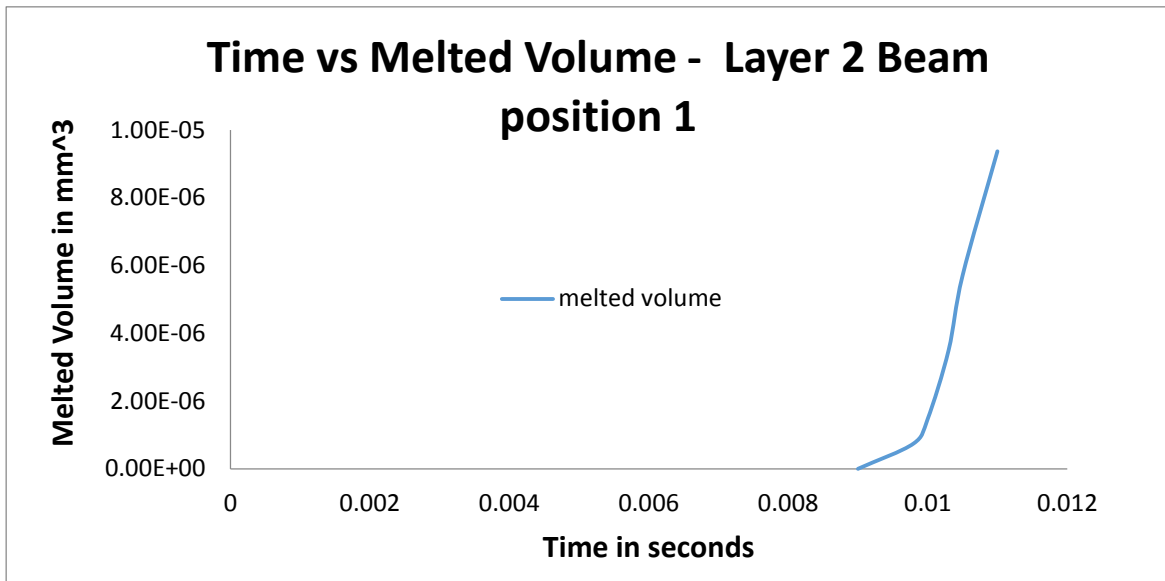


Figure 4-46 Time Vs Melted volume

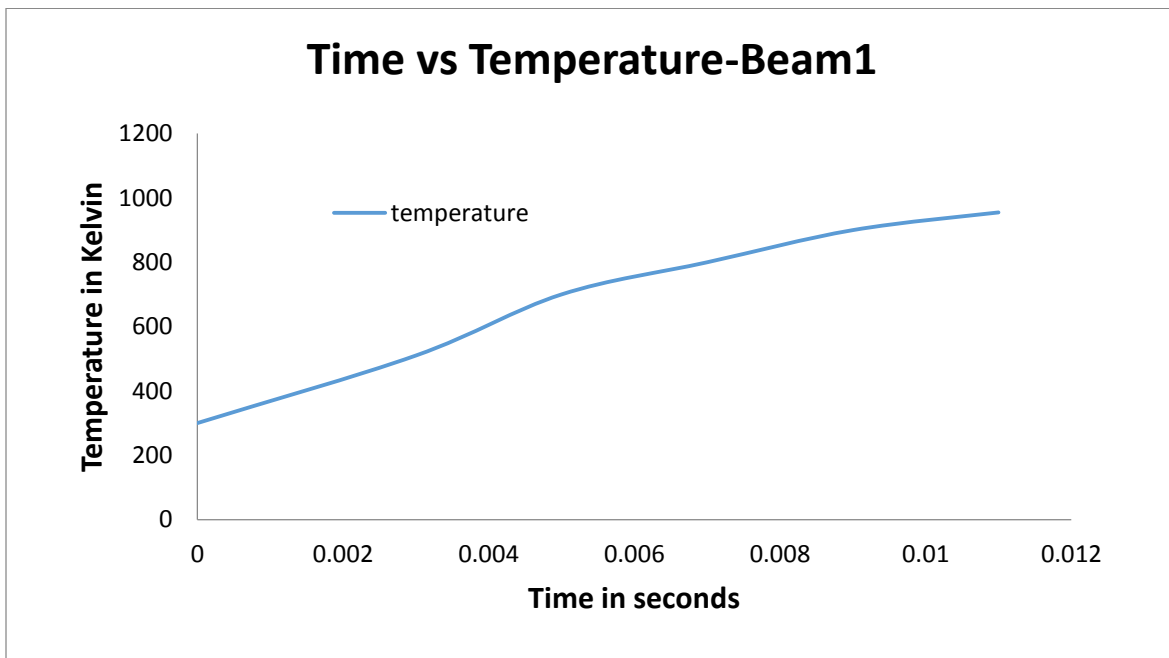


Figure 4-47 Process Time Vs Highest temperature

Layer 2 Beam position 2

Initial time = 0.002 sec

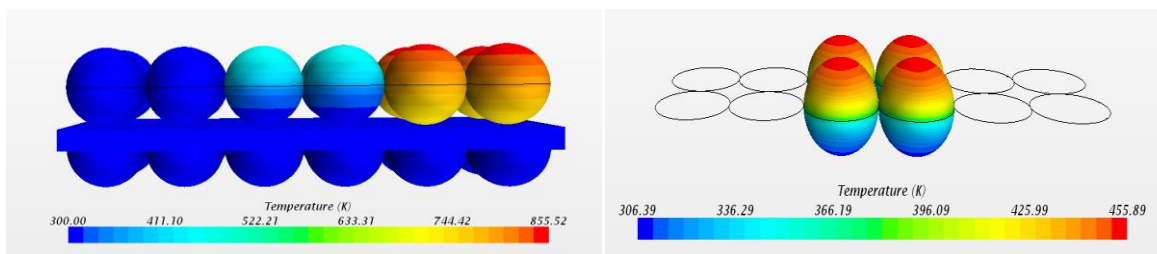


Figure 4-48 Initial temperature distribution at 0.002 sec

Time = 0.005 sec

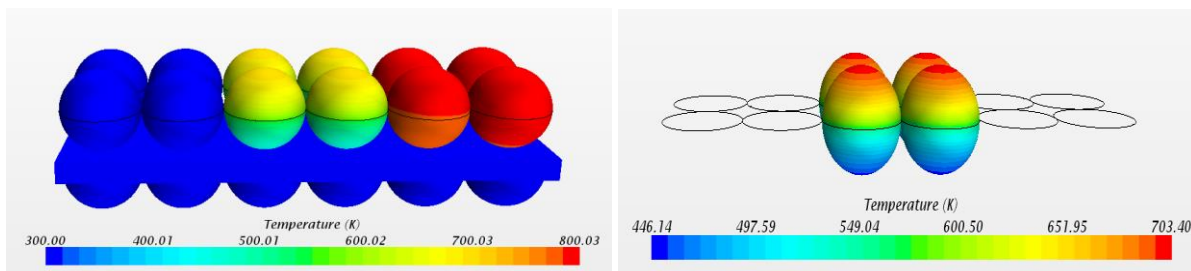


Figure 4-49 Temperature distribution at time 0.05 sec

Final Process Time = 0.011 sec

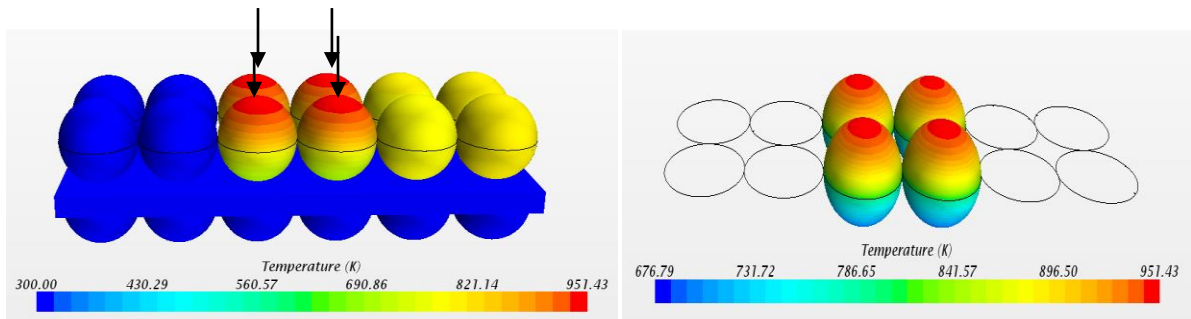


Figure 4-50 Temperature distribution for layer 2 beam position 2 at 0.011 sec

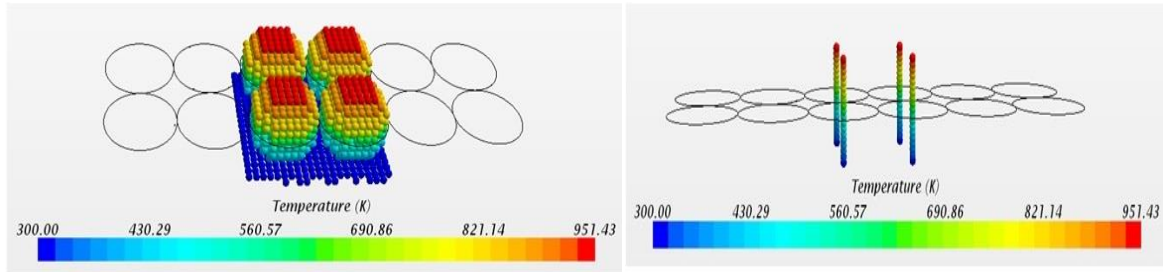


Figure 4-51 Point probes - Temperature distribution for layer 2 beam 2 position 2

The process time is 0.022 sec, when the beam is incident for the second time at position 2

Plots

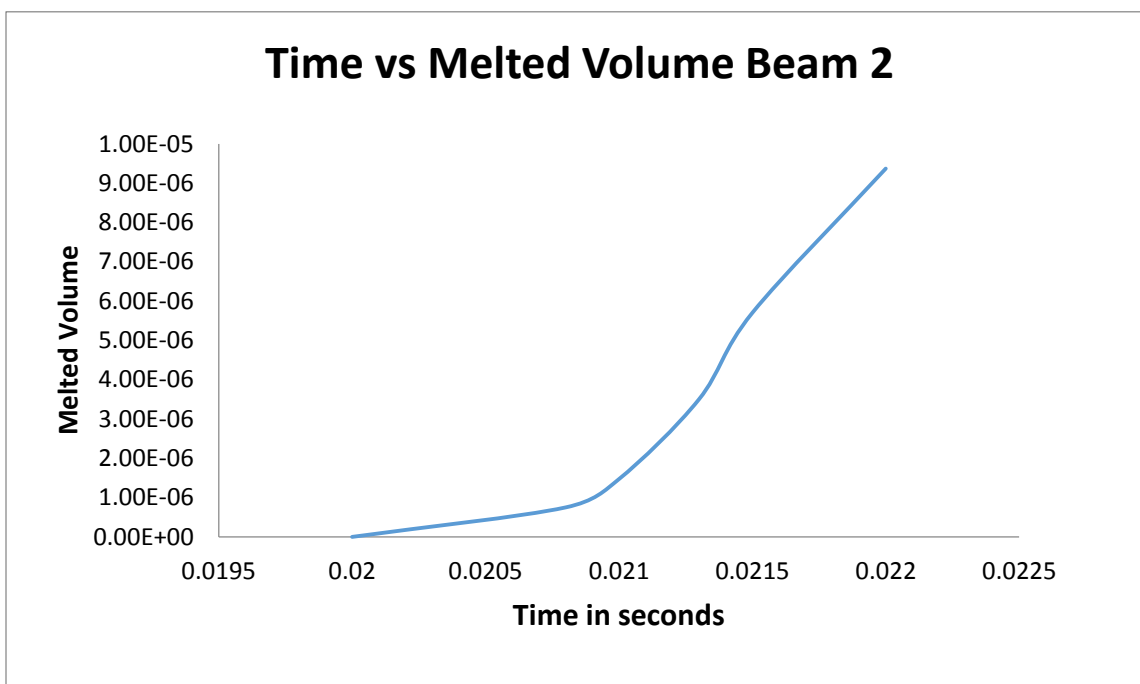


Figure 4-52 Time Vs Melted volume

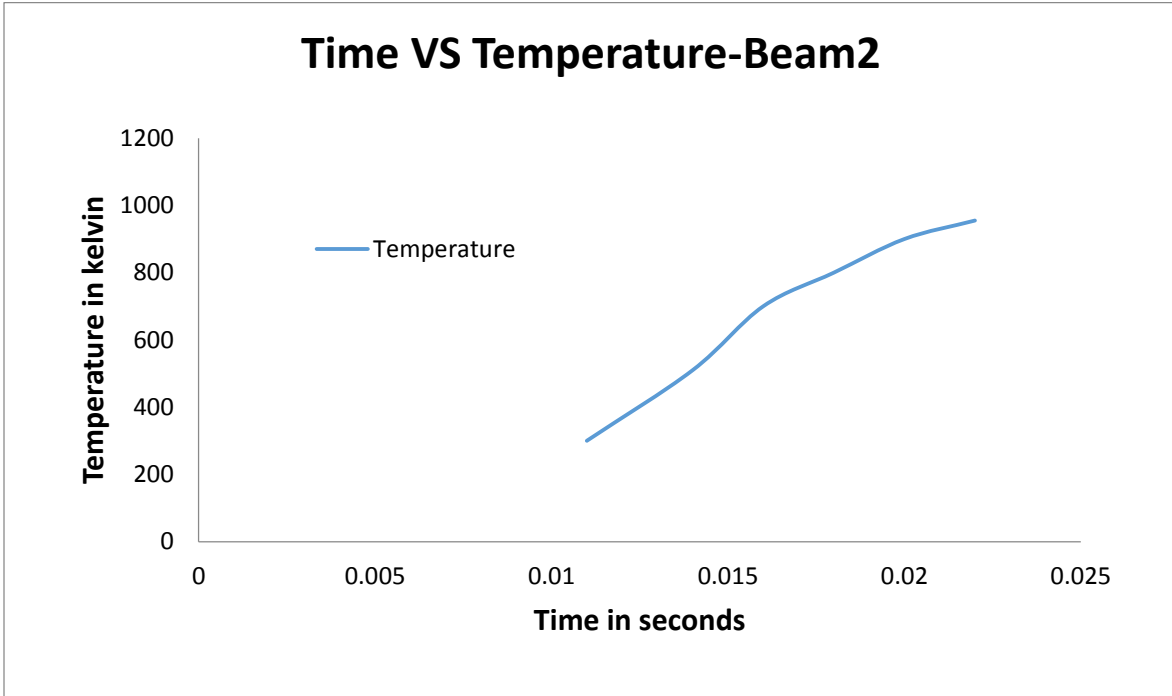


Figure 4-53 Process Time Vs Highest temperature

Layer 2 Beam position 3

Initial time 0.002 sec

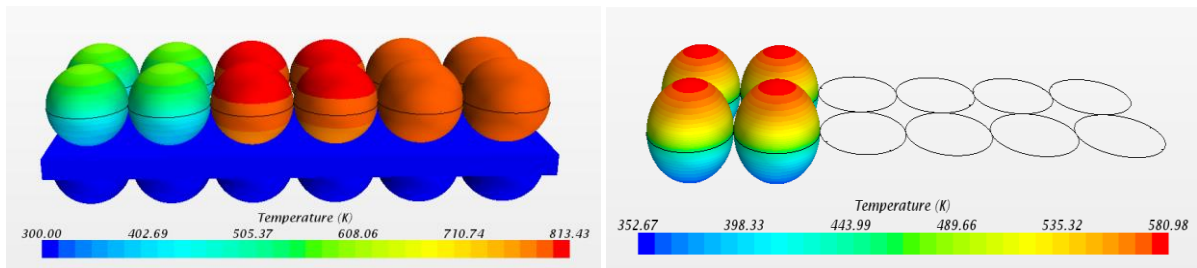


Figure 4-54 Temperature distribution at time 0.02 sec

Time 0.005 sec

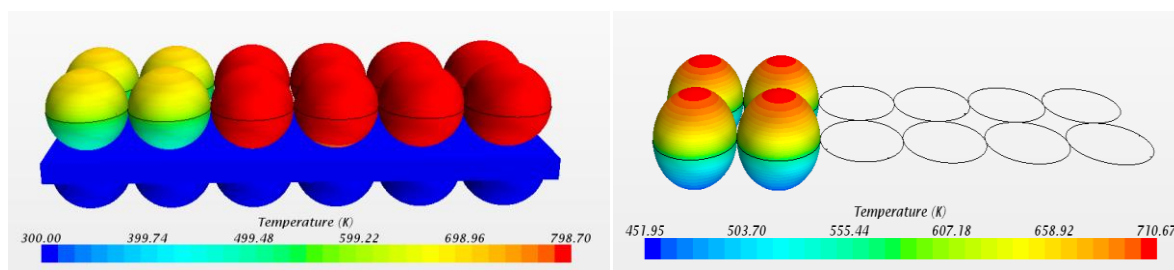


Figure 4-55 Temperature distribution at 0.05 sec

Final time 0.011sec

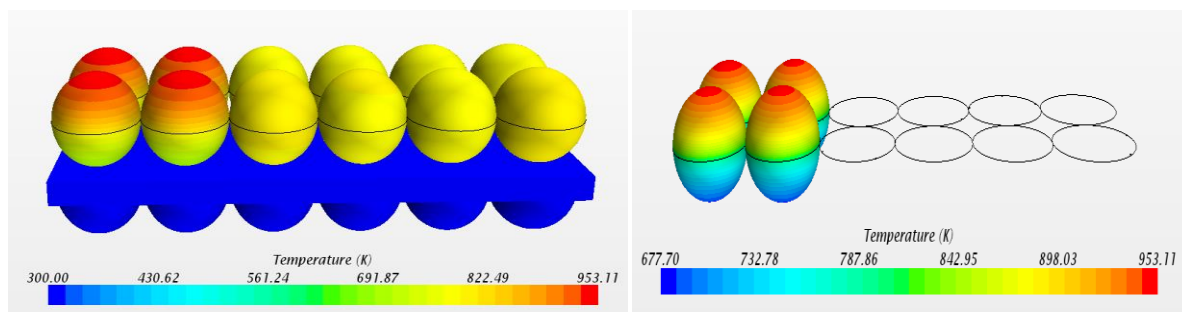


Figure 4-56 Temperature distribution for layer 2 beam position 3 at 0.011 sec

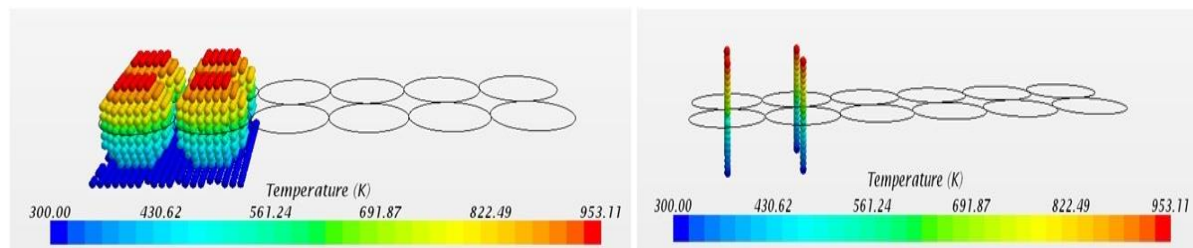


Figure 4-57 Point probes -Temperature distribution for layer 2 beam position 3

The final process time is 0.033sec

Plots

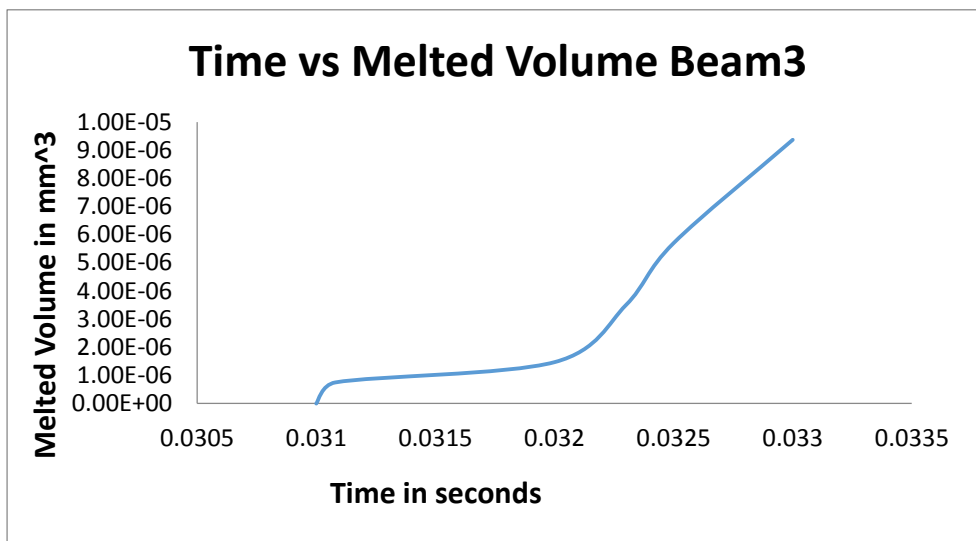


Figure 4-58 Time Vs Melted volume

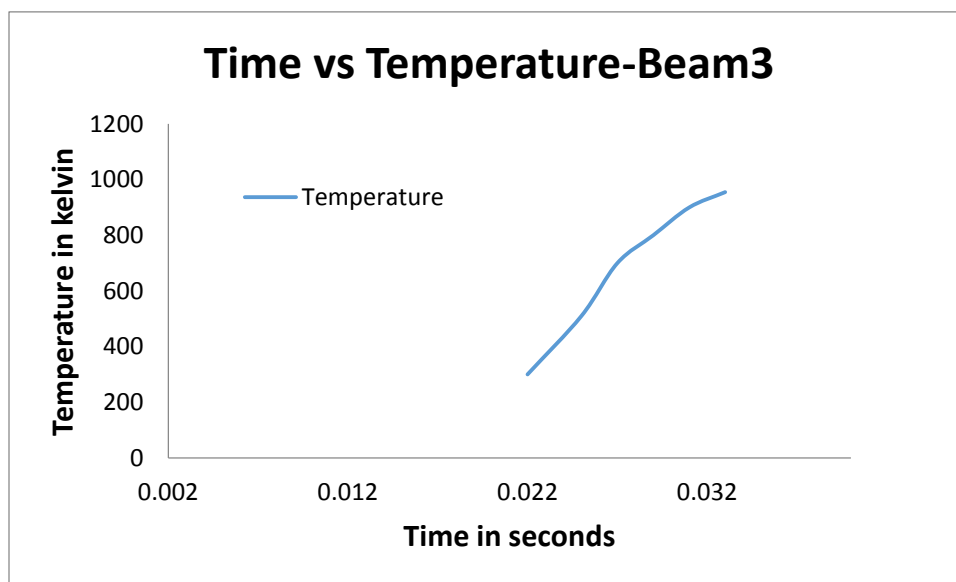


Figure 4-59 Time Vs Highest temperature

Enthalpy scenes

Layer 2 Beam position 1

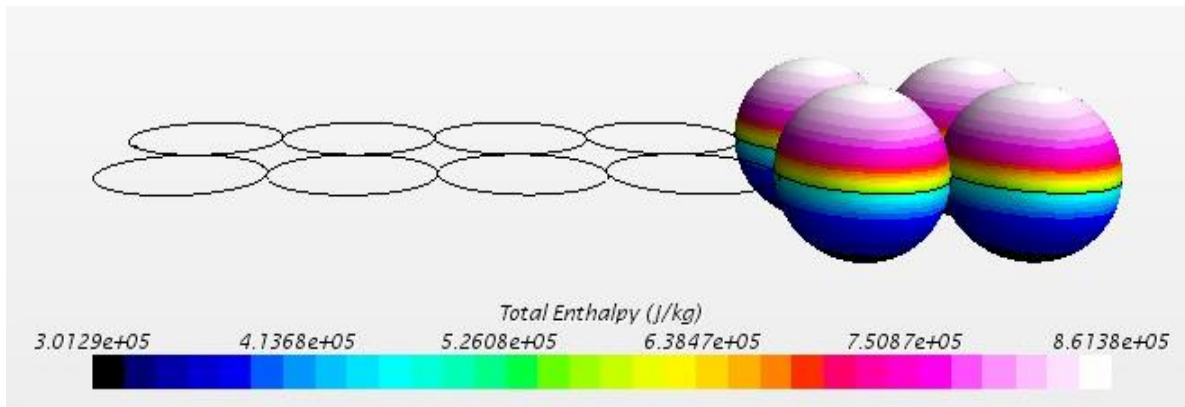


Figure 4-60 Enthalpy scene beam position 1

Enthalpy is 861380 J/kg

$$\begin{aligned}
 T_{\text{melt}} &= h_{\text{melt}}/C_p \\
 &= 861380/903 \\
 &= 952.8\text{k}
 \end{aligned}$$

So this is the temperature that we got from the temperature scene by projecting a laser beam on to the aluminum particles.

Beam position 2

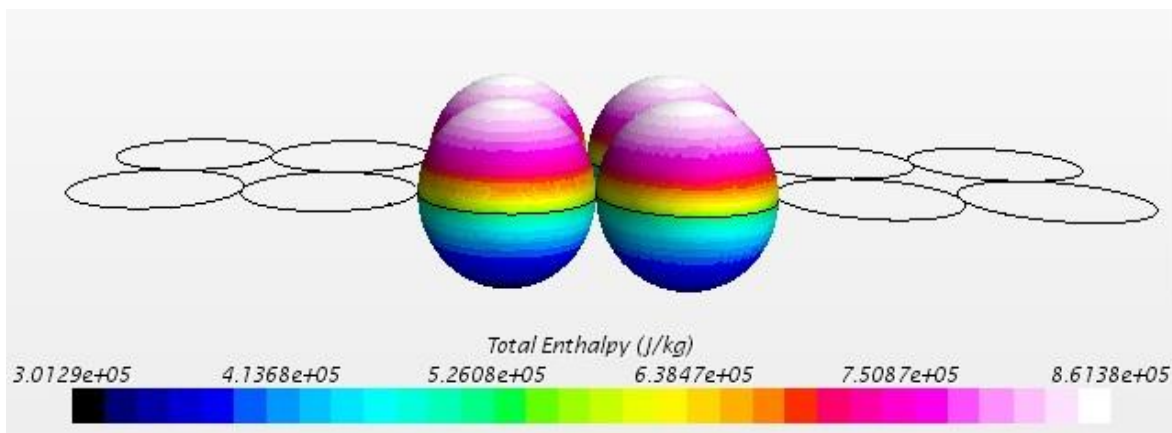


Figure 4-61 Enthalpy scene beam position 2

Beam position 3

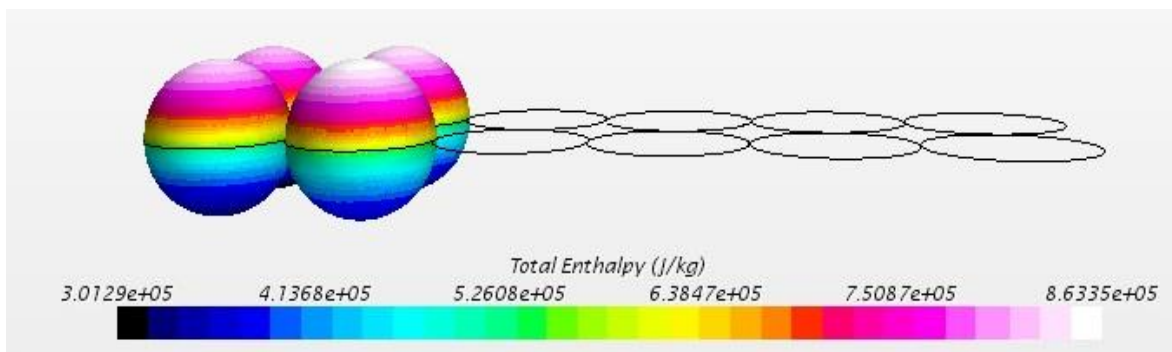


Figure 4-62 Enthalpy scene beam position 3

This is the part that is created after melting layer 2.

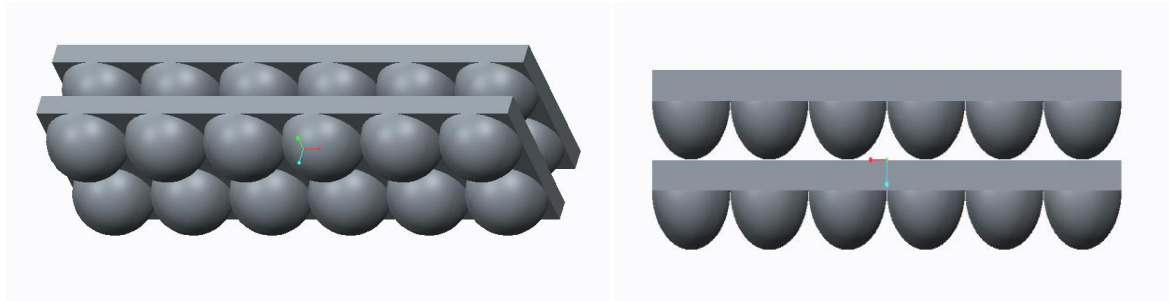


Figure 4-63 After melting and solidifying of layer 1 and 2

Spray a fresh layer of powder particles over the melted layers

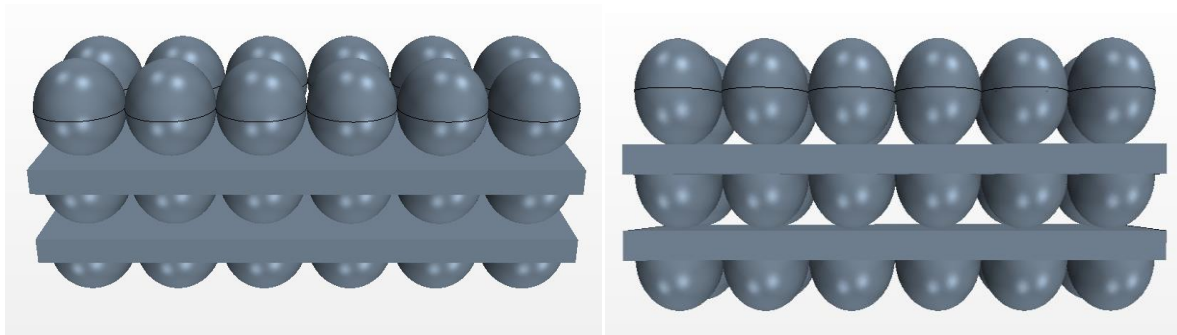


Figure 4-64 After spraying a new layer on the melted layer 1 and 2

Mesh scene

Base Size 0.001mm

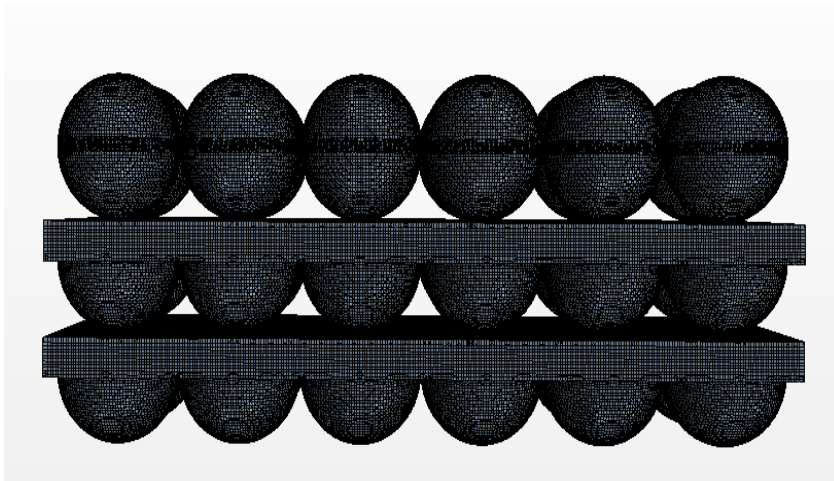


Figure 4-65 Mesh scene

Layer 3 Beam position 1

Initial time 0.002 sec

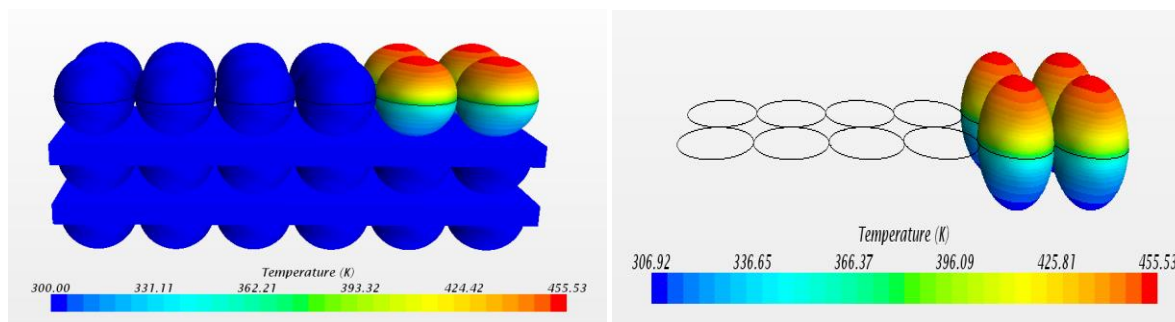


Figure 4-66 Temperature distribution at 0.002sec

Time 0.005 sec

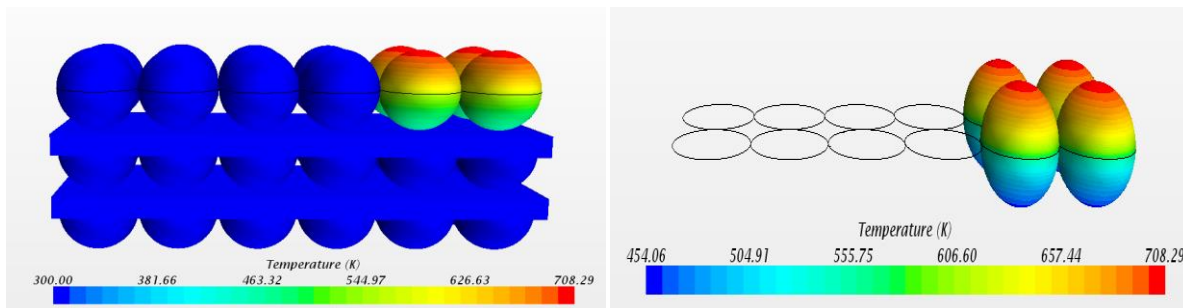


Figure 4-67 Temperature distribution at 0.005sec

Final time 0.011sec

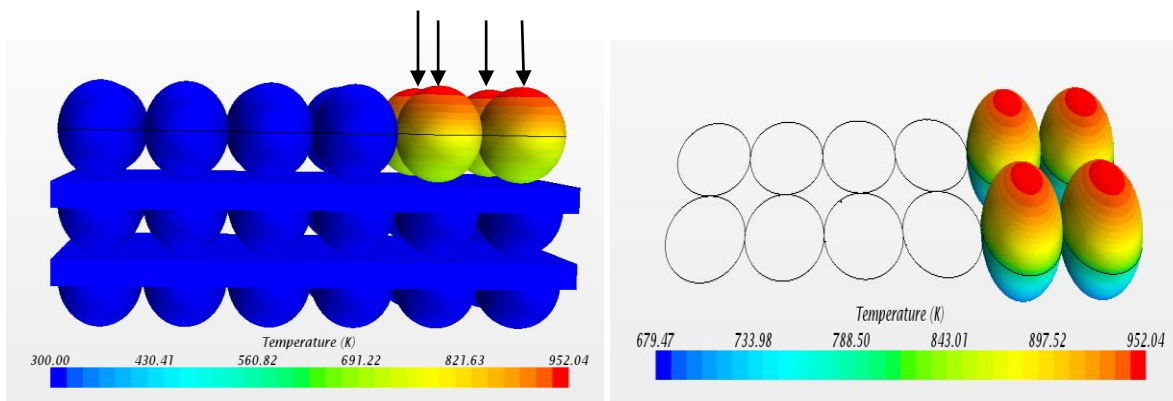


Figure 4-68 Temperature distribution for layer 3 beam position 1 at 0.011 sec

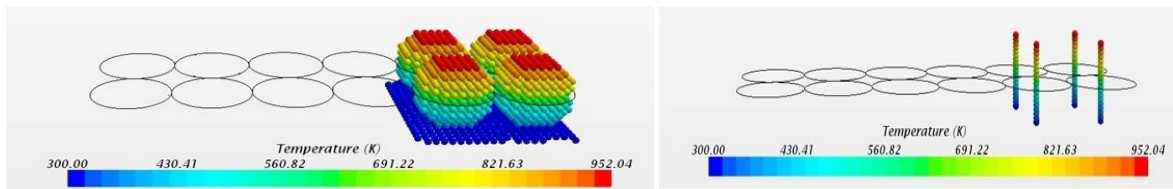


Figure 4-69 Point probes - Temperature distribution for layer 3 beam position 1

The final process time 0.011 sec

Plots

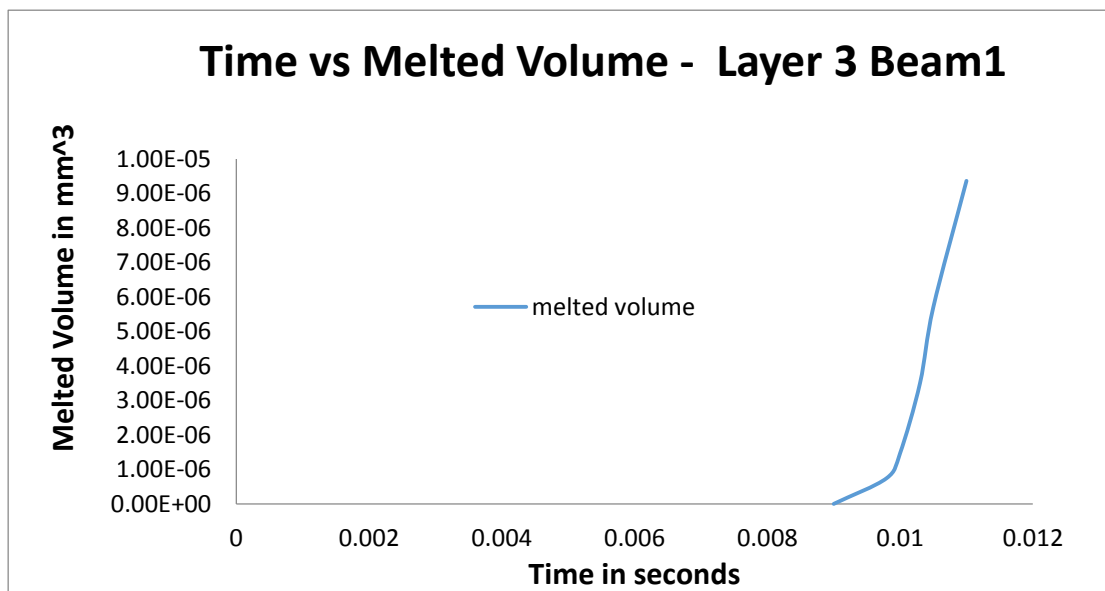


Figure 4-70 Time Vs Melted volume

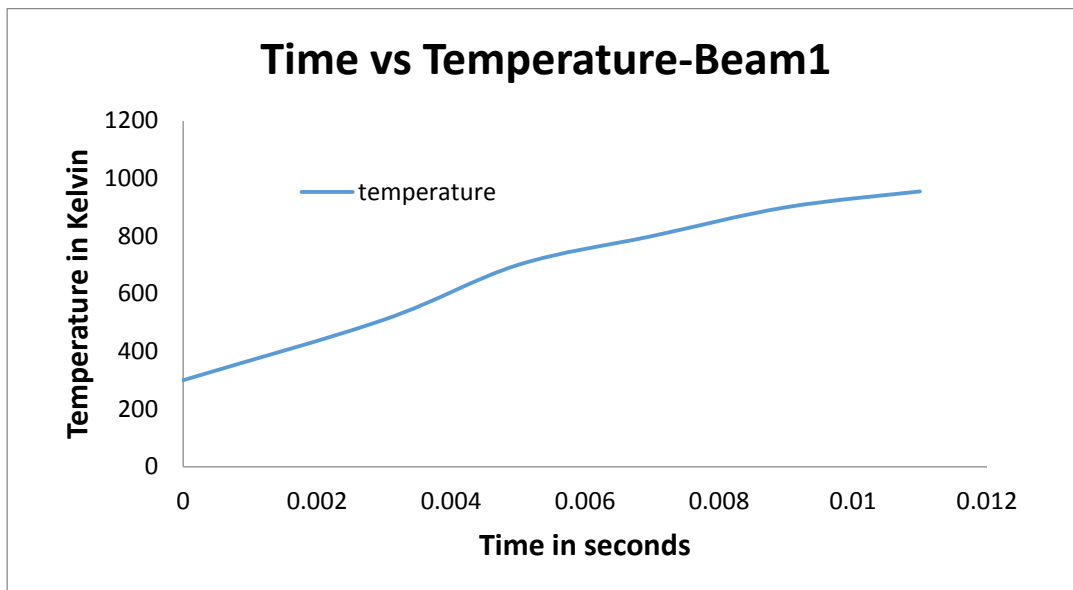


Figure 4-71 Process time Vs Highest temperature

Layer 3 Beam 2

Initially at time = 0.002 sec

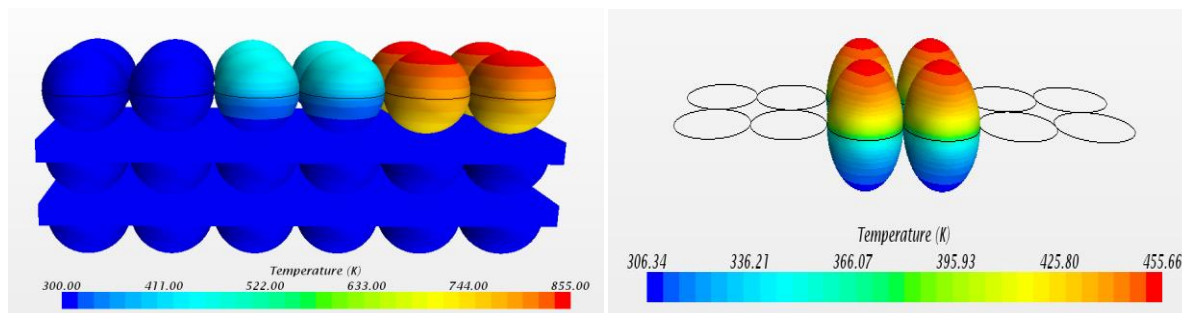


Figure 4-72 Temperature distribution at time 0.002 sec

Time = 0.005 sec

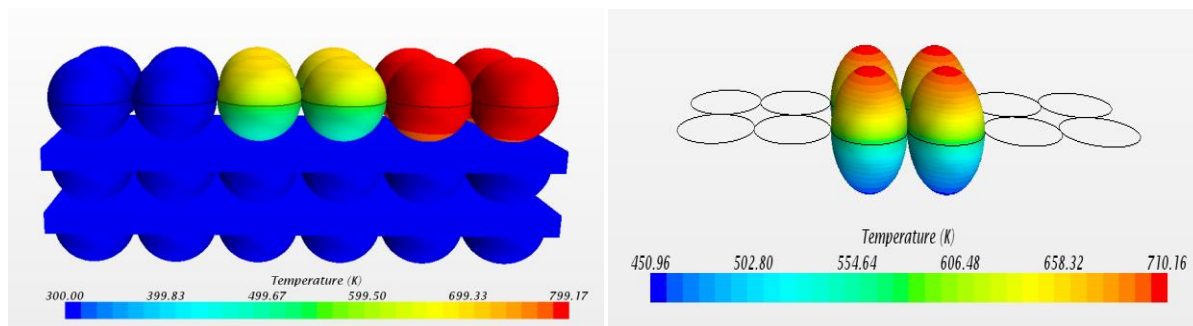


Figure 4-73 Temperature distribution at time 0.005 sec

Final time = 0.011sec

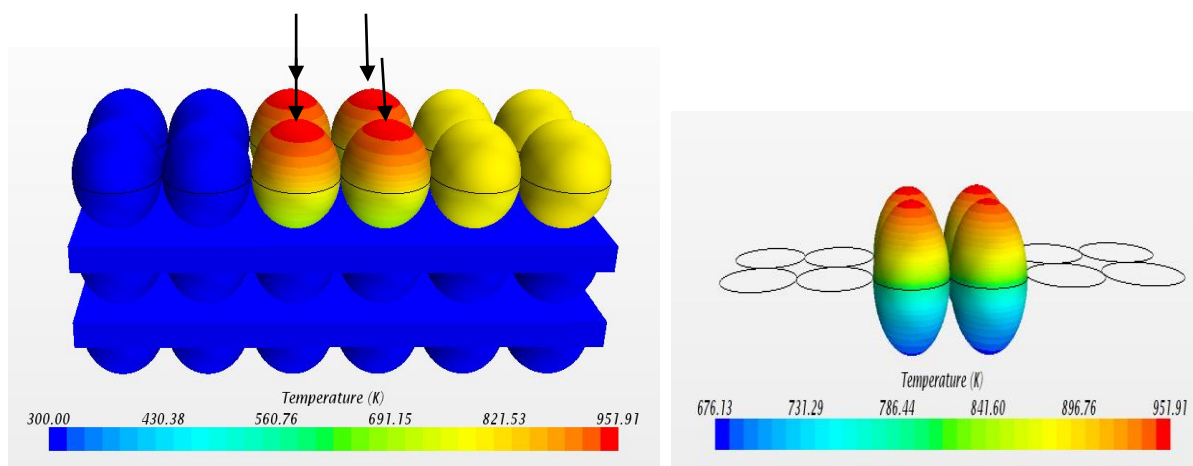


Figure 4-74 Temperature distribution for layer 3 beam position 2 at 0.011 sec

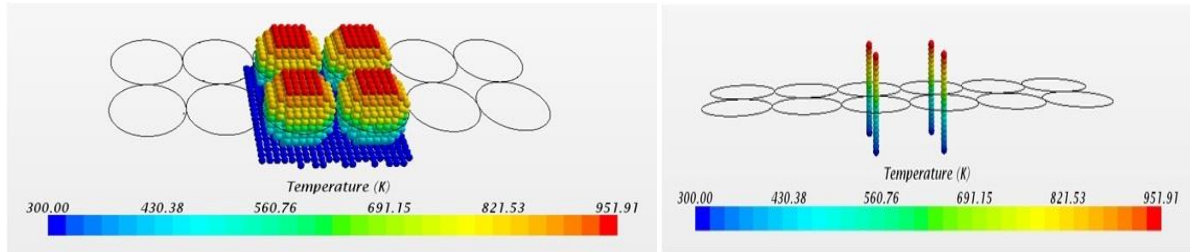


Figure 4-75 Point probes - Temperature distribution for layer 3 beam position 2

The process time is 0.022 sec.

Plots

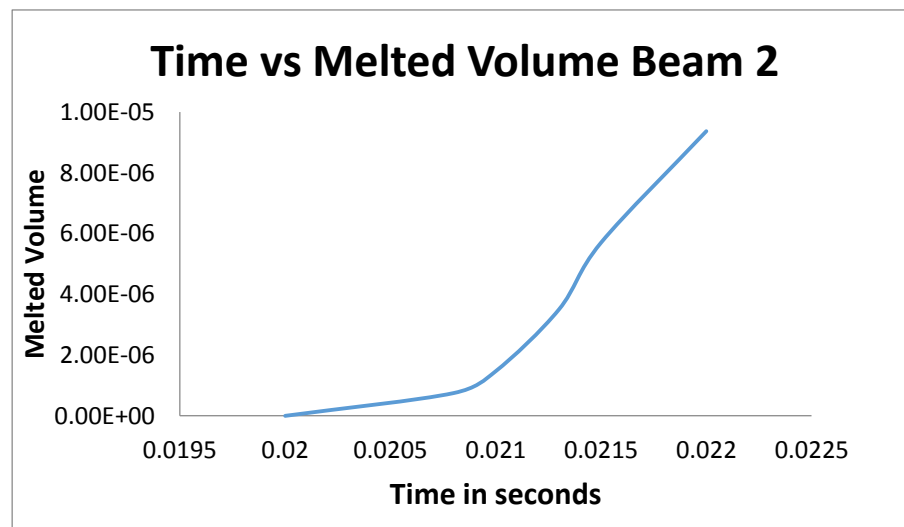


Figure 4-76 Time Vs Melted volume

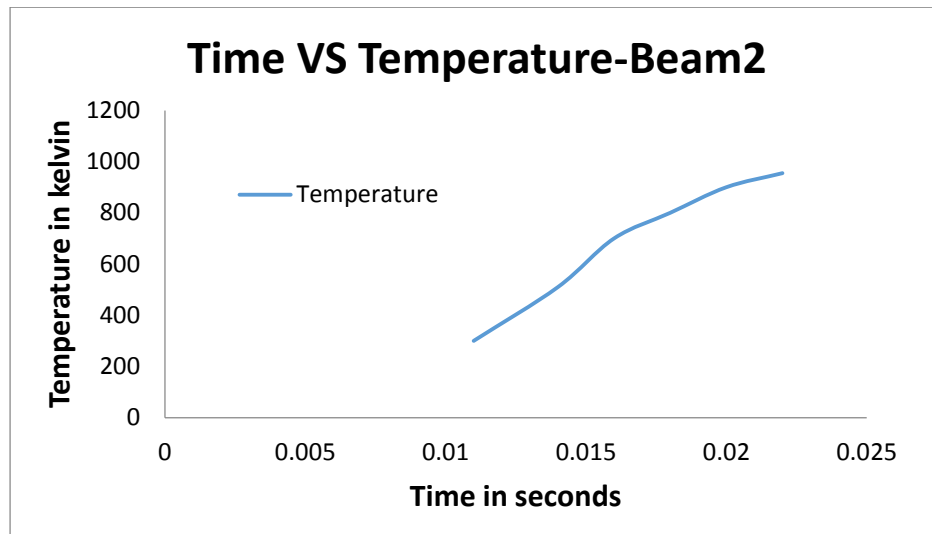


Figure 4-77 Process time Vs Highest temperature

Layer 3 Beam position 3

Initial time = 0.002 sec

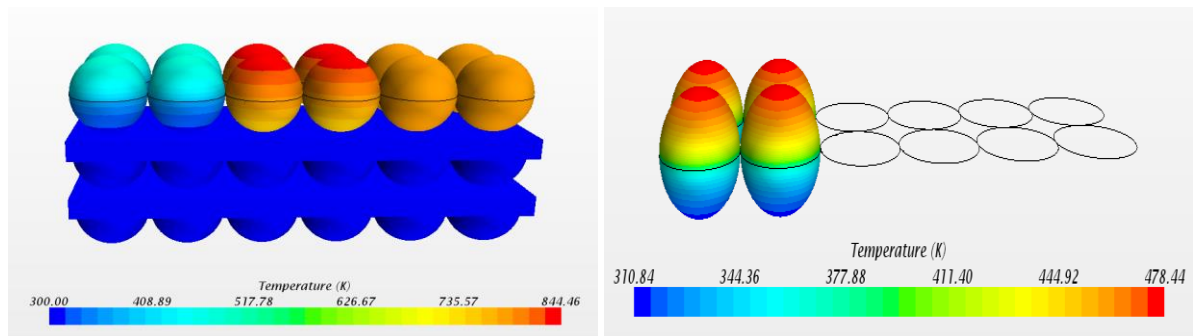


Figure 4-78 Temperature distribution at time 0.002 sec

At time 0.005 sec

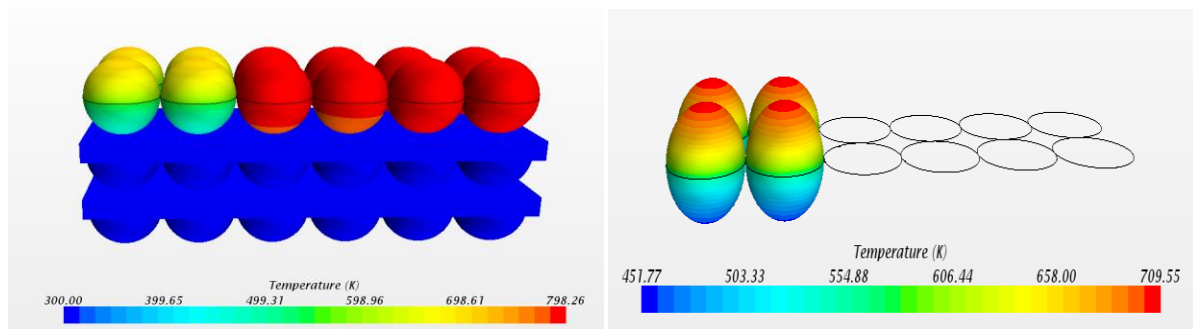


Figure 4-79 Temperature distribution for layer 3 beam 3 at time 0.005 sec

Final process time = 0.011 sec.

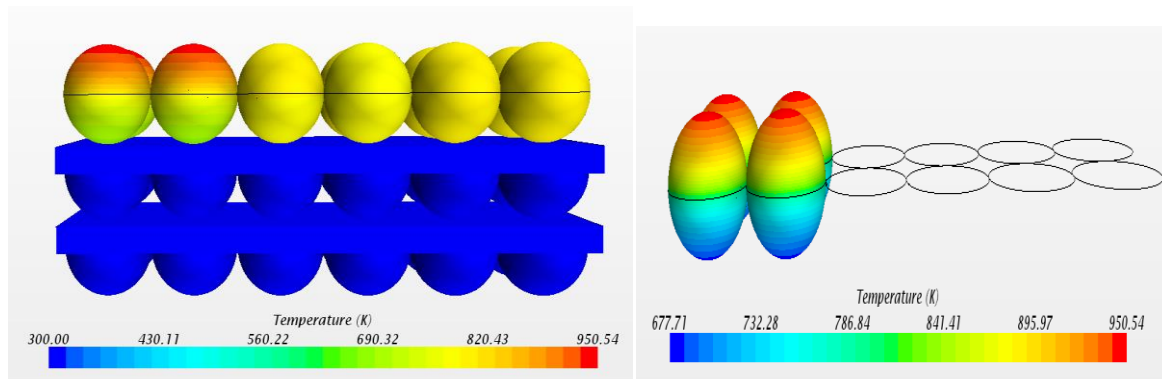
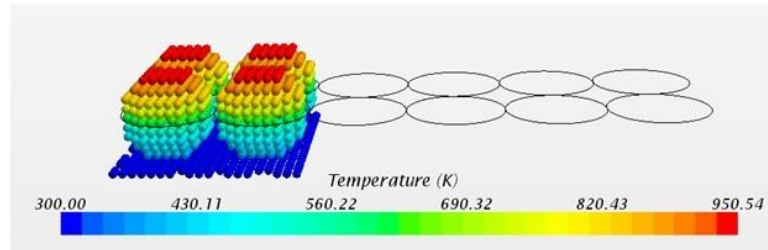
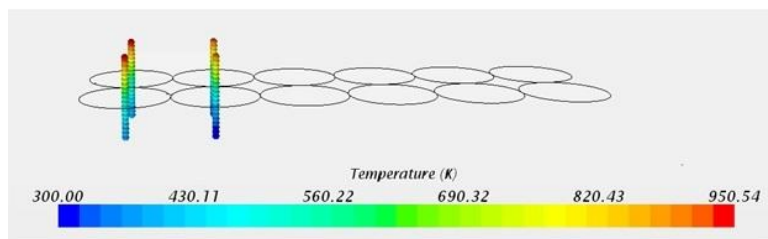


Figure 4-80 Temperature distribution for layer 3 beam position 3 at time 0.011 sec



(a)



(b)

Figure 4-81 Point probes - Temperature distribution for layer 3 beam position 3

Final Process time = 0.033sec

Plots

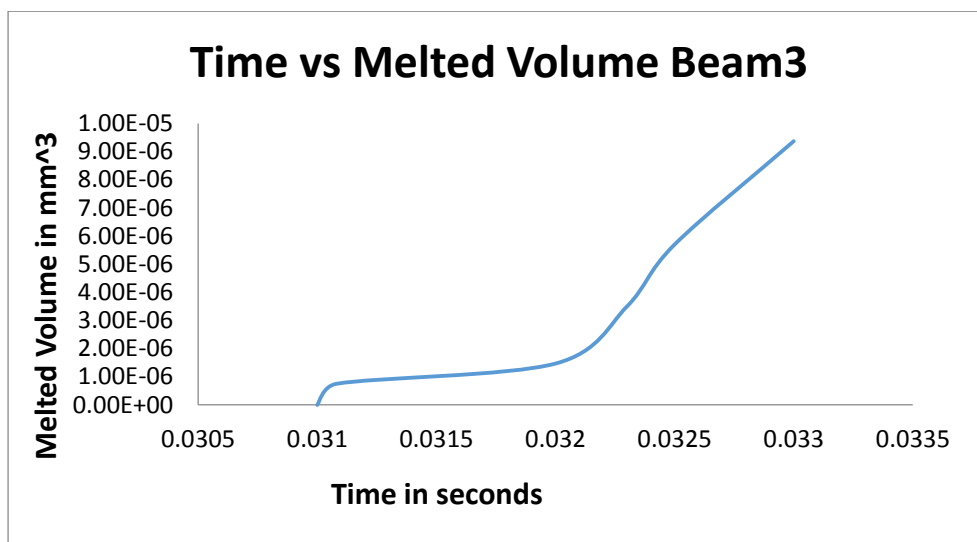


Figure 4-82 Time Vs Melted volume

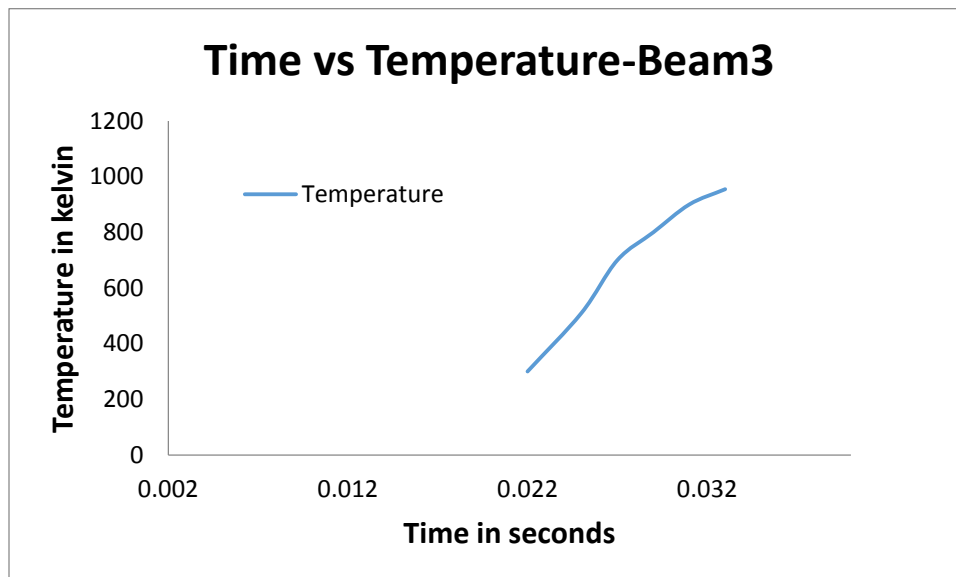


Figure 4-83 Time Vs Highest temperature

Enthalpy scenes

Beam position 1

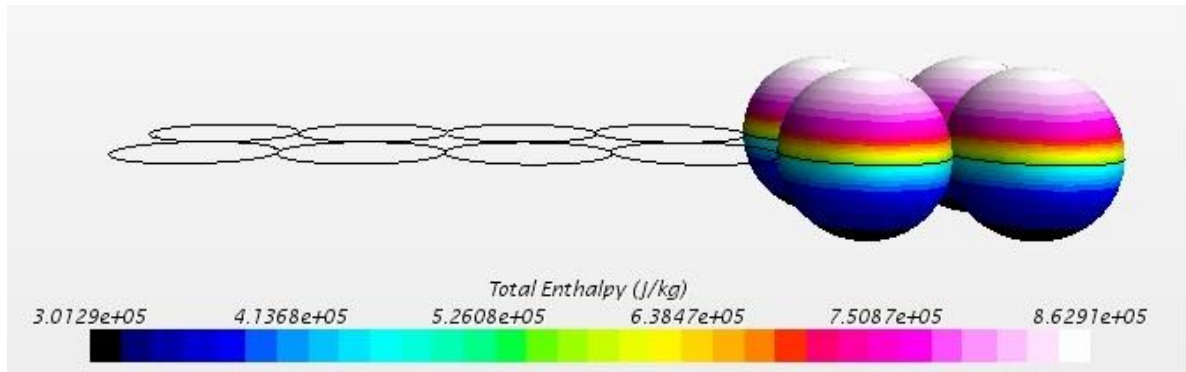


Figure 4-84 Enthalpy scene beam position 1

Enthalpy is 862190 J/kg

$$T_{\text{melt}} = h_{\text{melt}}/C_p$$

$$= 862190/903$$

$$= 952.8\text{k}$$

So this is the temperature that we got from the temperature scene by projecting a laser beam on to the aluminum particles.

Beam position 2

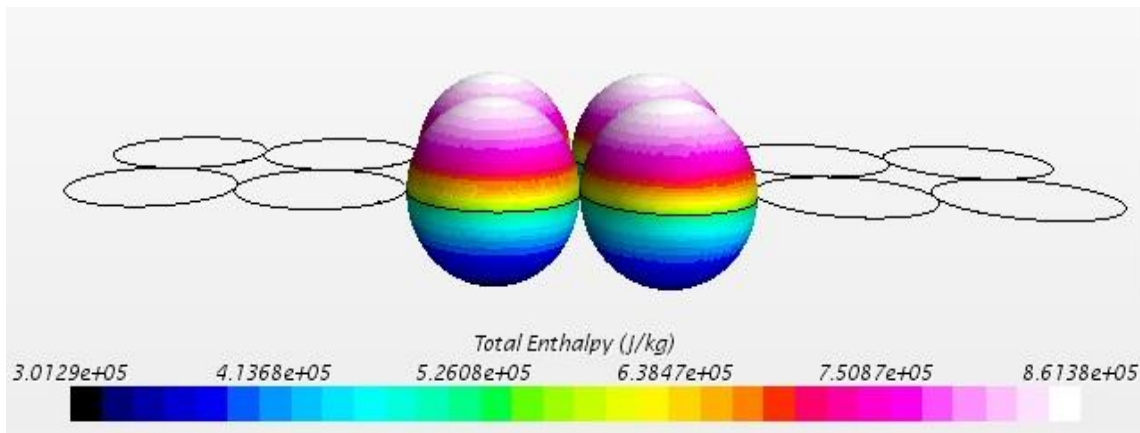


Figure 4-85 Enthalpy scene beam position 2

Beam position 3

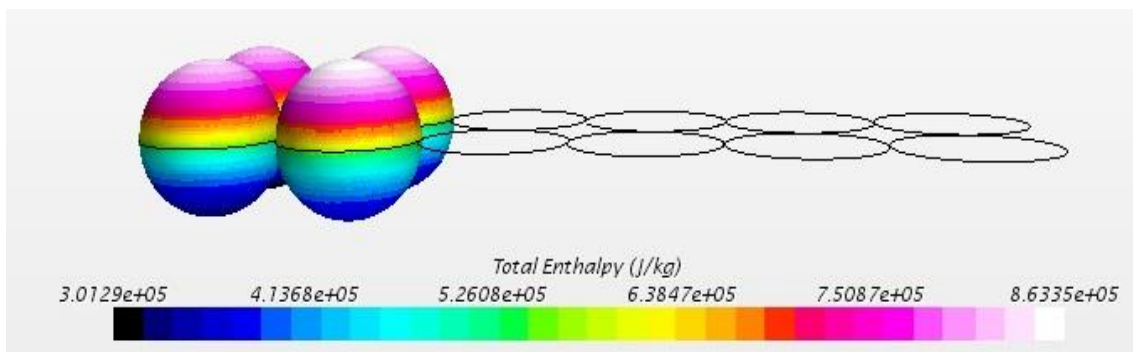


Figure 4-86 Enthalpy scene beam position 3

The final time taken to complete the manufacturing of the whole work piece, without considering the spraying time is 0.099 sec.

Scan speed of the laser beam = Distance travelled \div Time taken

Scan speed = $0.3 \div 0.033 = 9.09 \text{ mm/sec}$

4.4.2 Effect of particle size - 30microns:

For a particle size of diameter 30microns, we try to calculate the density of this part by melting the powder particles to such an extent that they fill up the void spaces. The procedure followed is the same as the one for the particle size of 50 microns. There is difference in the geometry but the physics models and the meshing models are the same. As these powder particles are comparatively smaller in size with the case before, it may require a less intense laser beam to do the same job.

Laser beam diameter is 67.08 microns

Geometry of the work piece is X axis -0.03 to 0.03; Y axis 0.015 to -0.165; Z axis -0.015 to 0.015

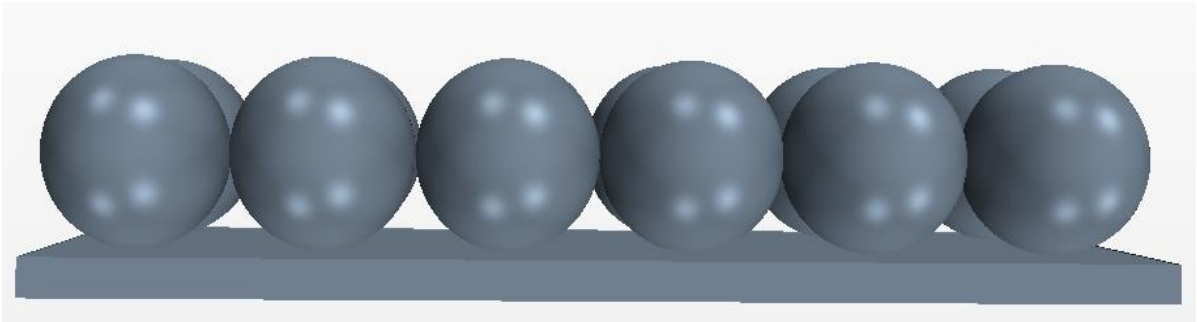


Figure 4-87 Geometry of work piece

Mesh size is 0.001mm

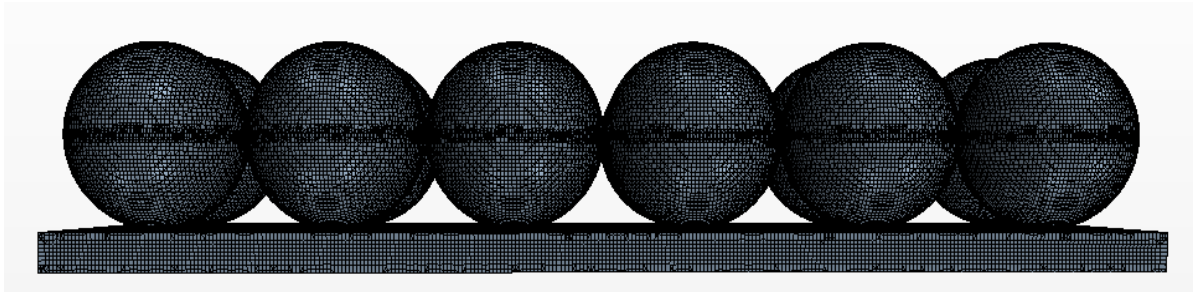


Figure 4-88 Mesh scene of the work piece

The mesh conditions and the physics applied for this part are the same as for the powder particles of 50 microns. The same manufacturing procedure is followed again.

After a few simulation trials, the laser beam intensity required to be melt the work piece as per the requirement is calculated to be $5 \cdot 10^8 \text{W/m}^2$.

Required molten volume to fill void spaces is $2.035 \cdot 10^{-6} \text{mm}^3$

Laser 1 Beam position 1

Process time = 0.008sec

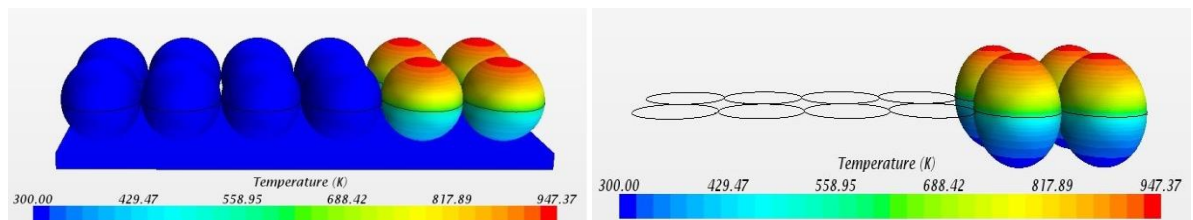


Figure 4-89 Temperature distribution for Layer 1 beam position 1 at time 0.008 sec

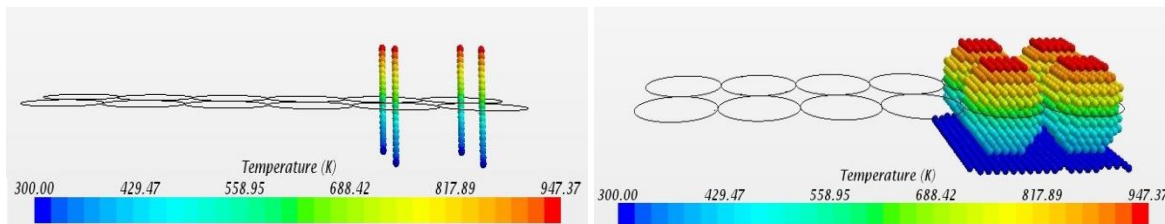


Figure 4-90 Temperature distribution for probe points

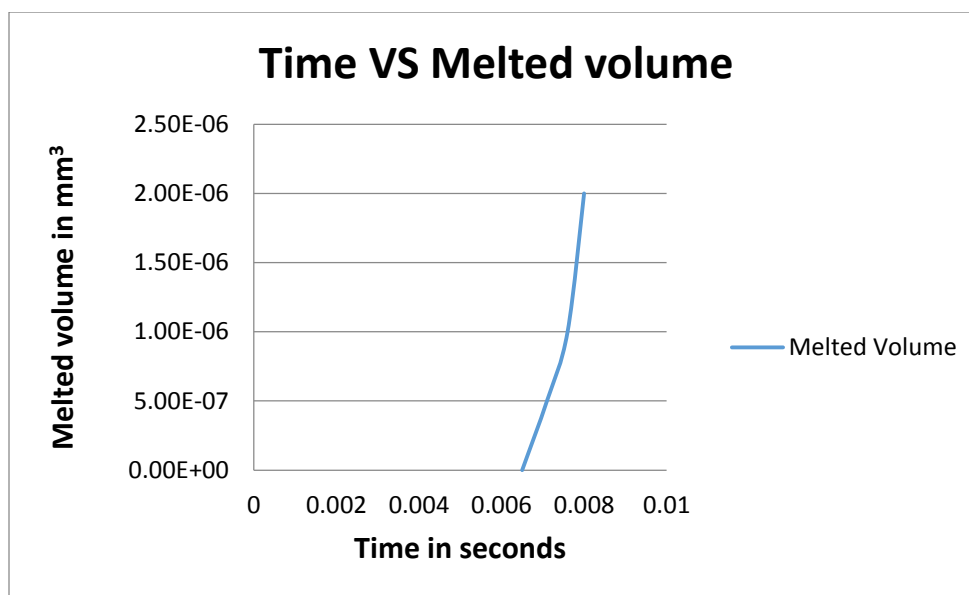


Figure 4-91 Time Vs Melted volume

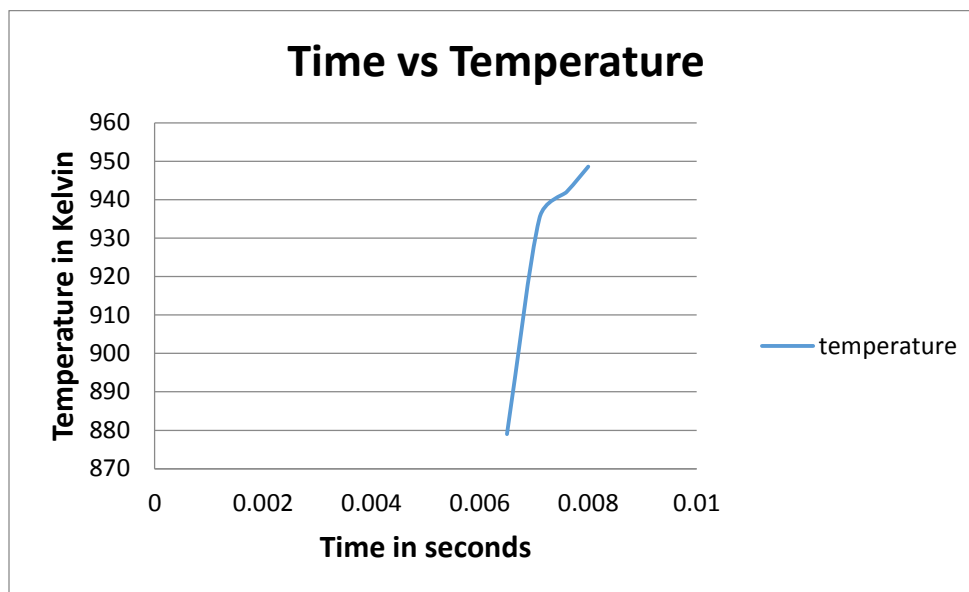


Figure 4-92 Time Vs Highest temperature

Layer 1 Beam position 2

Process time = 0.008 sec

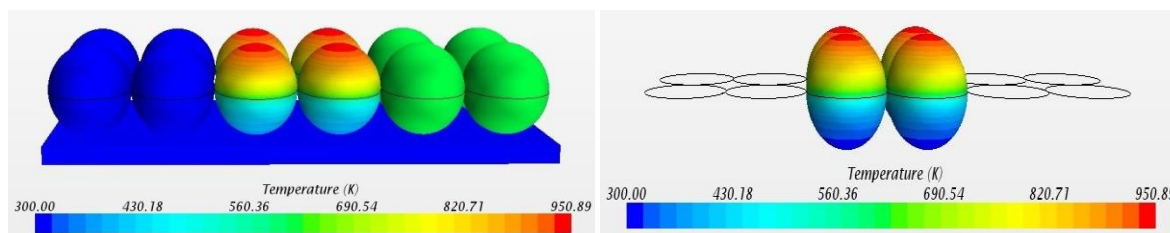


Figure 4-93 Temperature distribution for layer 1 beam position 2 at 0.016 sec

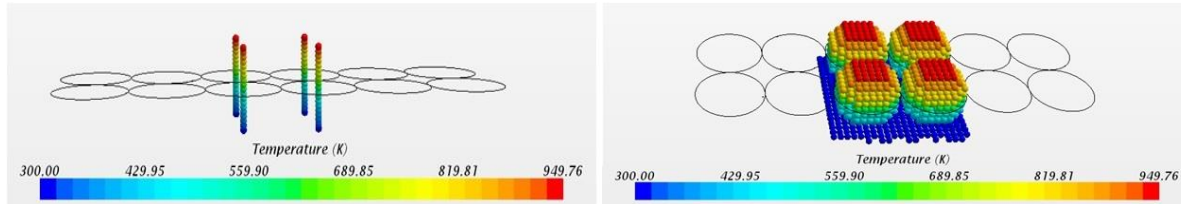


Figure 4-94 Temperature distribution for probe points

The final process time is 0.016 seconds

Plots

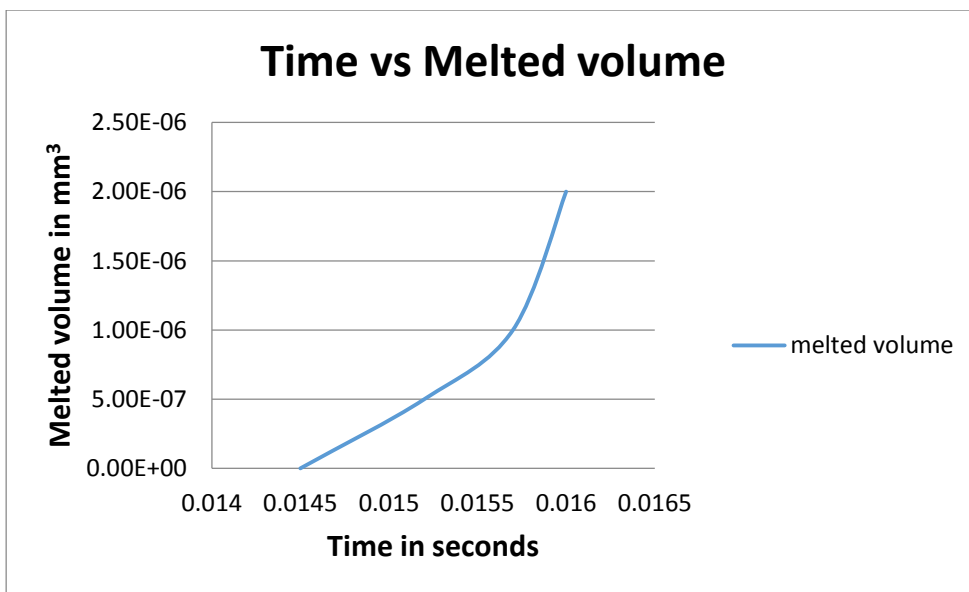


Figure 4-95 Time Vs Melted volume

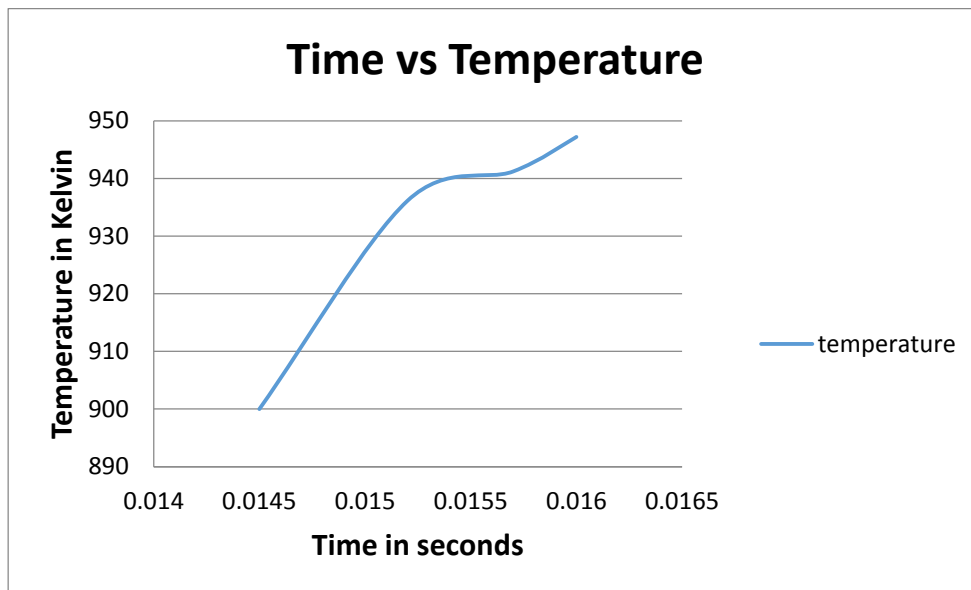


Figure 4-96 Time Vs Highest temperature

Laser 1 beam position 3

Process time = 0.008 sec

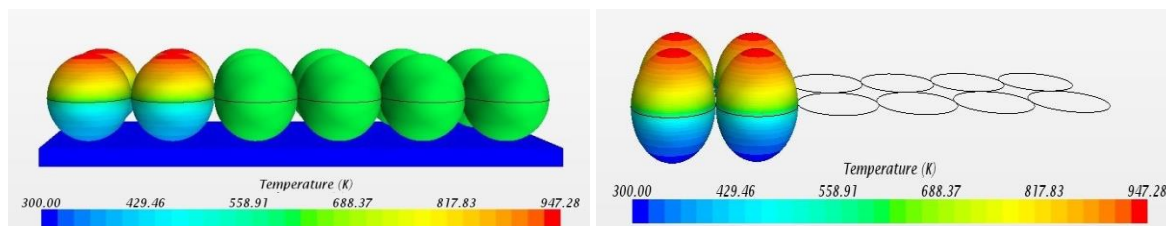


Figure 4-97 Temperature distribution for layer 1 beam position 3 at time 0.024 seconds

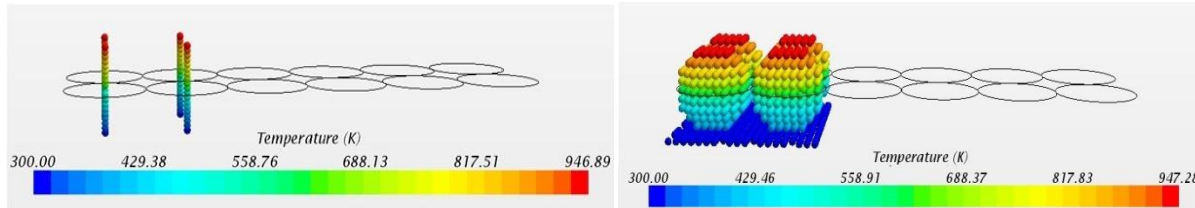


Figure 4-98 Temperature distribution for probe point

The final process time for completion of this layer is 0.024 sec

Plots

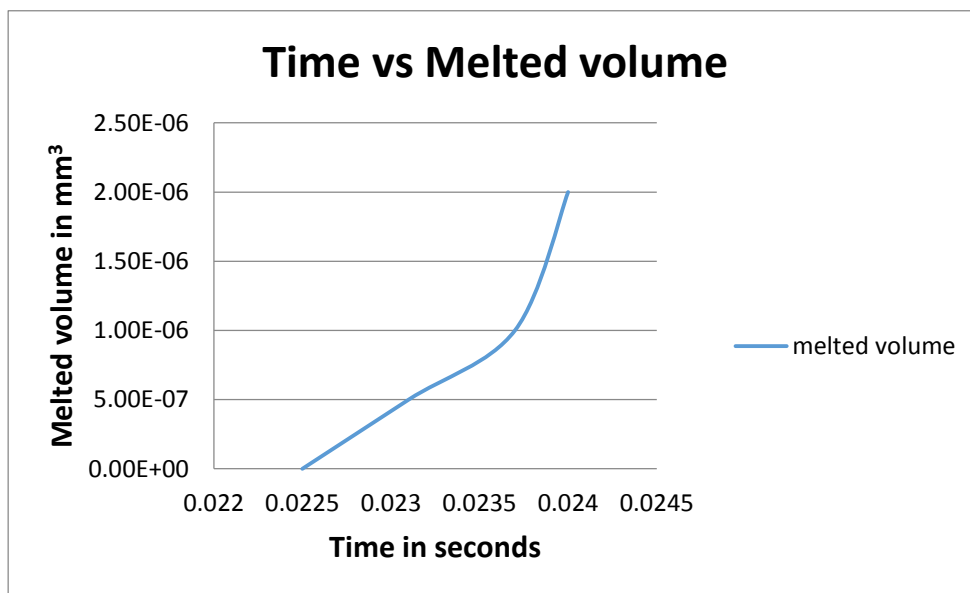


Figure 4-99 Time Vs Melted volume

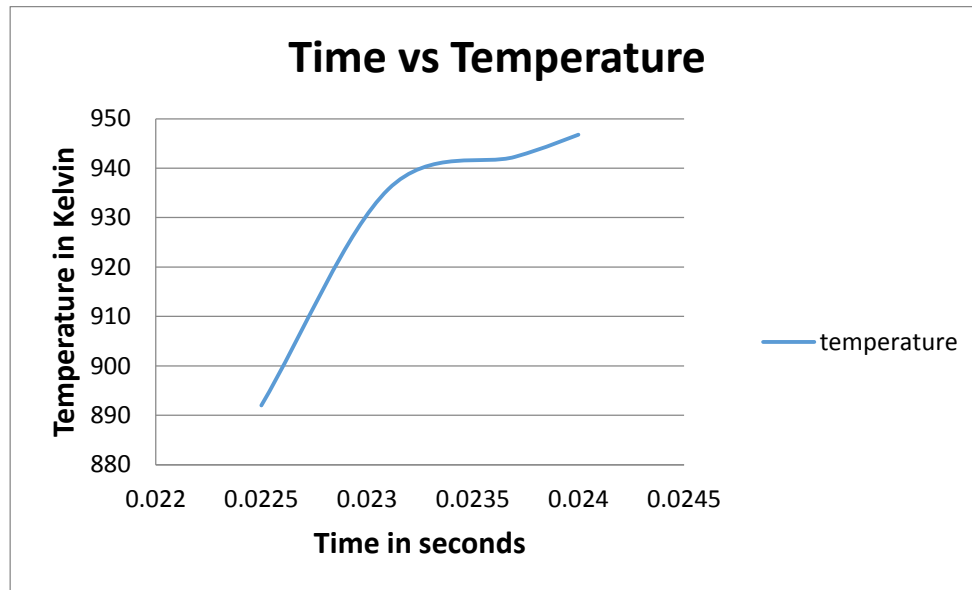


Figure 4-100 Time Vs Highest temperature

Enthalpy Validation

Beam position 1

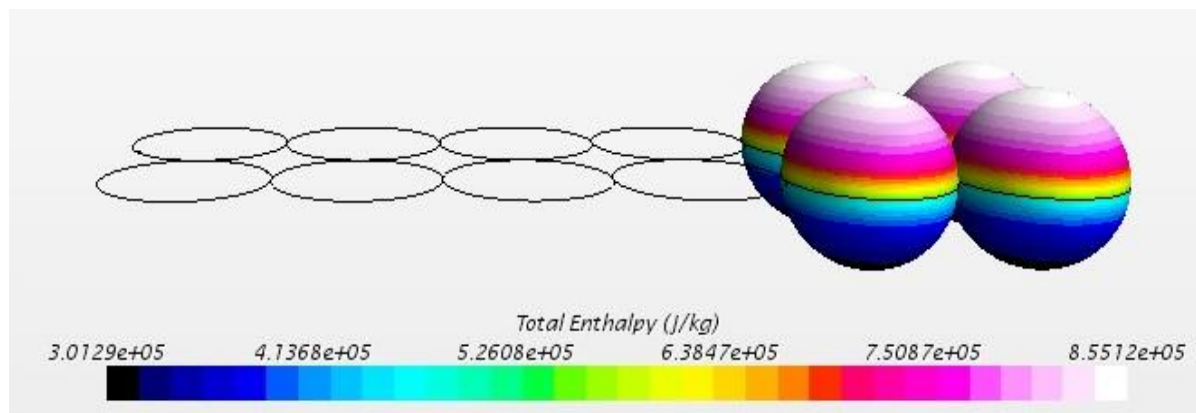


Figure 4-101 Enthalpy scene beam position 1

Enthalpy is 855120 J/kg

$$\begin{aligned}
 T_{\text{melt}} &= h_{\text{melt}}/C_p \\
 &= 855120/903 \\
 &= 946.97\text{k}
 \end{aligned}$$

So this is the temperature that we got from the temperature scene by projecting a laser beam on to the aluminum particles.

Beam position 2

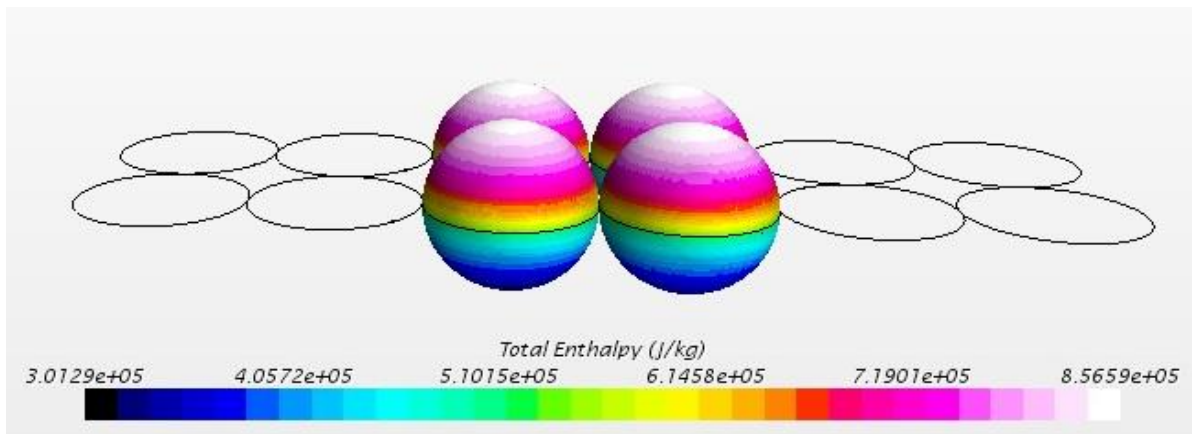


Figure 4-102 Enthalpy scene beam position 2

Enthalpy is 856590 J/kg

$$T_{\text{melt}} = h_{\text{melt}}/C_p = 856590/903 = 949.920\text{k}$$

Beam position 3

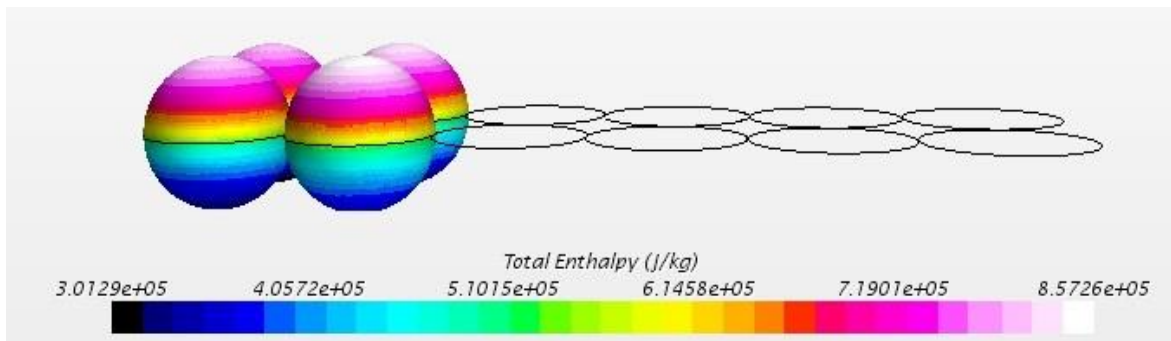


Figure 4-103 Enthalpy scene beam position 3

Enthalpy is 857260 J/kg

$$T_{\text{melt}} = h_{\text{melt}}/C_p = 857260/903 = 948.31\text{k}$$

The total process time to finish this operation is 0.024 sec

After the material processing, this is the part formed.



Figure 4-104 Part formed after melting layer 1

After spraying a fresh layer of powder particles over this,

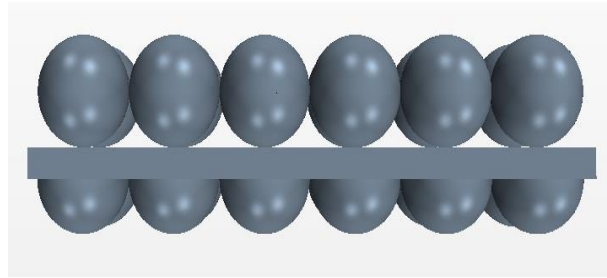


Figure 4-105 A new powder layer is sprayed over the processed layer

Mesh scene: Base size = 0.001mm

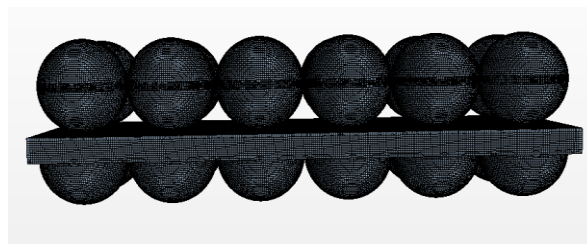


Figure 4-106 Mesh scene

As the physical properties of the material are the same. The meshing procedure and the physics applied to the part are the similar as for the layer 1. The same procedure is followed for second layer and for the following layers. The same case is ran for three layers for the all the three beam positions. To be precise and up to the point, all the cases are not showed for Layer 2 and Layer 3.

Layer 3 Beam position 3

Process time = 0.008 sec

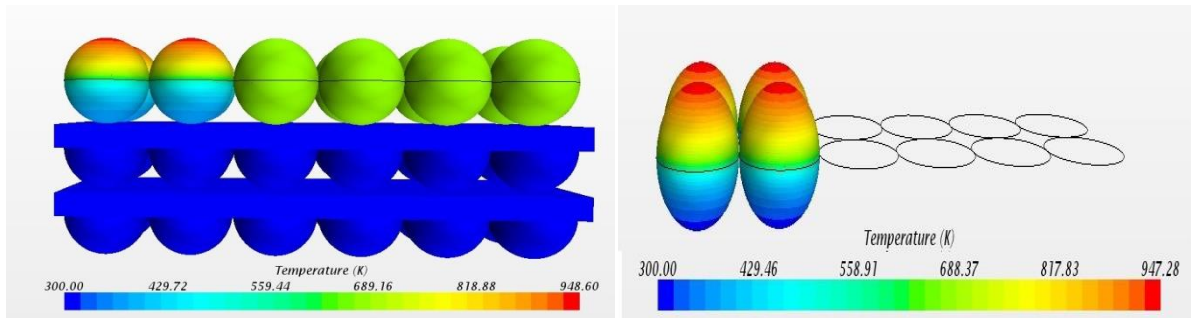


Figure 4-107 Temperature distribution for layer 1 beam position 1 at time 0.008 sec

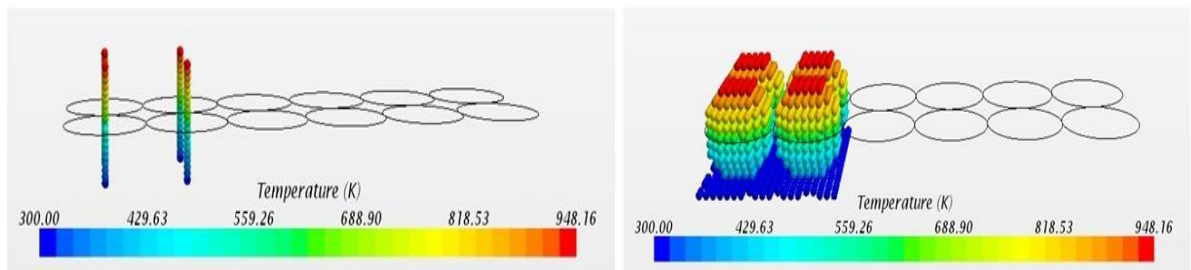


Figure 4-108 Temperature distribution for probe point

The final process time to form layer 3 is 0.024 sec

Enthalpy Scene

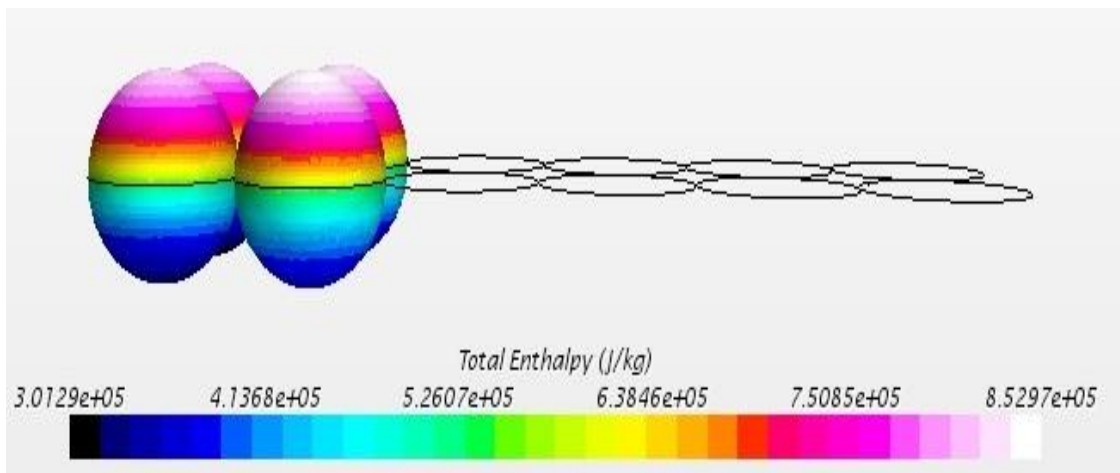


Figure 4-109 Enthalpy scene for layer 3 beam position 3

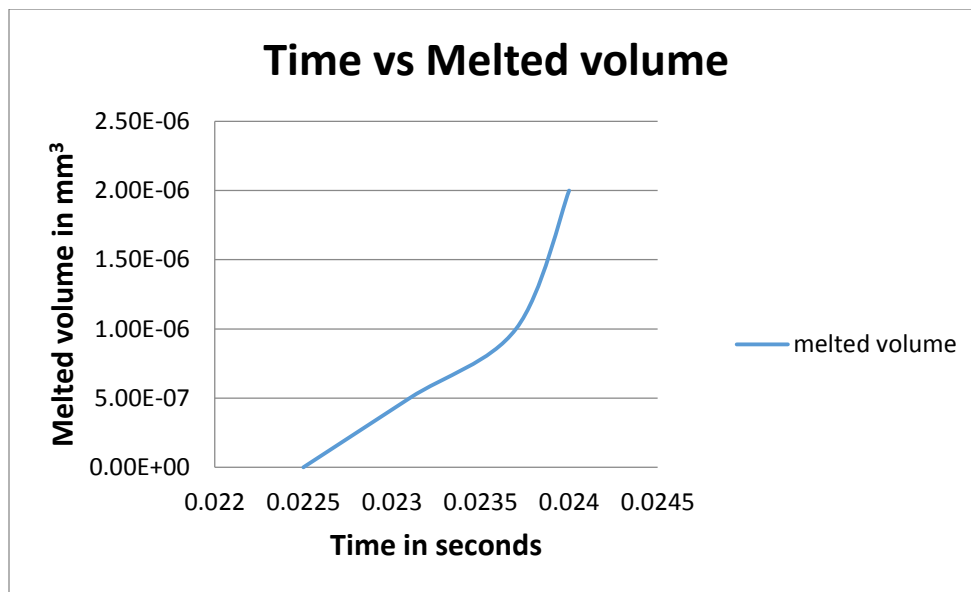


Figure 4-110 Time Vs Melted volume

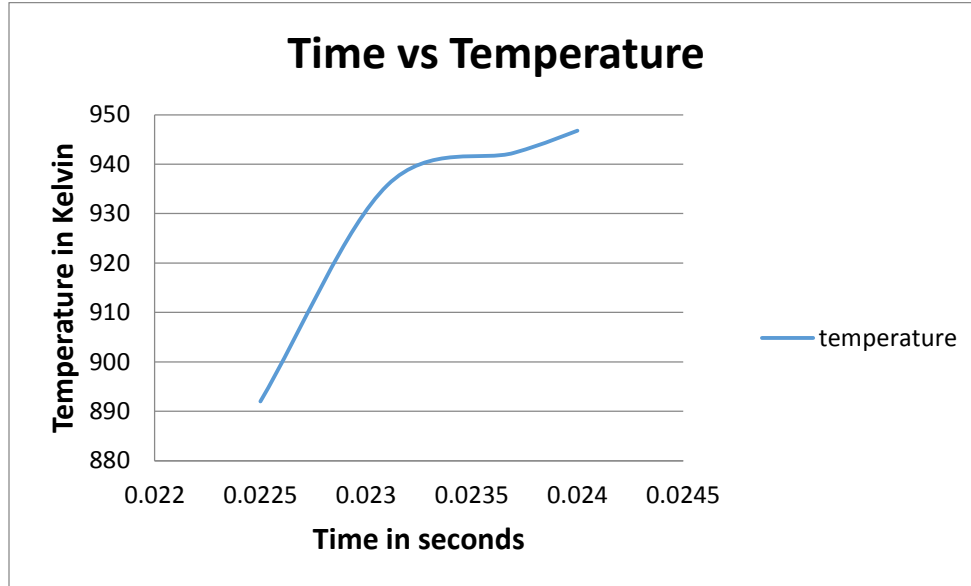


Figure 4-111 Time Vs Highest temperature

The final time taken to complete the manufacturing of the whole work piece, without considering the spraying time is 0.072 sec.

Scan speed of the laser beam = Distance travelled ÷ Time taken

Scan speed = $0.18 \div 0.024 = 7.5\text{mm/sec}$

4.4.3 Effect of particle size – 10microns

For a particle size of diameter 10microns, we try to calculate the density of this part by melting the powder particles to the meshing models are the same. The procedure followed is the same as the one for the particle size of 50, 30 microns. There is difference in the geometry but the physics models and smaller in size with the case before, it may require a less intense laser beam to do the same job.

The mesh conditions and the physics applied for this part are the same as for the powder particles of 50 and 30 microns. The same manufacturing procedure is followed again.

After a few simulation trials, the laser beam intensity required to be melt the work piece as per the requirement is calculated to be $3 \times 10^8 \text{W/m}^2$.

Required molten volume to fill void spaces is $7.12 \times 10^{-7} \text{mm}^3$

Layer 1 Beam Position 1

Beam diameter = 22.36 microns

Geometry X axis -0.01 to 0.01; Y axis 0.005 to -0.055; Z axis -0.005 to 0.005

Origin is (0, 0, 0)

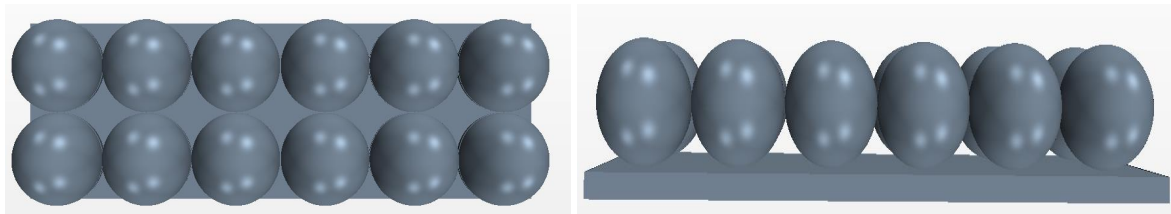


Figure 4-112 Geometry scene

Mesh scene:

Base size 0.001mm

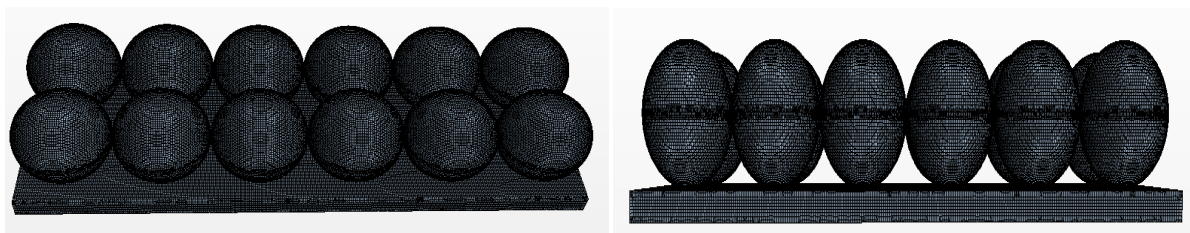


Figure 4-113 Mesh scene

Beam Intensity is $3.0 \times 10^8 \text{ W/m}^2$

Layer 1 Beam Position 1 Final Time 0.006sec

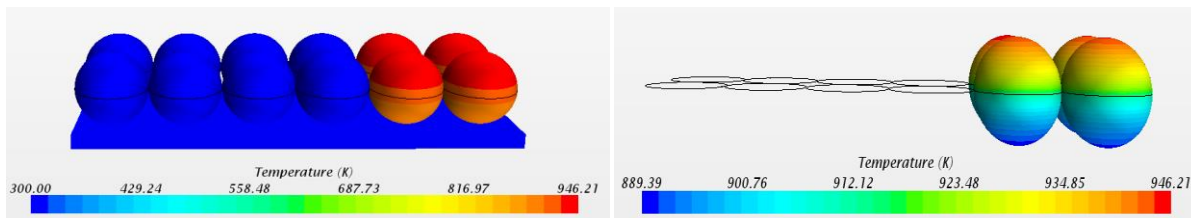


Figure 4-114 Temperature distribution for layer 1 and beam position 1 at 0.006 sec

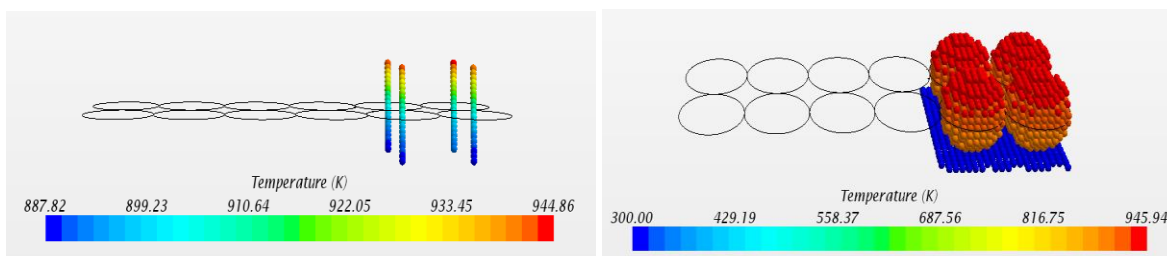


Figure 4-115 Temperature distribution for point probes

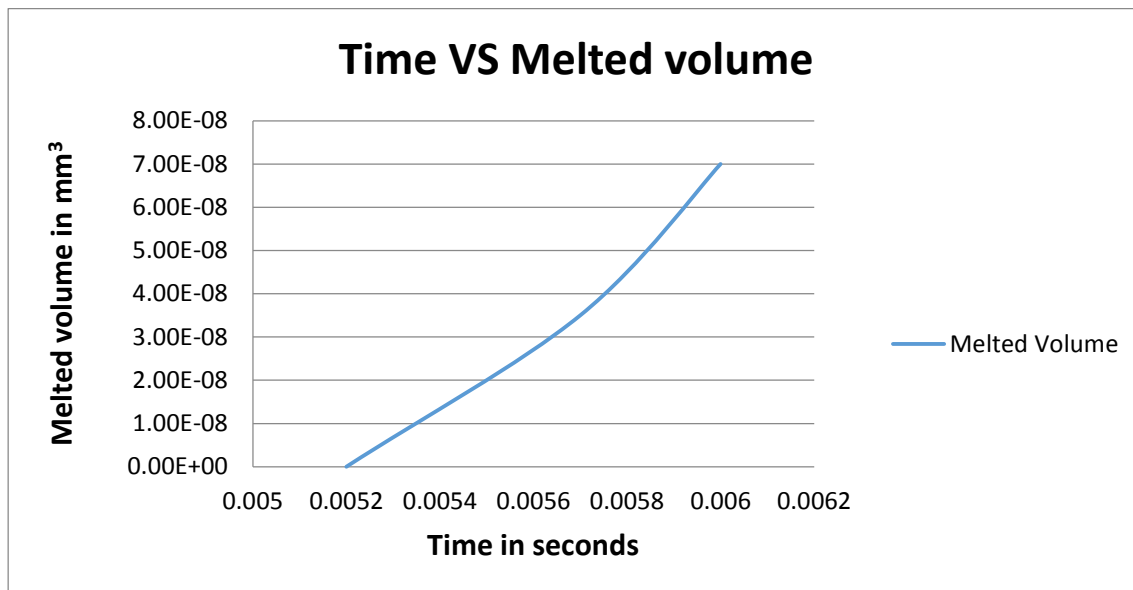


Figure 4-116 Time Vs Melted volume

The final process time for this process is 0.006 sec

(Layer 1 Beam 2) The beam is now shifted to second position

Process Time 0.012 sec

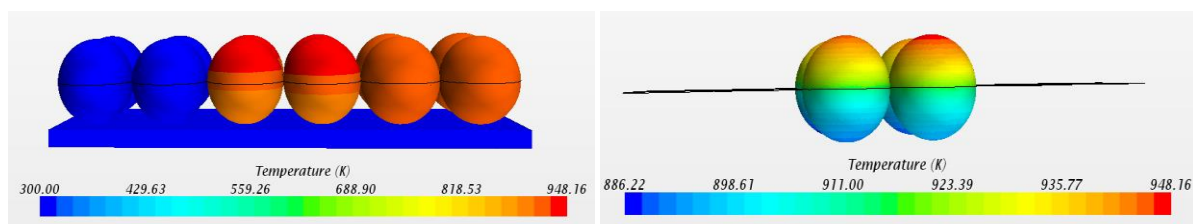


Figure 4-117 Temperature distribution for layer 1 beam position 2 at 0.012 sec

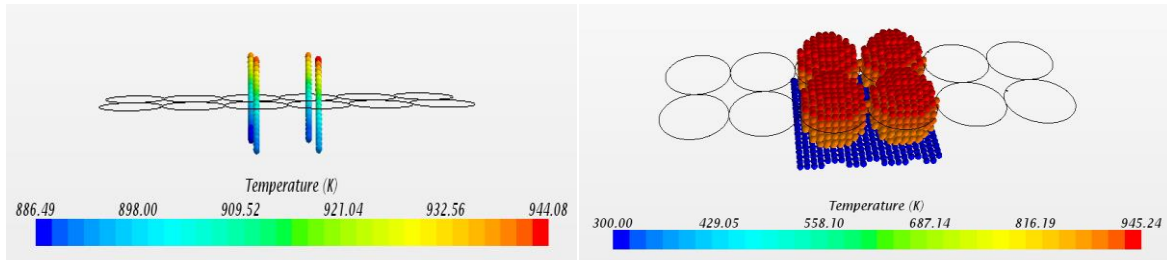


Figure 4-118 Probe points temperature distribution

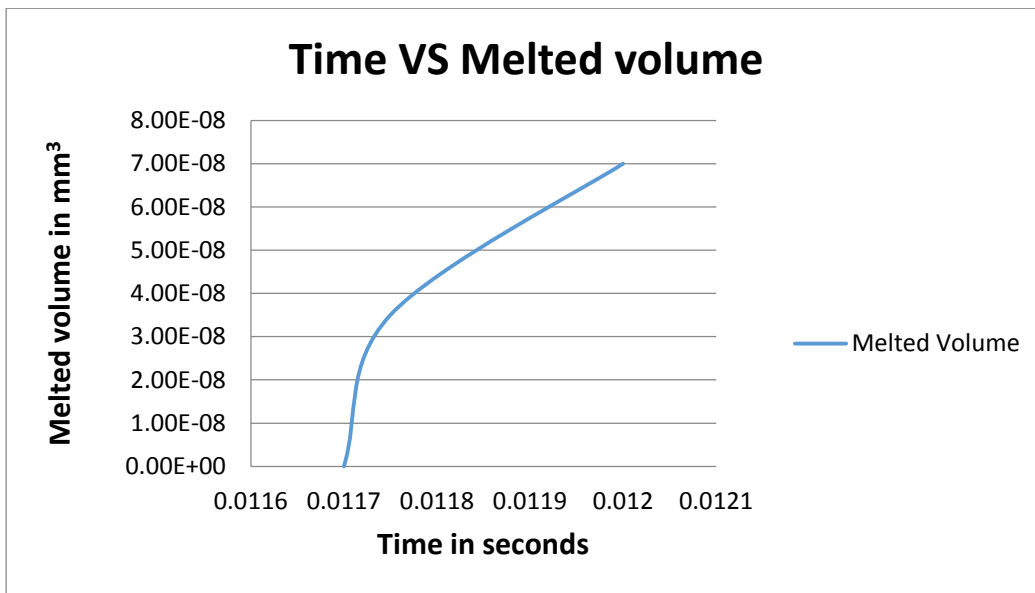


Figure 4-119 Time Vs Melted volume

The final process time after melting = 0.012 sec

Layer 1 Beam position 3

Beam is shifted and incident on position 3 for time 0.006 sec

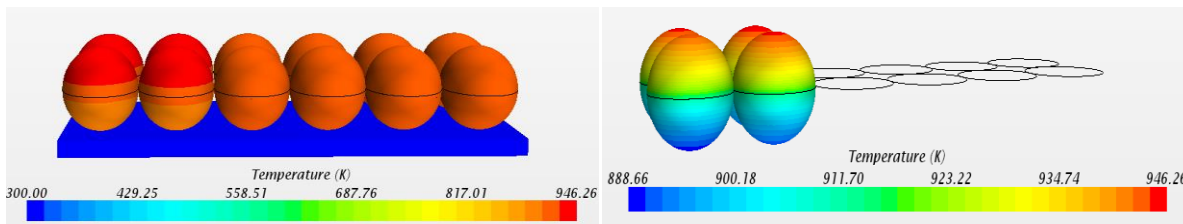


Figure 4-120 Temperature distribution of powder particles at 0.018 sec

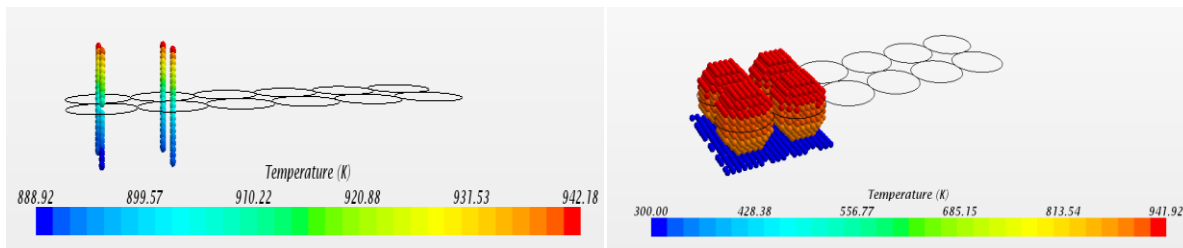


Figure 4-121 Temperature distribution for probe point

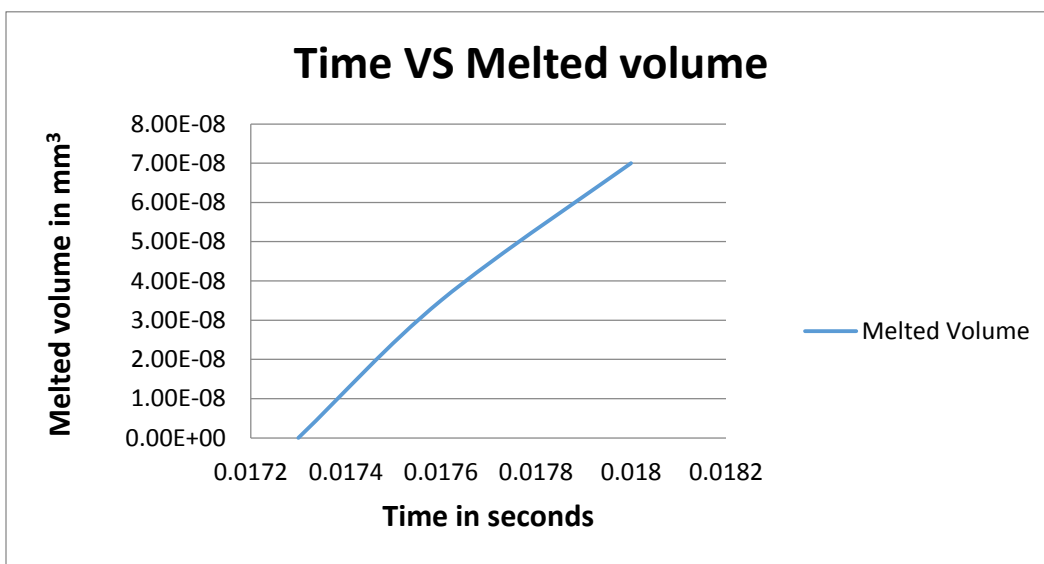


Figure 4-122 Time Vs Melted volume

Enthalpy Validation

Beam position 1

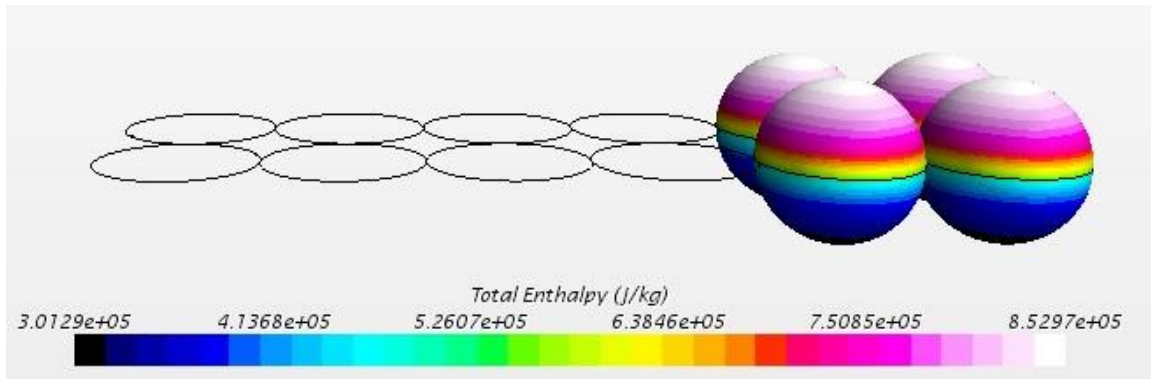


Figure 4-123 Enthalpy scene beam position 1

Enthalpy is 852970 J/kg

$$\begin{aligned}
 T_{\text{melt}} &= h_{\text{melt}}/C_p \\
 &= 852970/903 \\
 &= 945.98\text{k}
 \end{aligned}$$

So this is the temperature that we got from the temperature scene by projecting a laser beam on to the aluminum particles.

Beam position 2

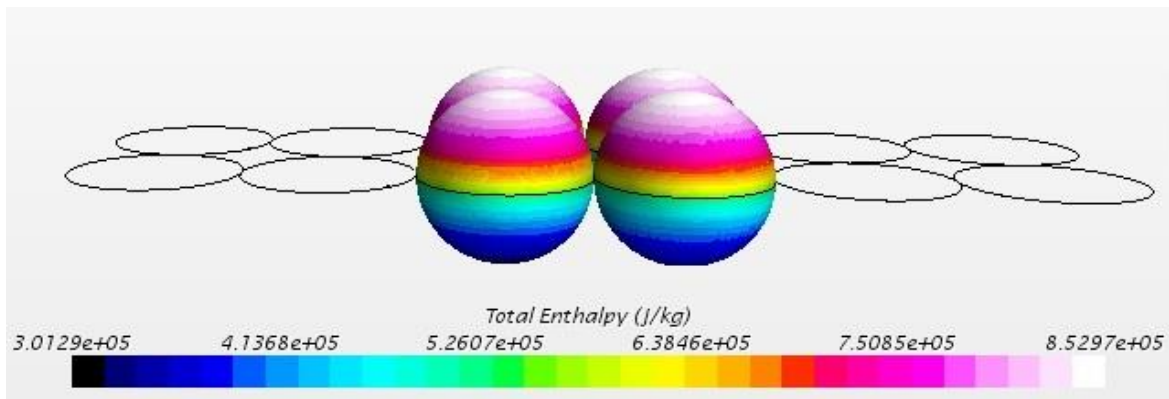


Figure 4-124 Enthalpy scene beam position 2

Enthalpy is 852970 J/kg

$$T_{\text{melt}} = h_{\text{melt}}/C_p = 852970/903 = 947.9\text{k}$$

Beam position 3

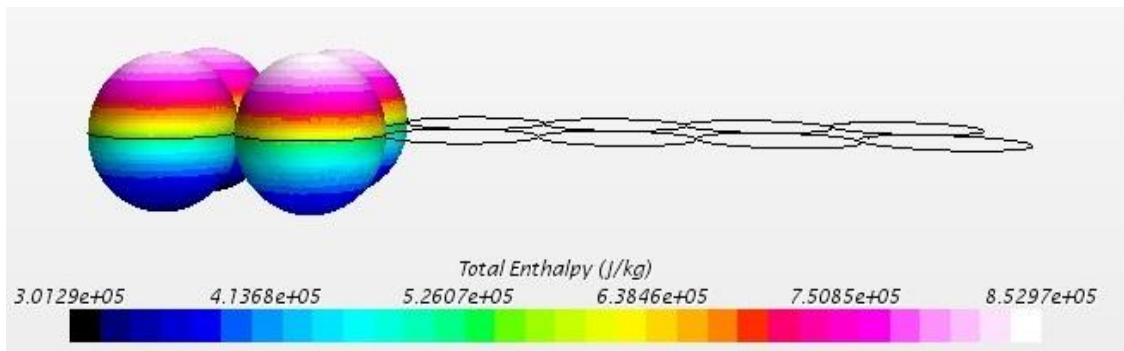


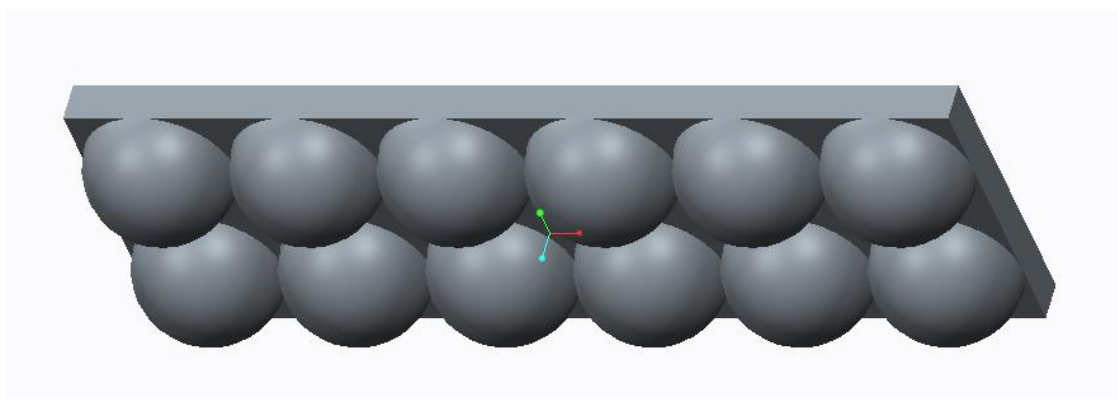
Figure 4-125 Enthalpy scene beam position 3

Enthalpy is 852970 J/kg

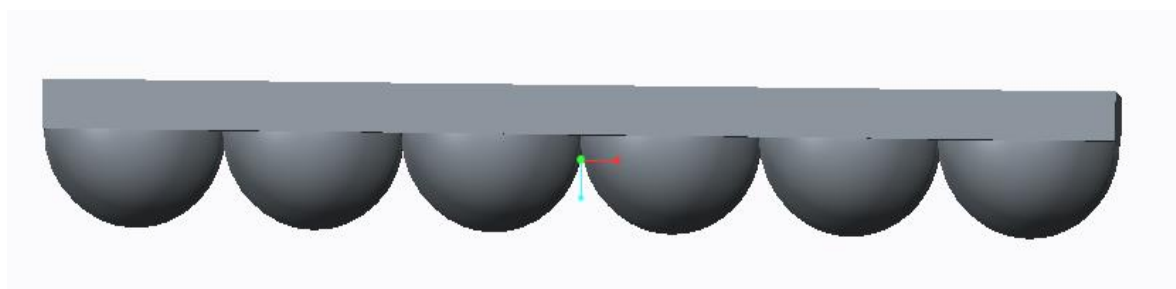
$$T_{\text{melt}} = h_{\text{melt}}/C_p = 852970/903 = 947.9\text{k}$$

The total process time to finish this operation is 0.018 sec

After melting the layer 1. This is the structure formed.



(a)



(b)

Figure 4-126 Geometry scene after melting the layer 1

Spray another fresh layer of powder over the melted one.

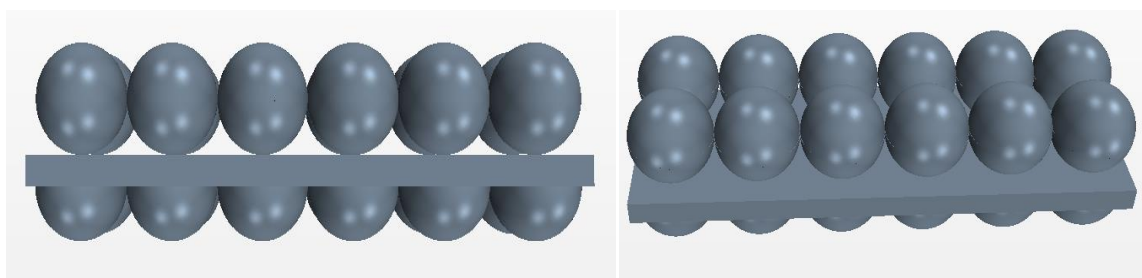


Figure 4-127 After spraying another layer of particles over the melted layer

As the physical properties of the material are the same. The meshing procedure and the physics applied to the part are the similar as for the layer 1. The same procedure is followed for second layer and the following layers. The same case is ran for three layers for the all the three beam positions. To be precise and up to the point, all the cases are not showed for Layer 2 and Layer 3. Now the beam is moved to position 3 (Layer 3 Beam 3)

Laser process time = 0.006 sec for layer 3 beam 3

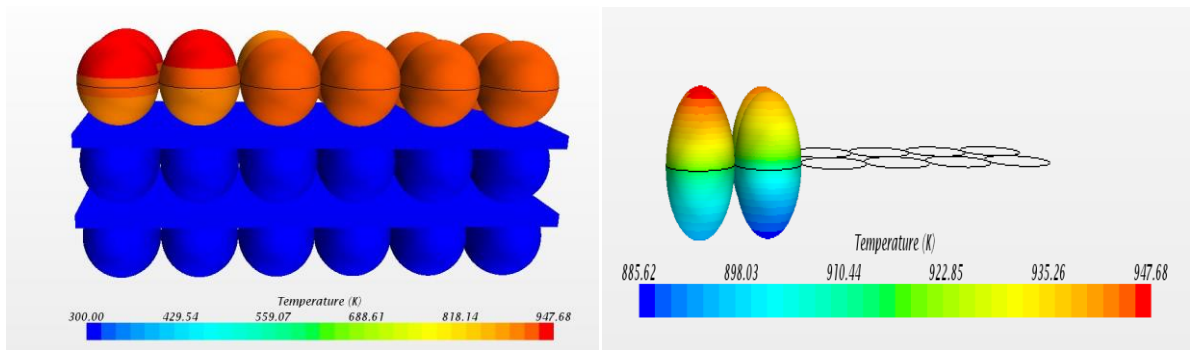


Figure 4-128 Temperature distribution of powder particles

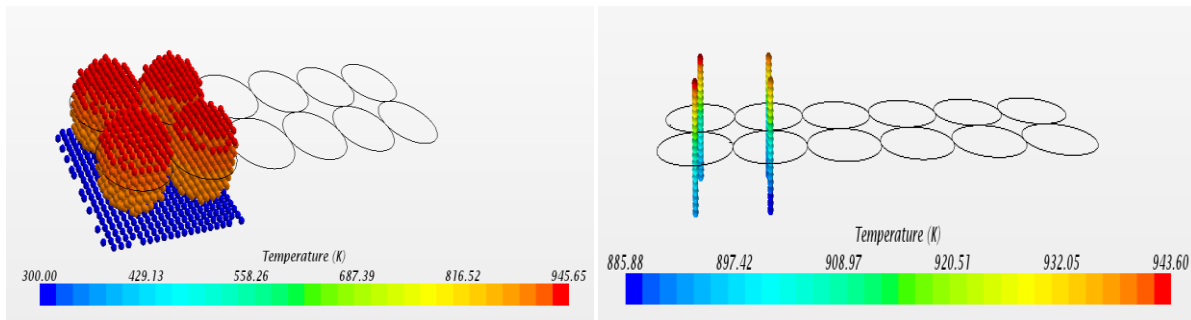


Figure 4-129 Temperature distribution for probe points

Enthalpy Scene for Layer 3 Beam position 3

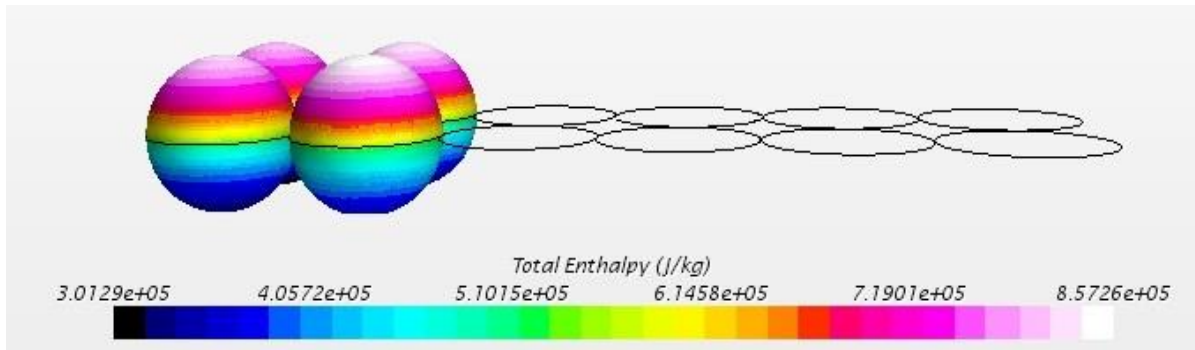


Figure 4-130 Enthalpy Scene for Layer 3 beam position 3

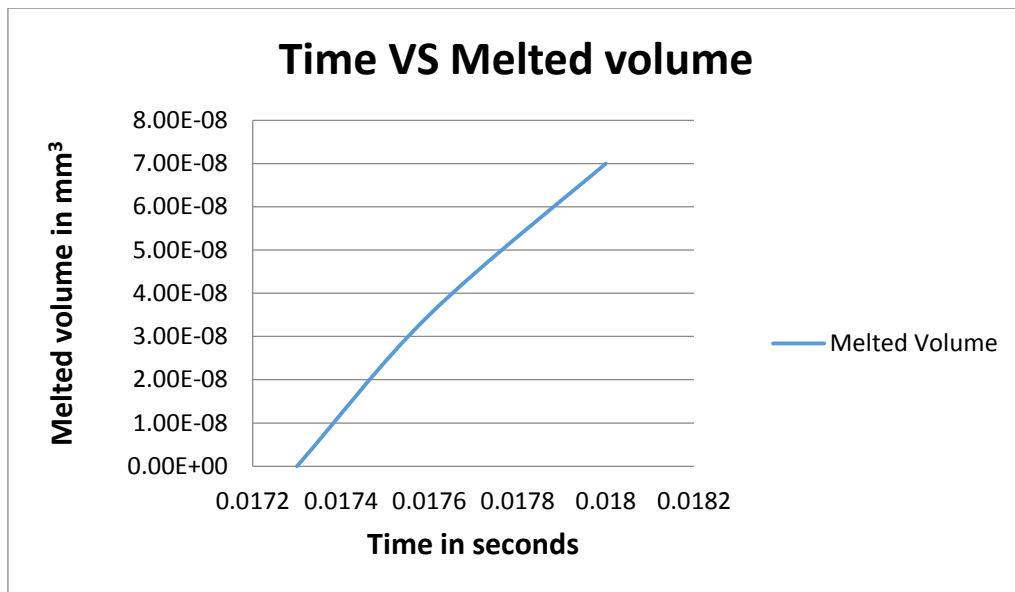


Figure 4-131 157 Time Vs Melted volume

The final process time is 0.018 sec

The final time taken to complete the manufacturing of the whole work piece, without considering the spraying time is $0.018 + 0.018 + 0.018 = 0.054$ sec.

Scan speed of the laser beam = Distance travelled \div Time taken

Scan speed = $0.06 \div 0.018 = 3.33$ mm/sec

4.5 Performing Sensitivity Analysis

After iterations, the optimum operating parameters in terms of the particles size and laser beam properties are calculated. Sensitivity analysis is performed for the desired part by calculating density of these spherical powder particles for different sizes.

4.5.1 Density calculation for particle of size 50microns

The total process to build three layers is **0.099sec**

$L=0.3$ mm, $b=0.1$ mm, **$h=0.15$ mm**

Volume = **0.0045 mm³**

After melting and processing

$L=0.3$ mm, $b=0.1$ mm, **$h=0.1124$ mm**

Volume = **0.00342 mm³**

Reduction in the volume = 0.00108 mm³

Mass of aluminum = number of particles * volume of each particle * density of pure aluminum

= $36 * (4/3\pi r^3) * 0.0027 = 0.0063 * 10^{-3}$ gm

Density = **Mass/Volume**

Density before melting = $0.0063 * 10^{-3}$ gm/ 0.0045 mm³ = $1.4089 * 10^{-3}$ gm/mm³

Density after melting = $0.0063 * 10^{-3}$ gm/ 0.00342 mm³ = $1.84 * 10^{-3}$ gm/mm³

4.5.2 Density calculation for particle of size 30microns

The total process to build three layers is **0.072sec**

Initially for three layers

L=0.18mm, b=0.06mm, **h=0.09mm**

Volume = **0.000972mm³**

After melting and processing

L=0.18mm, b=0.06mm, **h=0.06645mm**

Volume = **0.000717mm³**

Reduction in the volume = 0.002551mm³

Mass of aluminum = number of particles * volume of each particle * density of aluminum =

$$6*(4/3\pi r^3)*0.0027 = \mathbf{0.00136*10^{-3}gm.}$$

Density = Mass/Volume

$$\text{Density before melting} = \mathbf{0.00136*10^{-3}gm/0.000972mm^3 = 1.409*10^{-3}gm/mm^3}$$

$$\text{Density after melting} = \mathbf{0.00136*10^{-3}gm/0.000717mm^3 = 1.896*10^{-3}gm/mm^3}$$

4.5.3 Density calculation for particle of size 10microns

The total process to build three layers is **0.054sec**

Initially for three layers

L=0.06mm, b=0.02mm, **h=0.03mm**

Volume = **0.000036mm³**

After melting and processing

L=0.06mm, b=0.02mm, **h=0.02215mm**

Volume = **0.00002658mm³**

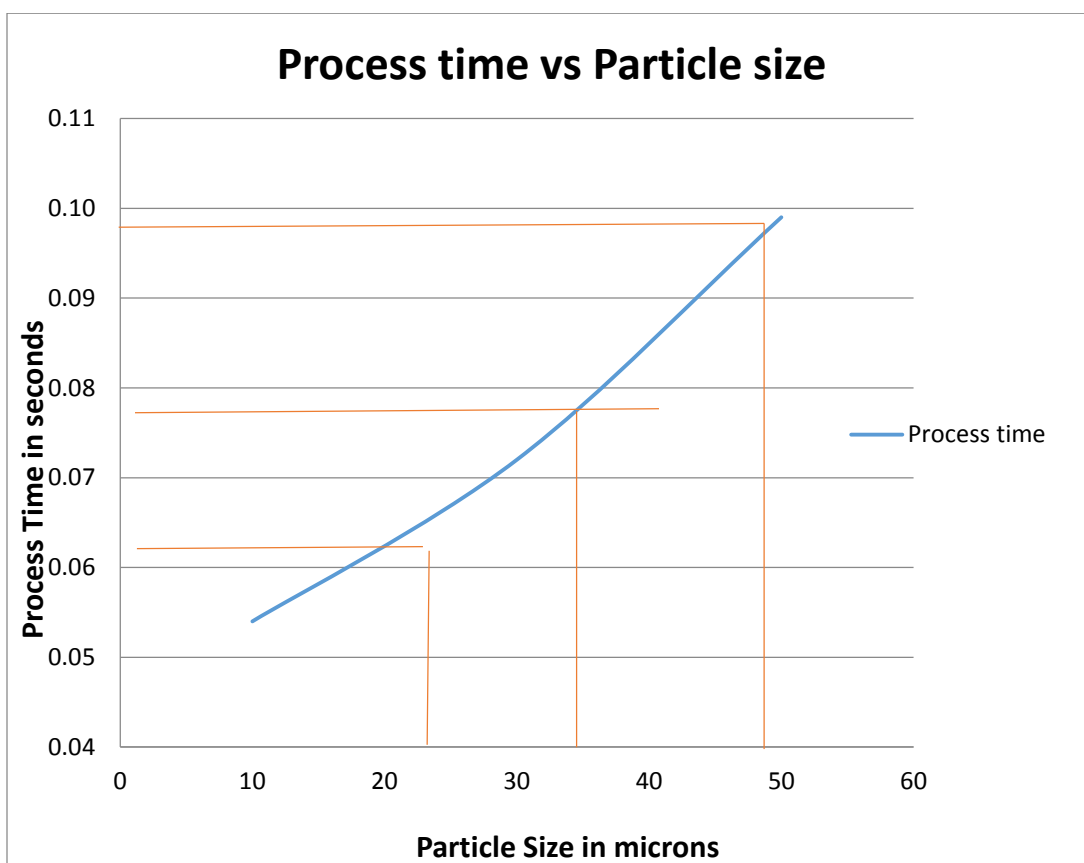
Reduction in the volume = 0.00000942mm^3

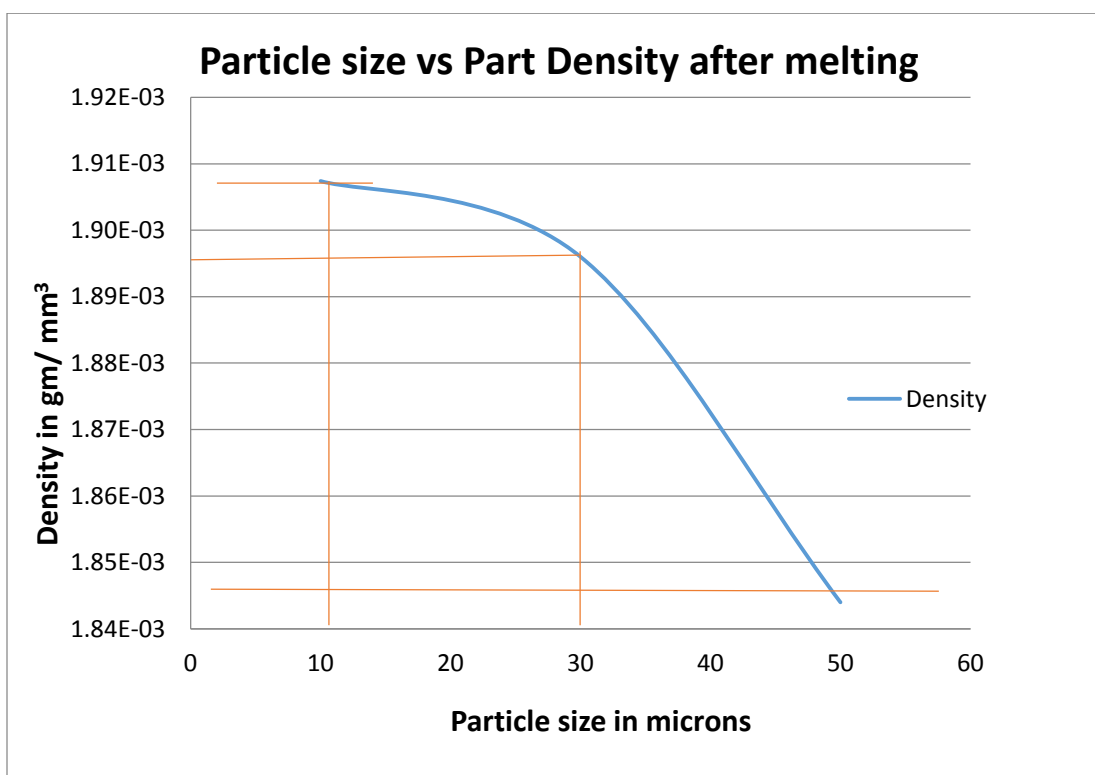
Mass of aluminum = number of particles * volume of each particle * density of aluminum =
 $6*(4/3\pi r^3)*0.0027 = \mathbf{0.0000507*10^{-3}\text{gm.}}$

Density = Mass/Volume

Density before melting = $\mathbf{0.0000507*10^{-3}\text{gm}/0.000036\text{mm}^3 = 1.41*10^{-3}\text{gm/mm}^3}$

Density after melting = $\mathbf{0.0000507*10^{-3}\text{gm}/0.00002658\text{mm}^3 = 1.907*10^{-3}\text{gm/mm}^3}$

Variation of Process Time with Particle Size**Figure 4-132 Particle size Vs Process time**

Variation of Particle size with Part Density**Figure 4-133 Particle size Vs Part density**

5 CONCLUSION AND FUTURE WORK

A number of bipolar plate designs have been considered throughout the study. A computational simulation model based on an enthalpy-based heat model was developed to characterize the SLM-AM process. An iterative methodology was presented to establish the beam power density and particle size needed to meet the target process time and part density. Performed sensitivity analysis for the desired part by heating and melting of spherical particles to establish the optimum operating parameters in terms of the particles size and laser beam properties, and also to develop a correlation of the fabricated part density with powder size for a given beam power density.

Future work should include establishing the operating beam parameter, particle size, operating scan speed for fabricating a bipolar plate using the SLM simulation model. Use the SLM simulation model to develop a CAD model for the fabrication of bi-polar plate and finally validate the SLM model with the manufactured fabricated bipolar plate.

6 REFERENCES

- [1] Gusarov, A. V., Yadroitsev, I., Bertrand, P., & Smurov, I. (2007). Heat transfer modelling and stability analysis of selective laser melting. *Applied Surface Science*, 254(4), 975-979.
- [2] Zeng, K., Pal, D., & Stucker, B. (2012, August). A review of thermal analysis methods in Laser Sintering and Selective Laser Melting. In *Proceedings of Solid Freeform Fabrication Symposium Austin, TX*.
- [3] Kruth, J. P., Mercelis, P., Van Vaerenbergh, J., Froyen, L., & Rombouts, M. (2005). Binding mechanisms in selective laser sintering and selective laser melting. *Rapid prototyping journal*, 11(1), 26-36.
- [4] Yadroitsev, I., Bertrand, P., & Smurov, I. (2007). Parametric analysis of the selective laser melting process. *Applied surface science*, 253(19), 8064-8069.
- [5] Li, R., Shi, Y., Liu, J., Yao, H., & Zhang, W. (2009). Effects of processing parameters on the temperature field of selective laser melting metal powder. *Powder Metallurgy and Metal Ceramics*, 48(3-4), 186-195.
- [6] Brown, M. S., & Arnold, C. B. (2010). Fundamentals of laser-material interaction and application to multiscale surface modification. In *Laser Precision Microfabrication* (pp. 91-120). Springer Berlin Heidelberg.

- [7] Kumar, S., & Pityana, S. (2011, June). Laser-based additive manufacturing of metals. In *Advanced Materials Research* (Vol. 227, pp. 92-95).
- [8] Yadroitsev, I., & Smurov, I. (2011). Surface morphology in selective laser melting of metal powders. *Physics Procedia*, 12, 264-270.
- [9] Basu, B., & Srinivasan, J. (1988). Numerical study of steady-state laser melting problem. *International journal of heat and mass transfer*, 31(11), 2331-2338.
- [10] Basu, B., & Date, A. W. (1990). Numerical study of steady state and transient laser melting problems—I. Characteristics of flow field and heat transfer. *International Journal of Heat and Mass Transfer*, 33(6), 1149-1163.
- [11] Ravindran, K., Srinivasan, J., & Marathe, A. G. (1994). Finite element study on the role of convection in laser surface melting. *Numerical Heat Transfer, Part A Applications*, 26(5), 601-618.
- [12] Sowdari, D., & Majumdar, P. (2010). Finite element analysis of laser irradiated metal heating and melting processes. *Optics & Laser Technology*, 42(6), 855-865.
- [13] Kasula, B., & Majumdar, P. (2003, January). Three-dimensional finite element analysis of melting in an alloy irradiated with a high energy laser beam. In *ASME 2003 International Mechanical Engineering Congress and Exposition* (pp. 81-87). American Society of Mechanical Engineers.
- [14] Zeng, K., Pal, D., & Stucker, B. (2012, August). A review of thermal analysis methods in Laser Sintering and Selective Laser Melting. In *Proceedings of Solid Freeform Fabrication Symposium Austin, TX*.

- [15] Mohammad, S. (2012). CFD analysis of blood flow through stented arteries. In *Masters Abstracts International* (Vol. 50, No. 06).